

# Degradation of chromogenic photoworks



Master's thesis

Cecilia Jespers, BSc

Supervisors: E. B. Reijers, MSc

Prof. Dr. L. W. Jenneskens

Organic chemistry and catalysis

Debye institute for Nanomaterials Science

October 28<sup>th</sup> 2015, Utrecht



## Abstract

Photographic artworks, especially those where photographs are combined with other materials, so called photoworks, show signs of aging through color shift which results in value loss of the artworks. In order to find more suitable ways to store them, an investigation is made of possible chemical reactions which may result in this change in color. Evidence is found for the presence of acetic acid, this pollutant will be a focus in this research. The generalized forms of three basic yellow, magenta and cyan dyes found in photographs are synthesized and treatment with acid was performed. UV-Vis spectroscopy and NMR spectroscopy were used to investigate the influence of acid on the dyes. Cyclovoltammetric measurements and DFT calculations were done in order to gather more information about the reactivity of the dyes and more specific, about the reactivity of the Schiff base. The dyes are changed irreversibly when treated with acid. Absorption of visible light happens at the same wavelength but with a lower intensity. Several derivatives of dyes were synthesized in order to investigate the degradation mechanism. The hypothesis of the hydrolysis of the Schiff base was tried to be approved but due to lack of evidence this hypothesis cannot be established.

## List of abbreviations

PMMA	Polymethylmethacrylaat
RH	Relative humidity
HOMO	Highest occupied molecular orbital
LUMO	Lowest unoccupied molecular orbital
TEA	Triethylamine
DCM	Dichloromethane
TFA	Trifluoroacetic acid
B3LYP	Becke 3 parameter Lee-Yang-Parr
SCRf	Self consistent reaction field

## Table of contents

<b>1</b>	<b>Introduction</b>	<b>7</b>
<b>2</b>	<b>Theoretical background</b>	<b>11</b>
2.1	<i>Color photography: The color formation process</i>	11
2.1.1	Initiation of the color formation process	14
2.1.2	Further steps in the development procedure	15
2.1.3	Dye molecules: Schiff bases and their reactivity	16
2.2	<i>Storage conditions of photoart</i>	17
2.2.1	Relative Humidity	17
2.2.2	Temperature	17
2.2.3	Acetic acid	18
2.2.4	Other pollutants	18
2.3	<i>Colors and conjugated systems</i>	19
2.3.1	Conjugated systems	19
2.3.2	HOMOs and LUMOs	20
2.3.3	2D and 3D structure of the dyes	21
2.4	<i>Solvatochromic effects</i>	21
<b>3</b>	<b>Experimental</b>	<b>22</b>
3.1	<i>Synthesis of yellow dye 1</i>	22
3.2	<i>Synthesis of magenta dye precursor 2</i>	23
3.3	<i>Synthesis of magenta dye 3</i>	23
3.4	<i>Synthesis of cyan dye 4</i>	24
3.5	<i>Synthesis of aminoquinone 5</i>	24
3.6	<i>Synthesis of aminoquinone 6</i>	25
3.7	<i>Synthesis of acetamidoquinone 7</i>	25
3.8	<i>Synthesis of acetamidoquinone 8</i>	25
3.9	<i>Synthesis of gelatin mixture</i>	26
3.10	<i>pH measurements</i>	26
3.11	<i>Extractions</i>	26
3.12	<i>Acid and base treatment</i>	26
3.13	<i>Dyes in acetic acid</i>	26
3.14	<i>Stock solution 3 dyes in acid</i>	27
3.15	<i>DFT calculations</i>	27
3.16	<i>CV measurements</i>	27
<b>4</b>	<b>Results and discussion</b>	<b>28</b>
4.1	<i>Syntheses</i>	28
4.2	<i>Analysis of dye degradation products</i>	30
4.2.1	Experimental setups	30
4.2.2	Dyes in diverse acidic pHs over time	30
4.2.3	Dyes in acid	31
4.2.4	Combined mixture of three dyes and acid	38
4.2.5	Acid and base treatment	39
4.3	<i>Dyes and reactivity: study of the molecular orbitals</i>	40
4.3.1	Cyclovoltammetric measurements	40
4.3.2	DFT calculations	41
4.3.3	Solvatochromic effects	43
4.4	<i>Dyes in photographic context</i>	45
4.4.1	Extractions	45
4.4.2	Dyes in gelatin	46
4.5	<i>Schiff base hydrolysis theory</i>	47
<b>5</b>	<b>Conclusion</b>	<b>50</b>

<b>6</b>	<b>Outlook</b>	<b>51</b>
6.1	<i>Dyes in solid gelatin</i>	51
6.2	<i>Analysis of reaction products</i>	51

## 1 Introduction

"Art: The expression or application of human creative skill and imagination, typically in a visual form such as painting or sculpture, producing works to be appreciated primarily for their beauty or emotional power."<sup>i</sup> (Oxford Dictionaries).

The concept of art is hard to describe unambiguously.<sup>ii</sup> It can help to express feelings and can also be used as entertainment. In the prehistory primitive forms of art are found like cave paintings and sculptures. Some of these artworks seem to have a religious purpose although it is hard to assign in most cases.<sup>iii</sup> More recently other materials have also been applied like photography, industrial dyes and plastics.

Photography is a medium that is used in the form of art since the movement of Pictorialism, an art movement that flowered between 1880 and 1920.<sup>iv</sup> Photography covers many techniques: black and white, sepia, color, digital and analogue are some examples. The technique of color photography finds its origin in 1861 when J. C. Maxwell made a photo of a ribbon (Figure 1) with red, yellow and blue filters.<sup>v</sup> In the early 20th century, different methods of color photography were developed. The brothers Lumière developed the first way of developing color photography commercially in 1907.<sup>vi</sup>



Figure 1: The first known color photograph, made by J. C. Maxwell in 1861.

Fine art photography, or photographic art, is a form of art where photographs are used as the medium and the photographer is considered as the artist. Photographs can be combined with other media, like canvas, drawings, paintings and objects. These combined words are called photoworks. Over the last decades, many artists made photoworks and they have thus become a vital part of our cultural heritage. In Figure 2, an example of a photowork is shown. This work, *Arranged* (1996, Jim Hodges) is a combination of a photograph and a sculpture.<sup>vii</sup> Another artist who used combinations of photography and other materials is the Dutch artist Ger van Elk (1941-2014). He made sculptures, short movies, paintings and also photoworks.



Figure 2: *Arranged*, (1996, Jim Hodges)

Photos can show several signs of aging like discoloration and brittleness of the photo. An example can be found in *Russian Diplomacy* (1972, Van Elk, Stedelijk Museum Amsterdam), shown in Figure 3. The photo used is a black and white image printed on chromogenic photographic paper. As seen in Figure 3 and in the close-up of the photowork Figure 4, a color shift is visible from black towards purple.



Figure 3: *Russian Diplomacy* (1972, Van Elk)





Figure 4: Close up of *Russian Diplomacy*.

*Russian Diplomacy* consists of a chromogenic photograph on resin-coated paper. Matte paint is added on the photograph, in the colors black, grey, yellow and white. The photowork is covered with PMMA and framed with a wooden frame. The artwork is adhered on a secondary support of PMMA. The work shows several signs of aging, one of these in the form of discoloration of the photo but also paint loss and stains are observed. Other photographs made in the same period show also color changes. In *The symmetry of diplomacy* (1974, Ger van Elk, Stedelijk Museum Amsterdam) the colors in the photograph seem shifted towards red and purple accents (Figure 5). The white parts of the photograph, which do not contain photographic dyes, are not shifted in color.<sup>viii</sup>



Figure 5: *The symmetry of Diplomacy I* (1971, Van Elk) with a close up of the right corner.

Although photography has been widely used for decades and fading of colors is reported extensively, the mechanistic reasons behind the change or fading of colors in photographs are still not been completely explained.<sup>ix</sup> In some of the photographs where several materials are combined (like *Russian Diplomacy*), additional degradation may occur due to interaction between these materials. In order to store them properly, it is necessary to investigate what influences the materials can have on each other.

Research has already been performed with *Russian Diplomacy*.<sup>viii</sup> This work was chosen as a research subject due to the clear shift of color. The physical properties and signs of aging of the artwork were recorded. When the glass was removed, a strong acetic acid odor was noticed. This is an indication for the presence of acetic acid in the air between the photo work and the protective material. Acetic acid can be a product of the reaction between water and the silicon glue, which is likely to be used to add the frame on top of the artwork. For these reasons, we set out to investigate the influence of acid on dyes used in photographs.

When photographs become significantly discolored they may no longer be considered suitable for expositions. Proper conservation can prevent or delay degradation of photographic artworks, which is of importance both financially and culturally. In order to elucidate the discoloration of photographs, in this thesis research concerning the mechanistic background of the discoloration is performed. This thesis is a part of the research funded by the NWO (Nederlandse Organisatie voor Wetenschappelijk Onderzoek).<sup>x</sup>

## 2 Theoretical background

### 2.1 Color photography: The color formation process

A color photograph is an image formed by a chemical reaction initiated by the presence of light. Photographic paper consists of a layer of paper, on which several layers of gelatin and protecting layers are added. A cross section is shown in Figure 6. Gelatin is made of collagen, a connective tissue protein that is present in animals in skin and bones. Collagen is partly hydrolyzed and the product is gelatin. Gelatin in photographs is derived from cow and pig skin and bones. It is applied as a thin layer (about  $1\ \mu\text{M}$ )<sup>xlii</sup> on the photographic paper. In the gelatin, dye precursors (coupling agents) are present. This is done in three layers, filters are present in order to make the three layers sensitive for different wavelengths. A protective gelatin layer is added on top.



Figure 6: Cross section of photographic paper.

There are three methods of developing a color photograph: the dye-coupled process, the instant photography process and the dye bleach process. Because the dye-coupled process is the most common used (including the selected photographic artwork *Russian Diplomacy*), this method will be the only one explained in this thesis.<sup>xi</sup> In Figure 7 and Figure 8 a schematic view is given of the two parts of the process: the formation of the negative and positive image.<sup>xi</sup> The negative image is used to make a positive image on photographic paper. Both processes, in chromogenic photography, use the formation of an imine bond between a coupling agent and an activated developing agent to form dyes. In the first step, light reflected from an object falls on the photographic paper. Silver halide, which is dispersed in the gelatin layers, absorbs the light which is passed through the filters (E and G in Figure 7 and D and F in Figure 8). The silver halide sites that are activated by light are reduced when a developing solution diffuses into the emulsion. The reduction takes place between a developing agent (*p*-phenylenediamine) and the activated silver halide. This results in silver metal and a quinonediaimine, which can react with coupling agents to form color dyes. Bleaching and fixing of the photographic paper results in the removal of silver metal and silver halide after development.

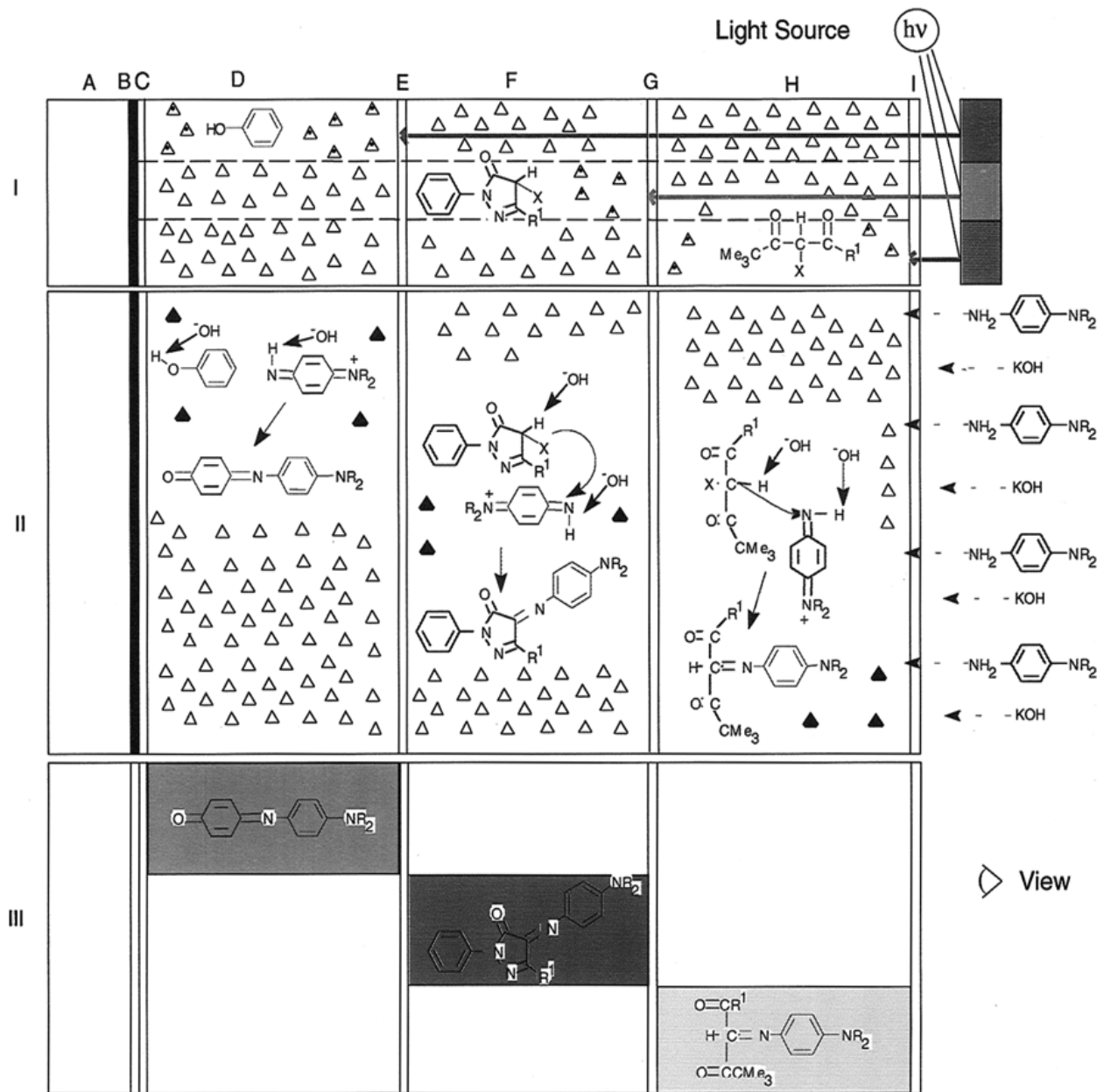


Figure 7: Processing of a color negative film by the dye-coupled process.

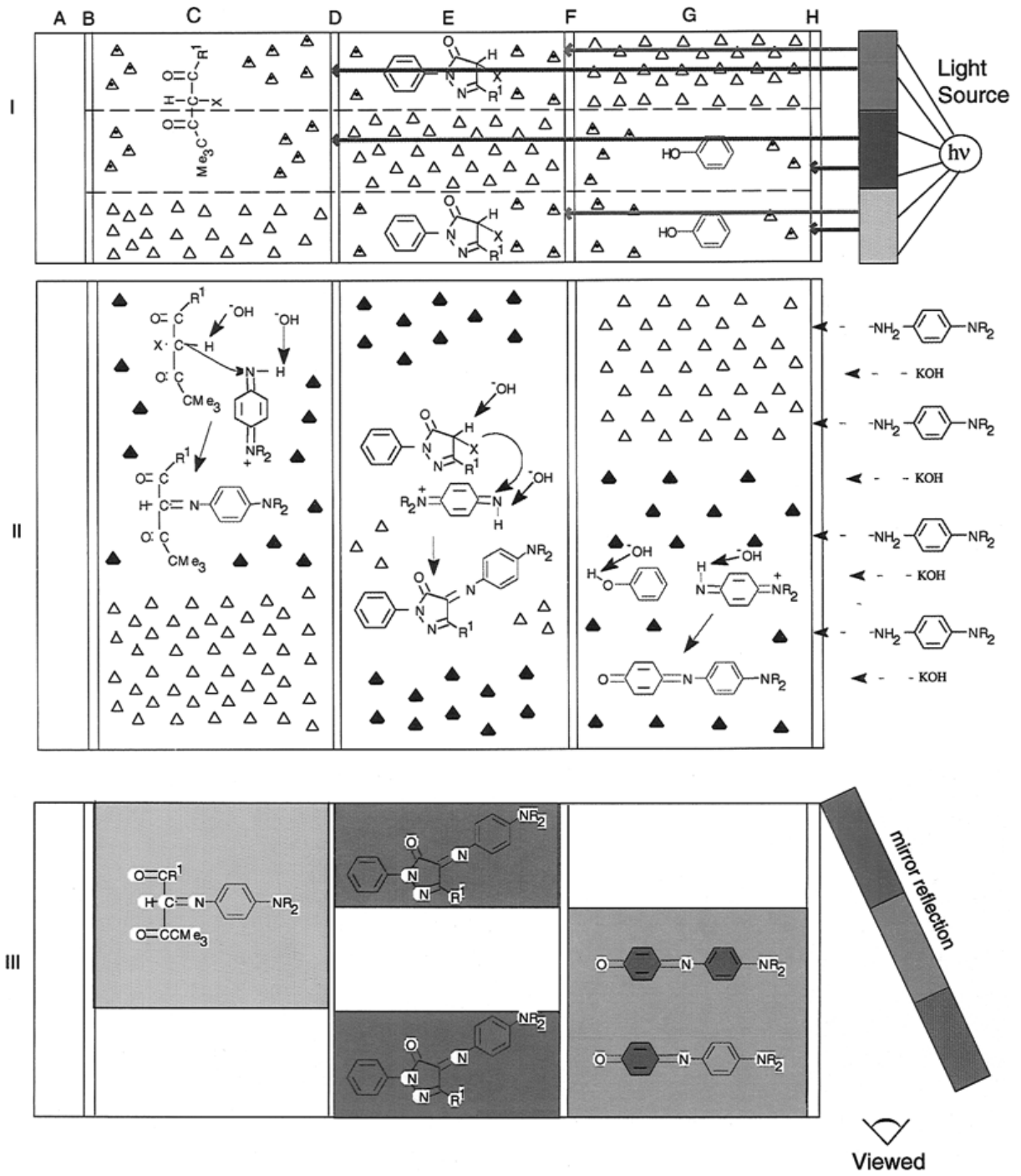


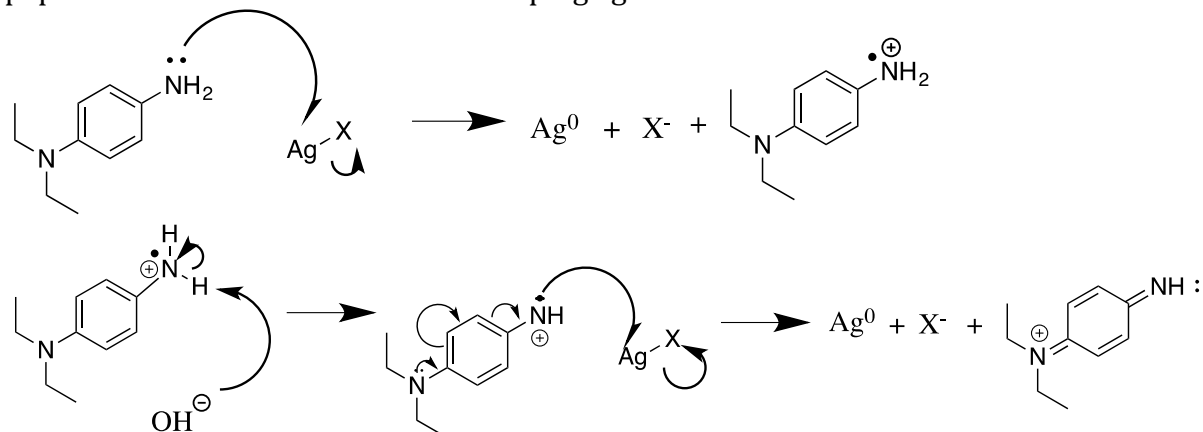
Figure 8: Processing of a color positive photographic image.



### 2.1.1 Initiation of the color formation process

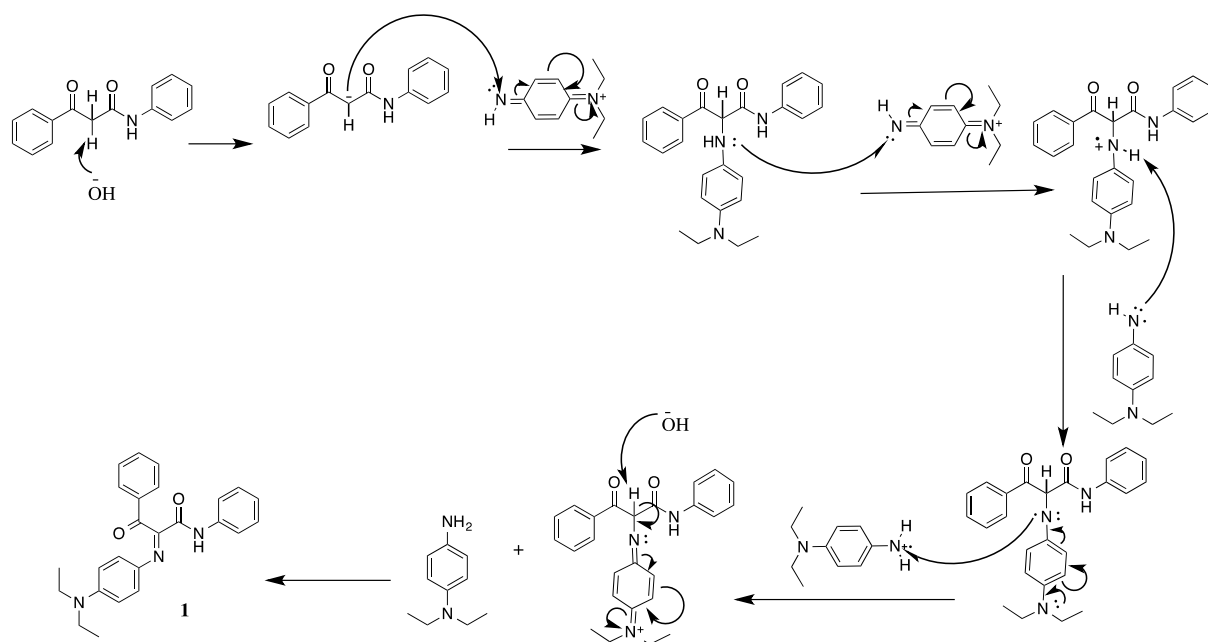
The attack of the diamine can only take place in so-called latent image sites. These are generated by the incoming electromagnetic waves (light), which create an electron-hole pair in AgX-clusters. A developing solution containing a *p*-phenylenediamine is diffused in the gelatin and can react with the activated silver halide.

The activated developing agent, a quinonediimine, is a product of several chemical reactions (Scheme 1) that take place in the gelatin emulsion of photographic film or paper. The result is an oxidized developing agent and a reduced silver atom.



**Scheme 1: Activation of the developing agent by oxidation with AgX.**

The activated developing agent can react with coupling agents that are present in the gelatin of the photographic film or paper. The mechanism of the reaction between the yellow dye coupler and the activated developing agent is given in Scheme 2. This mechanism is also representative for the cyan and magenta dye formation. The chemical reaction that results in an imine bond between a coupling agent and a dye coupler is initiated by the deprotonation of the dye coupler by a base (in this case NaOH). The carbanion of the dye coupler attacks the primary amine of the coupling agent. This leads to a secondary amine due to the formed bond between the dye coupler and the coupling agent. The secondary amine is again deprotonated by a base. A lone pair of the nitrogen atom will form a double bond between the amine and the carbon and in this process the carbon will lose the leaving group X. When X=H, the secondary amine will attack a second quinone molecule and this reaction will also result in the dye. At the end of the reaction, an imine bond is formed between the coupling and developing agent.<sup>xi</sup>



**Scheme 2: Dye formation by imine bond formation between coupling agent and activated developing agent.**

After coupling, the three dyes have the following general structure as shown in Figure 9.<sup>xii</sup> The coupling agent forms the mutual part of the dyes.

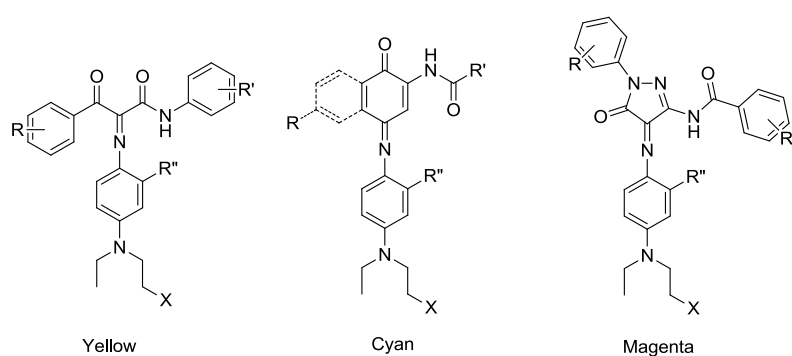


**Figure 9: General structures of the three dyes used in photographs, with R and X can be side chains.**

### 2.1.2 Further steps in the development procedure

After the formation of the color dyes, the remaining  $\text{AgX}$  and silver metal  $\text{Ag}^0$  are removed by bleaching and fixing the photographic film or paper. The bleaching process will convert the residual imaged silver to ionic silver. This is done by an oxidizing agent, typically a transition metal complex. The silver ions are removed by a fixing solution, commonly containing a thiosulfate (for example ammonium thiosulfate).

A negative image is made first and is then used to make the positive photographic image. The negative image is projected and enlarged on photographic paper, where a positive image is formed by the same process of the formation of the negative image (developing, bleaching and fixing). An overview of reactions that take place during the complete process of photography, from making a negative image on photographic film to fixing the positive image on photographic paper, is given in Table 1. Both the photographic and chemical terminology is given.

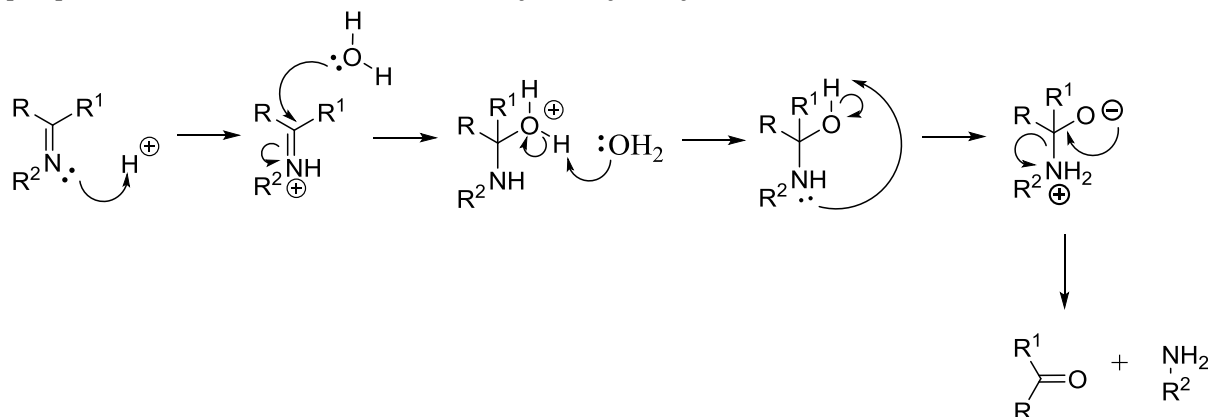
Reaction	Photographic name	Chemical name
$2\text{Ag}^+ + \text{D} \rightarrow 2\text{Ag}^0 + \text{D}_{\text{ox}}^+ + \text{H}^+$	Development	Reduction
$\text{D}_{\text{ox}}^+ + \text{C}^- \rightarrow \text{D-C}$	Color coupling	Nucleophilic attack
$\text{d-C} + \text{D}_{\text{ox}}^+ \rightarrow \text{Dye} + \text{D} + \text{H}^+$	4 eq. Dye formation	Oxidation
$\text{D-C} \rightarrow \text{Dye} + \text{HY}$	2 eq. Dye formation	Elimination of Electrophilic LG
$\text{Ag}^0 + \text{B}^{(n+1)} \rightarrow \text{Ag}^+ + \text{B}^{n+}$	Bleaching	Oxidation
$\text{AgX} + n\text{L}^{m+} \rightarrow \text{AgL}_n^{(m+1)-} + \text{X}^-$	Fixing	Complexation

**Table 1: Overview of reactions present in the development process, where D represents the developing agent, B represent the bleach solution, C is the coupler, Y is the leaving group of the coupler and L is the fixer.**

### 2.1.3 Dye molecules: Schiff bases and their reactivity

One of the main functional groups of the dyes, a Schiff base, consist of the double bond formed between the amine of the dye coupler and the carbanion of the activated developing agent as shown in Scheme 2. This functional group is present in all three dyes. The group contains of a lone pair on the nitrogen that can act as a base. Due to its reactivity this functional group is studied in this thesis. The Schiff base is an essential link in the conjugated system and therefore making the dyes applicable for absorbing light of the required wavelengths.<sup>xi</sup> A Schiff base is generally formed via a condensation reaction between a carbonyl and an amine moiety. The optimal pH conditions are mildly acidic.<sup>xiii, xiv</sup> In the case of dye formation, the Schiff base formation happens through an oxidative coupling as described in section 2.1.1.<sup>xi</sup>

The conditions in which photographs are stored, like relative humidity and temperature can have an influence on the reactions that can take place considering the dye molecules and can eventually result in a hydrolysis of the imine bond. Hydrolysis of the Schiff base will result in an amine and a carbonyl moiety as this is the reversed reaction of the Schiff base formation.<sup>xv</sup> This hydrolysis can be catalyzed by acidic or alkaline conditions. A proposed mechanism of the acid catalyzed hydrolysis is shown in Scheme 3.



**Scheme 3: Reaction mechanism of the hydrolysis of a Schiff base.**

Due to their sensitivity to both acidic and alkaline environments, hydrolysis of Schiff bases in dyes is mentioned in literature as one of the main reasons for dye degradation and therefore discoloration of photographs.<sup>xi, xvii</sup> In literature Schiff base hydrolysis catalyzed by sulfuric acid is mentioned.<sup>xvi, xvii</sup> However, the critical triketone product has not been conclusively observed so far, possibly due to its suspected instability.<sup>xviii</sup> Therefore, the Schiff base hydrolysis theory will be applied on the three dyes and the reaction products will be analyzed in order to determine if this reaction could cause the observed discoloration.



## 2.2 Storage conditions of photoart

The main factors that may have an influence on the aging process of a photograph are relative humidity, temperature and air pollutants.<sup>xxiii</sup> A focus will be on the effects of these factors on the color of a photograph and dye degradation, the degradation of structure of the gelatin layer (brittleness, mold etcetera) is not studied in this thesis. Another factor in the aging process of art is the microclimate that is created concerning the artwork. For example, the boxes in which art is stored or a glass plate that is added on top of an artwork can result in the concentration of pollutants and speed up the degradation processes. In the case of *Russian Diplomacy* a glass plate was added on top of the photowork, which created a microclimate where gas can be concentrated (in this case acetic acid).

### 2.2.1 Relative Humidity

The maximum amount of water vapor that the atmosphere can hold is temperature dependent. The relative humidity (RH) is a percentage of this maximum amount of water vapor. In Figure 10, the temperature dependence of the amount of water vapor (in mm Hg) of 4 RH values is shown.<sup>xix</sup>

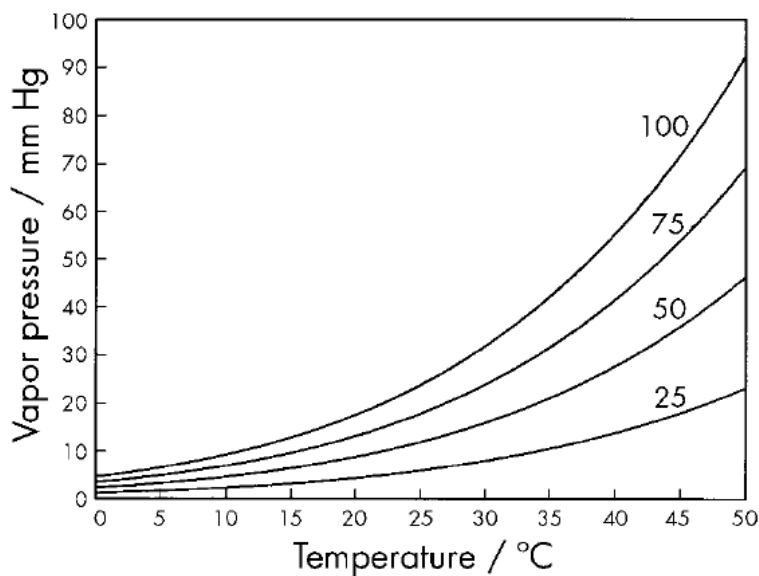


Figure 10: Temperature dependence of the relative humidity for 4 set percentages.

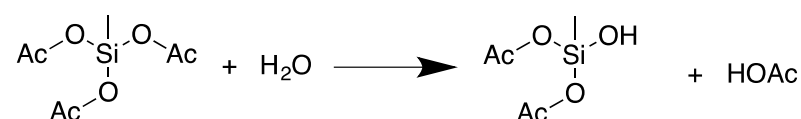
Humidity can have a large influence on the life span of photographs. Moisture can be absorbed by the gelatin of the photograph and causing the image and colors to distort.<sup>xxiii</sup> When the air is too dry (a RH lower than 20%) a photograph can become brittle and the gelatin can contract, resulting in a curling print. For photographs, a RH between 30 and 40% is advised as extended-term storage conditions (archival storage), when the artworks wanted to be kept as long as possible. At a temperature of 20°C and a RH of 40% gelatin can contain about 10 % moisture content.<sup>xxi</sup> The yellow dye is known as more sensitive for a high RH than the other two dyes.<sup>xxii</sup>

### 2.2.2 Temperature

Storage of photographs at a high temperature will increase the reaction speed and therefore increase the degradation process of the dyes compared with lower temperatures. A lower temperature is therefore recommended. For archival storage conditions, a maximum temperature of 2 °C is advised. When the temperature is too low, the humidity will also become too low and this can damage the photographs.<sup>xxiii</sup>

### 2.2.3 Acetic acid

Acetic acid is probably one of the main sources of acid and therefore a possible compound to react with the dyes.<sup>xxiii</sup> It not only affects the dyes but also the material of the photograph. It is known as the pollutant that is the most abundant in archives and as one of the most formed volatile organic compounds formed at the aging process of paper.<sup>xx, xxiv</sup> Acetic acid can also be formed via the hydrolysis of silicon glue that is commonly used to paste a photograph to the back support. In Scheme the formation of acetic acid is given.<sup>xxv</sup>



Scheme 4: Formation of acetic acid by hydrolysis of silicon glue.

### 2.2.4 Other pollutants

In archives other pollutants apart from acetic acid can be present. These can damage the stored photographs in several ways. In Table 2 an overview of possible pollutants in archives are listed with their effects on photographs over time.<sup>xxvi</sup> As listed to Table 2, SO<sub>x</sub>, NO<sub>x</sub>, oxidizing gases (like O<sub>3</sub> and H<sub>2</sub>O<sub>2</sub>) and carbonyl compounds can be present.<sup>xxiii</sup> Although several pollutants can be present in the atmosphere of the stored photoart, our initial research will focus on the reaction between acetic acid and photographic dyes. Acetic acid is the most likely to have a large influence on the color of the artworks and several reasons are mentioned previously for the assumption of the presence of acetic acid in the photographs.

Pollutant	Source	Possible effects on photographs
Sulfuric compounds	Low quality paper enclosures Outdoor (combustion and natural sources) Adhesives Bioeffluents Carpets	Fading of silver images Brown/yellow discoloration of silver images Fading of color images Brittleness of paper and emulsion
NO <sub>x</sub>	Cellulose nitrate film Collodion photographs Outdoor sources	Fading of silver images Fading of color images Brittleness of paper and emulsion Brittleness of nitrate film base
Other oxidizing gases (like O <sub>3</sub> and H <sub>2</sub> O <sub>2</sub> )	Outdoor (traffic and natural sources) Fresh paint Office machines Low quality paper enclosures	Fading of silver images Fading of color images Brittleness of paper and emulsion
Carbonyls (acids, aldehydes)	Cellulose acetate film Wood and wood-boards Various building materials	Brittleness and shrinkage of acetate film base Brittleness of paper and emulsion

Table 2: Overview of pollutants in archives.

## 2.3 Colors and conjugated systems

In a photograph, colors are formed via the subtractive color model. This model describes that light of certain wavelengths is absorbed by dyes and light that is not absorbed is observed by the human eye. This is illustrated in Figure 11. In photographs three general types of dyes are used: yellow, magenta and cyan dyes. These dyes have general structures as shown in Figure 9.<sup>xii</sup> Magenta dye absorbs light around 550 nm, cyan dye around 650 and yellow dye around 450 nm (Figure 12).<sup>xi</sup>

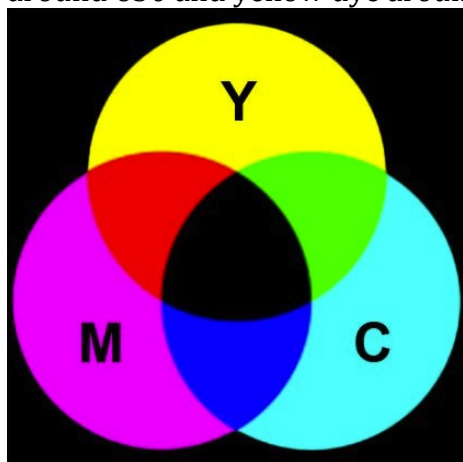


Figure 11: The YMCB (yellow, magenta, cyan and black) subtractive color model.

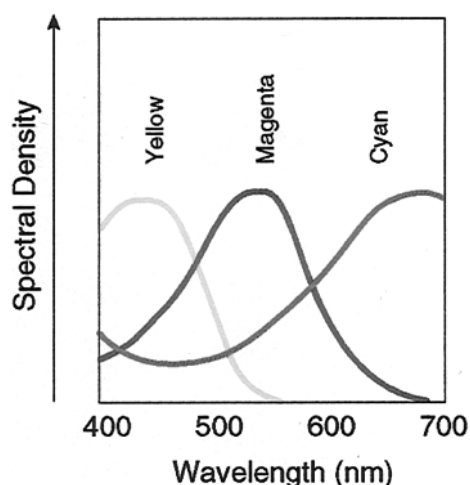


Figure 12: Absorption spectra of the three generalized dyes in photographs.

### 2.3.1 Conjugated systems

Colors in photographs are the result of absorption of light by the conjugated system present in the dyes. A conjugated system in organic chemistry consists of alternating double bonds and single bonds. The double bonds ( $\pi$ -bonds) are formed due to overlap of filled p-orbitals. Single bonds ( $\sigma$ -bonds) are formed due to overlap in sp-hybridized orbitals. When double and single bonds alternate, the molecular orbital formed is lowered in energy because of the overlap of all the p-orbitals (Figure 13).<sup>xxvii</sup>

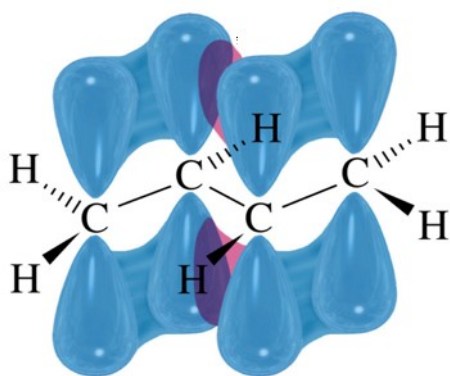


Figure 13: Butadiene, the  $\pi$ -bonds are represented in blue. Overlap between these bonds is shown in red.

Electron density of the  $\pi$ -bonds is delocalized over all the p-orbitals in the conjugated system. A typical example is an aromatic system such as benzene, where the electron density of the p-orbitals is delocalized over the ring system (Figure 14).<sup>xxviii</sup>

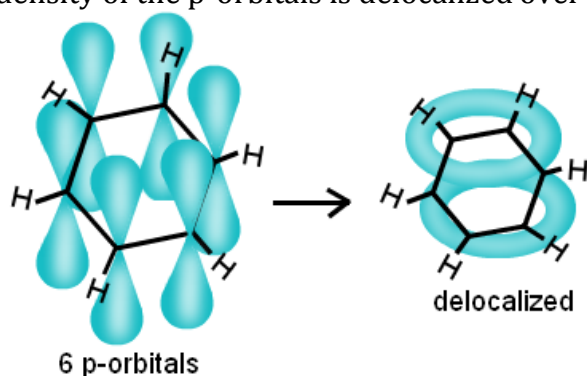


Figure 14: Benzene. Overlap between the p-orbitals leads to delocalization of electron density.

### 2.3.2 HOMOs and LUMOs

The energy of conjugated systems is quantized in discrete energy levels. The highest occupied molecular orbital (HOMO) and lowest unoccupied molecular orbital (LUMO) are well defined. The conjugated system can accept a photon of a certain wavelength (proportional to the energy difference between the HOMO and LUMO), which will excite an electron to the LUMO (Figure 15). This is known as a  $\pi \rightarrow \pi^*$  transition. The electron can relax back to the HOMO. The length of the conjugated system has an influence on the wavelength of the photon that can be accepted. A longer conjugated system can absorb a photon with lower energy because the energy gap between the HOMO and LUMO is smaller.

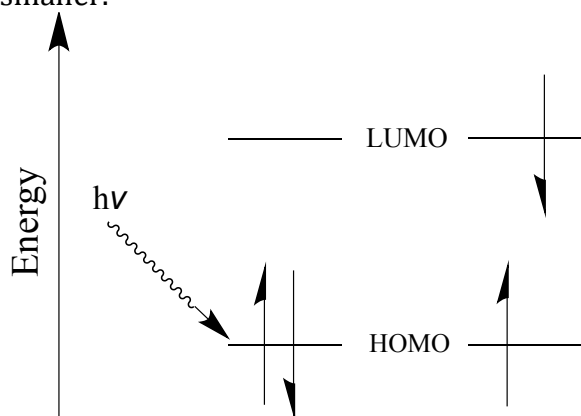


Figure 15: An electron from the HOMO in the ground state is excited by light ( $h\nu$ ) to the LUMO in the excited state.

DFT approximations of the HOMO and LUMO of the yellow dye are visualized in Figure 16.<sup>xxix</sup> These show electron density in the molecular orbitals. In the HOMO the electron density is localized at the phenylenediamine moiety and a lone pair is present at the nitrogen of the Schiff base, in the LUMO the electron density is mostly localized at the imine and keto moiety of the molecule.

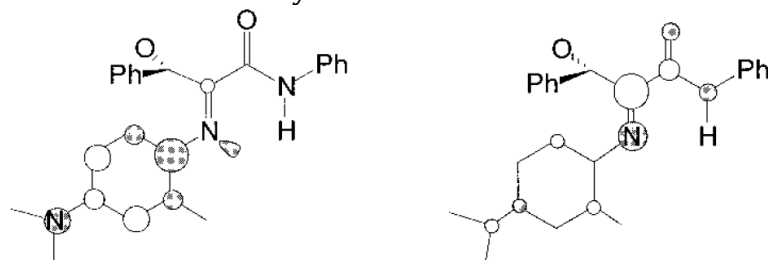


Figure 16: HOMO (left) and LUMO (right) of the yellow dye.

### 2.3.3 2D and 3D structure of the dyes

The dye molecules consist of several bulky groups like phenyl rings. These can result in a non-flat structure, which can have an important influence on the conjugation of the system. By density functional theory (DFT) calculations, predictions can be made about this three-dimensional structure of the dye molecules can be done. In Figure 17, the two geometries of the yellow dye calculated lowest in energy are given. The azomethine double bond results in two isomers, both are calculated. The left geometry is more stable than the right geometry. However, the overlap of the p-orbitals in both geometries is not optimal due to angle strain between the amine and keto moieties.

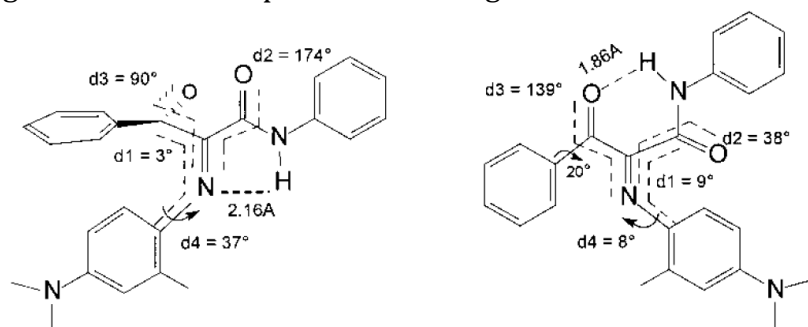


Figure 17: 3D structures of the yellow dye ground states calculated with DFT.

## 2.4 Solvatochromic effects

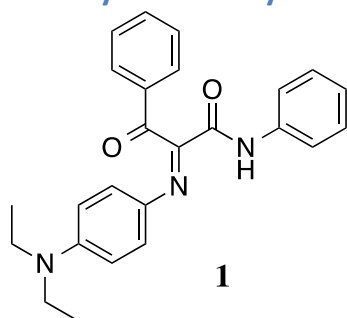
The solvatochromic effect describes the stabilization or destabilization of the HOMO and LUMO by solvents. In the ground state solvent molecules can coordinate around a molecule in such a way that the dipoles present in the compound are stabilized by the solvent. When the compound is excited, a change of the electron distribution can take place. This happens in a shorter time scale than the solvent molecules take to rearrange around the new electron distribution. The solvent molecules then rearrange around the compound in such a way that the new dipoles or charges are stabilized.

In the case of the photographic dyes polar solvents will lower the energy gap between the HOMO and the LUMO due to their ability to arrange around the excited molecules. This is called a bathochromic shift. Apolar solvents cannot stabilize the charge transfer and therefore enlarge the energy gap between the HOMO and LUMO and will result in absorption of photons with a higher energy so a lower wavelength.<sup>xxx, xxxi</sup>

### 3 Experimental

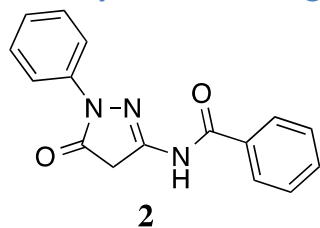
The compounds synthesized were analyzed at 298 K with  $^1\text{H}$  NMR on a 400 MHz Varian spectrometer and  $^{13}\text{C}$  NMR on a 100 MHz Varian spectrometer. UV-VIS spectroscopic measurements were done with either a PerkinElmer Lambda 950 or PerkinElmer Lambda 35. CV measurements were done with the Ivium vertex potentiostat. Solvents were used as received unless mentioned. NMR spectra can be found in appendix B. DFT calculations were done with LISA on SURFsara.

#### 3.1 Synthesis of yellow dye 1



Synthesis was based on literature procedure.<sup>xxxii</sup> A solution of 603 mg NaOH (15 mmol) in 30 mL H<sub>2</sub>O was added to 504 mg 2-benzoylacetanilide (2.11 mmol) and 0.66 mL *N,N*-Diethyl-*p*-phenylenediamine (3.97 mmol). A solution of 224 mg (NH<sub>4</sub>)<sub>2</sub>S<sub>2</sub>O<sub>8</sub> (1.07 mmol) in 20 mL H<sub>2</sub>O was added dropwise to the reaction mixture. Dye formation was visible immediately; the reaction mixture had an opaque orange color. The solution was stirred for 80 minutes at room temperature. The dye was subsequently extracted with DCM. The organic layer was then dried over MgSO<sub>4</sub> and filtered. All solvents were evaporated. Recrystallization from boiling EtOH was performed and the solution was cooled down and put in a freezer (-30°C) over the weekend. The solution was filtered and the residue was washed over DCM. An extraction was done with DCM and water. The organic layer was dried over MgSO<sub>4</sub> and all solvents were evaporated *in vacuo*. The obtained solid was washed over hexane. The product was isolated as a yellow powder in a yield of 12.2% (103 mg, 2.58 mmol).  $^1\text{H}$  NMR (CDCl<sub>3</sub>):  $\delta$  9.43 (s, 1H, NH) 7.89 (dd, 2H, Ar-H,  $J^3 = 8.4$  Hz,  $J^4 = 1.4$  Hz) 7.70 (dd, 2H, Ar-H,  $J^3 = 8.5$  Hz,  $J^4 = 0.84$  Hz) 7.58 (t, 1H, Ar-H,  $J^3 = 7.5$  Hz) 7.43 (t, 2H, Ar-H,  $J^3 = 7.7$  Hz) 7.35 (t, 2H, Ar-H,  $J^3 = 7.8$  Hz) 7.17 (d, 2H, Ar-H,  $J^3 = 9.2$  Hz) 7.12 (t, 1H, Ar-H,  $J^3 = 7.3$  Hz) 6.49 (d, 2H, Ar-H,  $J^3 = 9.2$  Hz) 3.32 (q, 4H, NCH<sub>2</sub>CH<sub>3</sub>,  $J^3 = 7.0$  Hz) 1.12 (t, 6H, NCH<sub>2</sub>CH<sub>3</sub>,  $J^3 = 7.24$  Hz).  $^{13}\text{C}$  NMR (CDCl<sub>3</sub>):  $\delta$  198.5, 161.2, 151.0, 148.5, 137.5, 134.6, 134.3, 132.1, 129.1 (2x), 128.9, 127.3, 124.3, 119.4, 111.3, 44.5, 12.5. UV-VIS in acetone/H<sub>2</sub>O (1:1 v/v):  $\epsilon = 2.26 \cdot 10^4$ ,  $\lambda_{\text{max}} = 438$  nm.

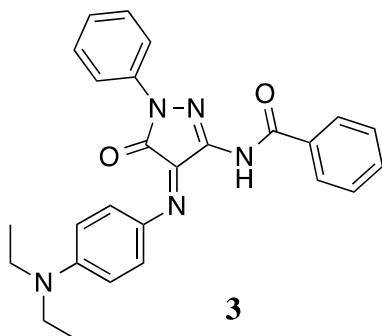
### 3.2 Synthesis of magenta dye precursor 2



Synthesis was based on literature procedure.<sup>xxxiii</sup> Under N<sub>2</sub> atmosphere, 377 mg benzoic acid (3.09 mmol) was dissolved in 4 mL SOCl<sub>2</sub>. The remainder of the SOCl<sub>2</sub> was distilled and after cooling to room temperature quenched with ethanol. To the benzoic chloride, 3 mL dry dioxane and 556 mg 3-amino-1-phenyl-2-pyrazolin-5-one (3.17 mmol) were added. The reaction mixture was stirred overnight at 60 °C. The next day, the mixture was cooled down, quenched with water and filtered over Celite. The filtrate was extracted with MeOH and DCM. The organic layers were combined and all solvents were evaporated *in vacuo*. The product was isolated as a brown powder in a yield of 68% (584 mg, 2.092 mmol).

<sup>1</sup>H NMR (CDCl<sub>3</sub>): δ 8.66 (s, 1H, NH) 7.89 (d, 2H, Ar-H, J<sup>3</sup> = 8.5 Hz) 7.84 (d, 2H, Ar-H, J<sup>3</sup> = 8.5 Hz) 7.63 (t, 1H, Ar-H, J<sup>3</sup> = 7.7 Hz) 7.53 (t, 2H, Ar-H, J<sup>3</sup> = 7.8 Hz) 7.39 (t, 2H, Ar-H, J<sup>3</sup> = 8.0 Hz) 7.18 (t, 1H, Ar-H, J<sup>3</sup> = 7.3 Hz) 4.21 (s, 2H, COCH<sub>2</sub>CNNH).

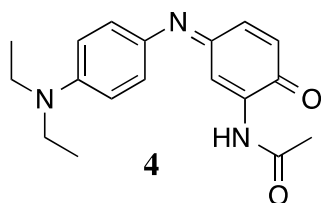
### 3.3 Synthesis of magenta dye 3



Synthesis was based on literature procedure.<sup>xxxiv</sup> In 30 mL EtOH, 30 mL EtOAc and 6 mL 30% NH<sub>4</sub>OH in 36 mL H<sub>2</sub>O 206 mg pyrazolone 2 (0.738 mmol) from the first step was added. In 15 mL H<sub>2</sub>O 677 mg AgNO<sub>3</sub> (3.99 mmol) was dissolved. This mixture was added dropwise to the pyrazolone mixture and the reaction was stirred for 45 minutes. Dye formation was visible immediately. The mixture was filtrated over Celite. The filtrate was washed with warm EtOAc and subsequently extracted with DCM. The solution was dried with MgSO<sub>4</sub> and solvents were removed *in vacuo*. The product was obtained as a purple solid in a yield of 65% (192 mg, 0.46 mmol). <sup>1</sup>H NMR (CDCl<sub>3</sub>): δ 8.87 (s, 1H, NH) 8.42 (d, 2H, Ar-H, J<sup>3</sup> = 8.5 Hz) 8.09 (d, 2H, Ar-H, J<sup>3</sup> = 8.7 Hz) 7.99 (d, 2H, Ar-H, J<sup>3</sup> = 7.7 Hz) 7.61 (q, 1H, Ar-H, J<sup>3</sup> = 4.1 Hz) 7.55 (t, 2H, Ar-H, J<sup>3</sup> = 7.1 Hz) 7.42 (t, 2H, Ar-H, J<sup>3</sup> = 7.2 Hz) 7.18 (t, 1H, Ar-H, J<sup>3</sup> = 7.2 Hz) 6.80 (d, 2H, Ar-H, J<sup>3</sup> = 8.4) 3.53 (q, 4H, NCH<sub>2</sub>CH<sub>3</sub>, J<sup>3</sup> = 6.9 Hz) 1.29 (t, 6H, NCH<sub>2</sub>CH<sub>3</sub>, J<sup>3</sup> = 7.17 Hz). <sup>13</sup>C NMR (CDCl<sub>3</sub>): δ 163.4, 152.7, 152.2, 144.0, 138.8, 135.1, 130.0, 133.8, 133.5, 132.5, 129.0, 128.6, 128.0, 124.7, 119.1, 111.5, 45.4, 12.8. UV-VIS in acetone/H<sub>2</sub>O (1:1 v/v): ε = 5.06\*10<sup>4</sup>, λ<sub>max</sub> = 546 nm.



### 3.4 Synthesis of cyan dye 4

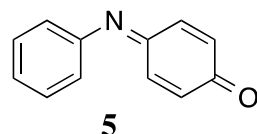


Synthesis was based on literature procedure.<sup>xxxv</sup> In 20 mL H<sub>2</sub>O 1.46 g NaCl (25 mmol) and 3.73 g AgNO<sub>3</sub> (22 mmol) were added. A solution containing 2.05 g Na<sub>2</sub>CO<sub>3</sub> (19 mmol) in 10 mL H<sub>2</sub>O was added. In 20 mL EtOH 385 mg 2-acetamidophenol (2.8 mmol) was dissolved and added to the reaction mixture. In an addition funnel 374 mg *N,N*-diethyl-*p*-phenylenediamine (2.3 mmol) was dissolved in 12 mL 0.25 M HCl. This solution was added dropwise to the reaction mixture, which was stirred during the reaction. The reaction mixture turned blue immediately. The dye was extracted with EtOAc and DCM and filtered over Celite. The organic layer was dried with MgSO<sub>4</sub> and the solvents were evaporated *in vacuo*. The crude product was purified with silica chromatography, using a mixture of DCM and 1% TEA as the eluent. A second column was performed with EtOAc. The product was isolated as a deep blue solid in a yield of 83% (591 mg, 1.97 mmol)

<sup>1</sup>H NMR (C<sub>6</sub>D<sub>6</sub>): δ 8.87 (d, 1H, Ar-*H*, J<sup>4</sup> = 2.6 Hz) 7.90 (s, 1H, NH) 7.43 (td, 2H, Ar-*H*, J<sup>3</sup> = 8.9 Hz, J<sup>4</sup> = 1.9 Hz) 7.24 (dd, 2H, Ar-*H*, J<sup>3</sup> = 10.0 Hz, J<sup>4</sup> = 1.5 Hz) 6.48 (d, 1H, Ar-*H*, J<sup>3</sup> = 9.8 Hz) 6.36 (td, 2H, Ar-*H*, J<sup>3</sup> = 9.2 Hz, J<sup>4</sup> = 2.2 Hz) 2.71 (q, 4H, NCH<sub>2</sub>CH<sub>3</sub>, J<sup>3</sup> = 7.0 Hz) 1.31 (s, 3H COCH<sub>3</sub>) 0.68 (t, 6H, NCH<sub>2</sub>CH<sub>3</sub>, J<sup>3</sup> = 7.0 Hz).

UV-VIS in acetone/H<sub>2</sub>O (1:1 v/v): ε = 3.2\*10<sup>4</sup>, λ<sub>max</sub> = 651 nm.

### 3.5 Synthesis of aminoquinone 5



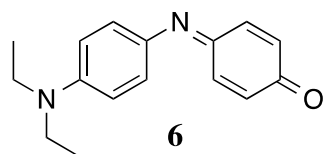
Synthesis was based on literature procedure.<sup>xxxvi</sup> In 16 mL H<sub>2</sub>O 226 mg 4-hydroxydiphenylamine (1.23 mmol) and 844 mg lead (IV)oxide (3.53 mmol) were added. The mixture was stirred for 80 minutes at room temperature. The mixture was filtered and the residue was extracted with DCM. To this mixture 734 mg lead(IV)oxide (3.07 mmol) was added and this was stirred at room temperature for 30 minutes. The mixture was filtrated over Celite, the residue was extracted with DCM. Extraction of the mixture was performed with DCM and water for 4 times until the water layer was white. The organic layer was dried with MgSO<sub>4</sub> and solvents were evaporated *in vacuo*. The product was obtained as a grey powder in a yield of 24.7% (55 mg, 0.302 mmol)

<sup>1</sup>H NMR (CDCl<sub>3</sub>): δ 7.41 (t, 2H, Ar-*H*, J<sup>3</sup> = 7.8 Hz) 7.30 (dd, 1H, Ar-*H*, J<sup>3</sup> = 9.7 Hz, J<sup>4</sup> = 1.96 Hz) 7.24 (t, 1H, Ar-*H*, J<sup>3</sup> = 7.11 Hz) 7.08 (dd, 1H, Ar-*H*, J<sup>3</sup> = 11.3 Hz, J<sup>4</sup> = 2.1 Hz) 6.89 (d, 2H, Ar-*H*, J<sup>3</sup> = 7.31 Hz) 6.69 (dd, 1H, Ar-*H*, J<sup>3</sup> = 10.1 Hz, J<sup>4</sup> = 1.5 Hz) 6.59 (dd, 1H, Ar-*H*, J<sup>3</sup> = 10.4 Hz, J<sup>4</sup> = 1.4 Hz). <sup>13</sup>C NMR (CDCl<sub>3</sub>): δ 187.6, 157.4, 149.4, 141.9, 133.5, 132.9, 129.1, 128.3, 126.2, 120.7.

UV-VIS in acetone/H<sub>2</sub>O (1:1 v/v): ε = 2.84\*10<sup>3</sup>, λ<sub>max</sub> = 451 nm.

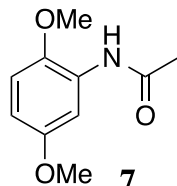


### 3.6 Synthesis of aminoquinone 6



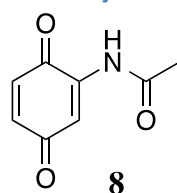
A solution of 1.5 g NaCl (26 mmol) and 4.3 g AgNO<sub>3</sub> (26 mmol) in 20 mL H<sub>2</sub>O was made. To this mixture 2.5 g Na<sub>2</sub>CO<sub>3</sub> (24 mmol) dissolved in 10 mL H<sub>2</sub>O was added. In 20 mL EtOH 261 mg phenol (2.78 mmol) was dissolved and added to the reaction mixture. In an addition funnel 40 mL EtOH, 3 mL 1 M HCl and 0.4 mL *N,N*-diethyl-*p*-phenylenediamine (2.44 mmol) were mixed and this was added dropwise to the reaction mixture. A color change was visible immediately, from grey to blue. After 2 h the mixture was filtered and extracted in DCM with brine, NaOH (4 M in H<sub>2</sub>O) and H<sub>2</sub>O. MgSO<sub>4</sub> was used to remove the water and the remaining solvents were evaporated *in vacuo*. The product was obtained as a blue solid in a yield of 61% (378 mg, 1.64 mmol). <sup>1</sup>H NMR (CDCl<sub>3</sub>): δ 7.35 (dd, 2H, Ar-*H*), 7.33 (dd, 2H, Ar-*H*, ) 7.06 (td, 2H, Ar-*H*, J<sup>3</sup> = 8.9, J<sup>4</sup> = 2.0 Hz) 6.71 (td, 2H, Ar-*H*, J<sup>3</sup> = 8.9 J<sup>4</sup> = 2.1 Hz) 6.6 (dd, 1H, Ar-*H*) 3.44 (q, 4H, NCH<sub>2</sub>CH<sub>3</sub>, J<sup>3</sup> = 7.2 Hz) 1.23 (t, 6H, NCH<sub>2</sub>CH<sub>3</sub>, J<sup>3</sup> = 7,2 Hz). <sup>13</sup>C NMR (CDCl<sub>3</sub>): 188.1, 153.1, 148.5, 139.1, 128.9, 127.1, 111.9, 44.9, 12.9. UV-VIS in acetone/H<sub>2</sub>O (1:1 v/v): ε = 2.73\*10<sup>4</sup>, λ<sub>max</sub> = 645 nm.

### 3.7 Synthesis of acetamidoquinone 7



Synthesis was based on literature procedure.<sup>xxxvii</sup> In 250 mL DCM 7.406 g 2,5-dimethoxyaniline (48 mmol) was dissolved. The mixture was cooled with an ice bath. To the mixture 8.4 mL TEA and 4.5 mL acetyl chloride was added. Gas formation was observed. After 45 minutes the ice bath was removed and the mixture was stirred for another hour. The mixture was washed two times with water. The organic layer was dried with MgSO<sub>4</sub> and the solvents were removed *in vacuo*. The product was isolated as a brown solid in a yield of 92.04% (8.69 g, 45 mmol). <sup>1</sup>H NMR (CDCl<sub>3</sub>): δ 8.09 (d, 1H, Ar-*H*, J<sup>4</sup> = 2.9 Hz) 7.77 (s, 1H, NH) 6.77 (d, 1H, Ar-*H*, J<sup>3</sup> = 8.9 Hz) 6.55 (dd, 1H, Ar-*H*, J<sup>3</sup> = 9.0 Hz, J<sup>4</sup> = 3.0 Hz) 3.82 (s, 3H, OMe-*H*) 3.77 (s, 3H, OMe-*H*) 2.18 (s, 3H, COCH<sub>3</sub>).

### 3.8 Synthesis of acetamidoquinone 8



Synthesis was based on literature procedure.<sup>xxxviii</sup> In a mixture of 0.25 mL MeOH and 4.75 mL H<sub>2</sub>O 1.002 g diacetoxyiodobenzene (3.11 mmol) and 509 mg compound 7 (2.6

mmol) were dissolved. This mixture was stirred for 1.5 h. The solvents were evaporated *in vacuo*. A column was performed with petroleum ether/ EtOAc (1:1 v/v). The product was obtained as an orange solid in a yield of 28.4% (122.3 mg, 0.74 mmol).

$^1\text{H}$  NMR ( $\text{CDCl}_3$ ):  $\delta$  8.09 (s, 1H, NH) 7.54 (d, 1H, Ar-H,  $J^4 = 2.3$  Hz) 6.73 (m, 2H, Ar-H) 2.22 (s, 3H,  $\text{COCH}_3$ ).  $^{13}\text{C}$  NMR ( $\text{CDCl}_3$ ): 24.9, 114.7, 133.2, 138.1, 138.2, 169.4, 182.6, 188.0.

### 3.9 Synthesis of gelatin mixture

In 70 mL water 3.5 g gelatin (Gelatin Photographic grade, Talas nr 30002) was added. This mixture was heated up to 80 °C and stirred. When the gelatin was dissolved, the mixture was cooled to room temperature and a gel was obtained. This mixture was used as stock solution. If needed, the gel can be liquefied several times by reheating to about 50 °C.

### 3.10 pH measurements

A set with increasing pH-values (from 1 to 7) was made of compound **1**, **3** and **4** in solutions of acetone/aqueous acid (1:1 v/v). For pH 1, 2 and 3 HCl (1 M) was used. Buffers of acetic acid/sodium acetate were used for pH 3.5, 4, 4.5, 5, 5.5, 6, 6.5 and 7. Pure acetic acid (99.6%) was mixed with a 0.1 M NaOAc aqueous solution to make the buffers. UV-Vis measurements were done at  $t = 1, 30, 103, 150, 342$  and 720 hour. Sample concentrations were 15  $\mu\text{M}$  for the yellow dye, 8  $\mu\text{M}$  for the cyan dye and 9  $\mu\text{M}$  for the magenta dye.

### 3.11 Extractions

Extractions of the dyes were done with Fujicolor calibration papers (Fujicolor Chrystal Archive Paper Supreme <sup>HD</sup> for digital premium). Pieces of photographic paper with one color (yellow, magenta or cyan) were used. The method was based on literature procedure.<sup>xxxix</sup> Ethanol and TFA were mixed in the appropriate ratios (2/1 and 1/1 v/v), cooled in an ice bath and used to extract dyes from photographic paper. After stirring, the mixtures were left for four hours. The colors of the photographic paper were faded and the solvent was colored. The solvents were evaporated. During the evaporation, a color change at the cyan and magenta paper was visible from dye color to yellow. The extract was obtained as a light yellow gel. When acetone was added, the color of the dye reappeared.

### 3.12 Acid and base treatment

In 27 mL acetone 31 mg yellow dye **1** (76.6  $\mu\text{mol}$ ) was dissolved and 3 mL 1M HCl was added. The mixture was stirred for 1 hour. After the addition of the acid a color change was observed from yellow to orange. After 1 h 3 mL 1 M aqueous NaOH was added to the mixture, a color shift was observed from orange to yellow. The mixture was stirred for another 2 hours, then DCM and water were added. For both the organic and water the solvents were evaporated *in vacuo*.  $^1\text{H}$  NMRs of the water layer and organic layer were taken.  $^1\text{H}$  NMR analysis of the organic layer showed a complex mixture.  $^1\text{H}$  NMR ( $\text{D}_2\text{O}$ ):  $\delta$  7.29 (td, 2H, Ar-H,  $J^3 = 9.4$  Hz,  $J^4 = 2.3$  Hz) 6.99 (td, 2H, Ar-H,  $J^3 = 9.0$  Hz,  $J^4 = 2.1$  Hz) 3.55 (s, 4H,  $\text{NCH}_2\text{CH}_3$ ) 1.08 (t, 6 H,  $\text{NCH}_2\text{CH}_3$ ,  $J^3 = 7.6$  Hz).

### 3.13 Dyes in acetic acid

Compound **1**, **3** and **4** ( $\pm 25$  mg) were dissolved in  $\pm 50$  mL acetic acid. This was heated up to 130 °C and stirred and refluxed for 24 h. After a day the color was changed in the case of magenta and yellow dye. Extractions were performed with DCM and water. Analysis of the organic layer was done with GC/MS, UV-Vis and  $^1\text{H}$  NMR. Analysis of the

water layer was only performed with the cyan dye due to the absence of color of the water layer in the magenta and yellow dye reactions. All  $^1\text{H}$  NMRs show complex mixtures.

### 3.14 Stock solution 3 dyes in acid

Compound **1**, **3** and **4** were combined in a stock solution of 1 L acetone. Dye concentrations were 138  $\mu\text{M}$  for compound **1**, 48  $\mu\text{M}$  for compound **3** and 106  $\mu\text{M}$  for compound **4** in the stock solution. Samples were prepared containing stock solution and water (1:1 v/v) or acetone and a buffer (1:1 v/v) (NaOAc/AcOH) of 0.1 M. UV-Vis measurements were done with samples with pH 7 and pH 3.5. At a pH of 3.5 the intensity was measured every hour from  $t=1$  to  $t=17$  hours after addition of the acid buffer. Measurements were performed at set wavelengths: 450 nm for yellow dye, 545 nm for magenta dye and 650 nm for cyan dye, as the three peak positions are from the three dyes measured separately in the same solvent.

### 3.15 DFT calculations

All the calculations were done via LISA on SURFsara. For the time-independent calculations basis set 6-31g\* was used with hybrid B3LYP. For the cyan dye a time-dependent measurement was done to visualize the UV-spectrum. This was done by: 6-31g\* with B3LYP, SCRF (Solvent=Ethanol).

### 3.16 CV measurements

Measurements were carried out with an Ivium potentiostat, Vertex standard, 100 mA/10V. Samples contained  $\pm 5$  mg compound with 5 mL electrolyte (0.1 M  $\text{NBu}_4\text{PF}_6$  in MeCN). The working electrode was a glassy carbon electrode, the counter electrode consisted of a Pt wire and the reference electrode was an Ag/AgNO<sub>3</sub> in MeCN electrode. The measuring speed was 100 mV/s.

## 4 Results and discussion

### 4.1 Syntheses

The yellow, magenta and cyan dyes were synthesized by the coupling of a developing agent with color couplers.<sup>xi</sup> The reaction is initiated by an electron transfer reaction between  $\text{Ag}^+$  and a developing agent, in this case diamine **10**. The activated developing agent can then be attacked by a deprotonated coupling agent. A C-N bond is formed and two equivalents of developing agent are used to first oxidize and then deprotonate the dye, which results in a Schiff base formation. Thus, in total 4 equivalents of developing agents are used for the synthesis of the dye. A proposed mechanism is given in Scheme 2.

Several variants of the cyan dye, compound **5** and **6** and **8** were synthesized in order to elucidate the reaction mechanism of the acid catalyzed degradation of the dyes. Compound **5** was synthesized by an oxidation with  $\text{PbO}_2$  and compound **6** was accessed via a synthetic route analogous to the synthesis of cyan dye. Compound **8** was synthesized via an oxidation of acetamidoquinone **7**.

The synthesized compounds were analyzed with  $^1\text{H}$  NMR,  $^{13}\text{C}$  NMR and UV-Vis spectroscopy. All compounds were pure according to NMR data. UV-Vis measurements were done in acetone/water 1:1 v/v because experiments with acid were planned and therefore a protic solvent like water is necessary. The dyes do not dissolve completely in water so acetone was used to dissolve the dye. Data are given in Table 3.

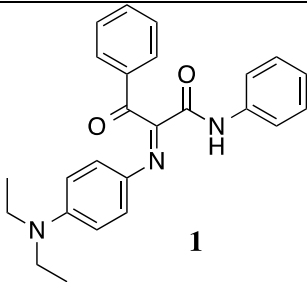
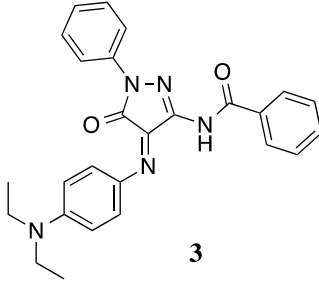
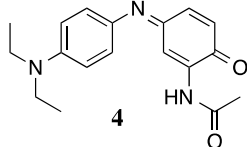
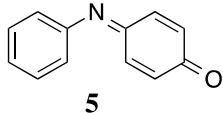
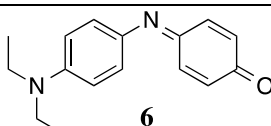
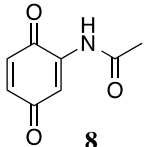
compound	Structure	Yield (%)	Extinction coefficient	$\lambda_{\max}$ (nm) acetone/water 1:1 v/v
<b>1</b> (Yellow dye)		12	$2.26 \cdot 10^4$	438
<b>3</b> (magenta dye)		65	$5.06 \cdot 10^4$	546
<b>4</b> (cyan dye)		83	$3.2 \cdot 10^4$	651
<b>5</b> (aminoquinone)		25	$2.84 \cdot 10^3$	451
<b>6</b> (aminoquinone)		61	$2.73 \cdot 10^4$	645
<b>8</b> (acetamido-quinone)		28		384

Table 3: Data from synthesized compounds.

## 4.2 Analysis of dye degradation products

### 4.2.1 Experimental setups

Indications are given for the presence of acid in the artwork: acetic acid was smelled when the glass plate was tilted. Acetic acid is known in literature as a degradation product of the silicon glue, which is probably used to add the glass on the front of the artwork, and as a degradation product of the paper, which is a part of the photograph. In literature it is known that the yellow dye is more sensitive for acidic conditions than the cyan and magenta dye.<sup>xvii</sup> Some experiments were done in order to gather more information about the influence of acid on color changes and therefore possible explanations for the observed changes on *Russian Diplomacy*.

### 4.2.2 Dyes in diverse acidic pHs over time

Compound 1, 3 and 4 were dissolved in acetone/water (1:1 v/v) with HCl or acetone/buffer solutions and the absorption was measured over time with UV-Vis spectroscopy in a period of a month (720 hour). In Figure 18, Figure 19 and Figure 20 the absorption of the yellow, magenta and cyan dye are shown at the peak positions at selected pHs. For the cyan dye, the peak position shifts at lower pH. After 720 h at pH 4 the magenta dye has lost only 11% of its intensity compared to pH 7 at  $t = 0$  h, where the cyan dye lost 48% of its intensity after 720 hours and the yellow dye even 96% of its intensity.

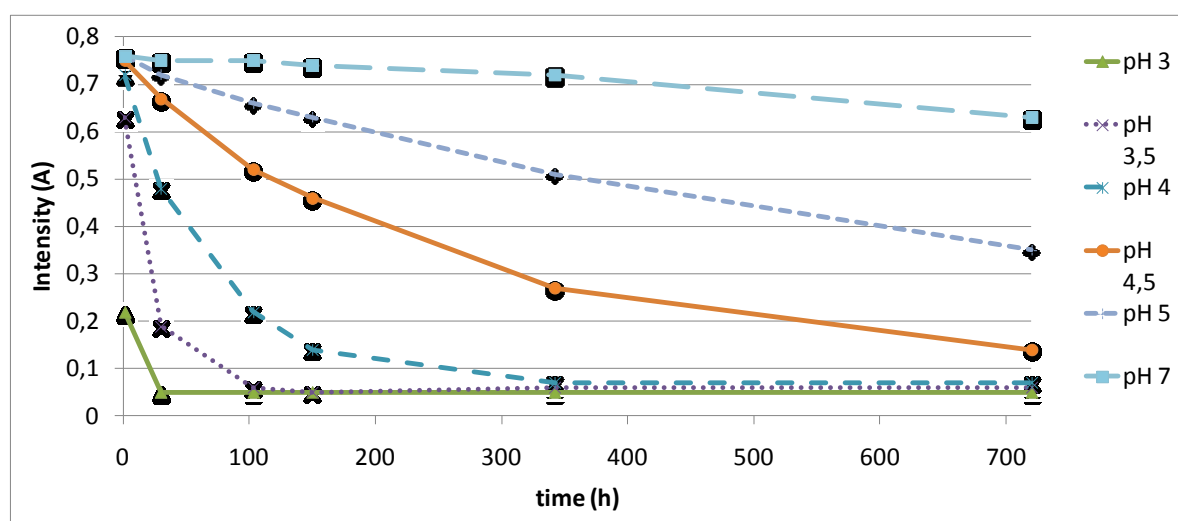


Figure 18: UV- Vis data of yellow dye in different pHs over time with  $\lambda_{\max} = 438$  nm.

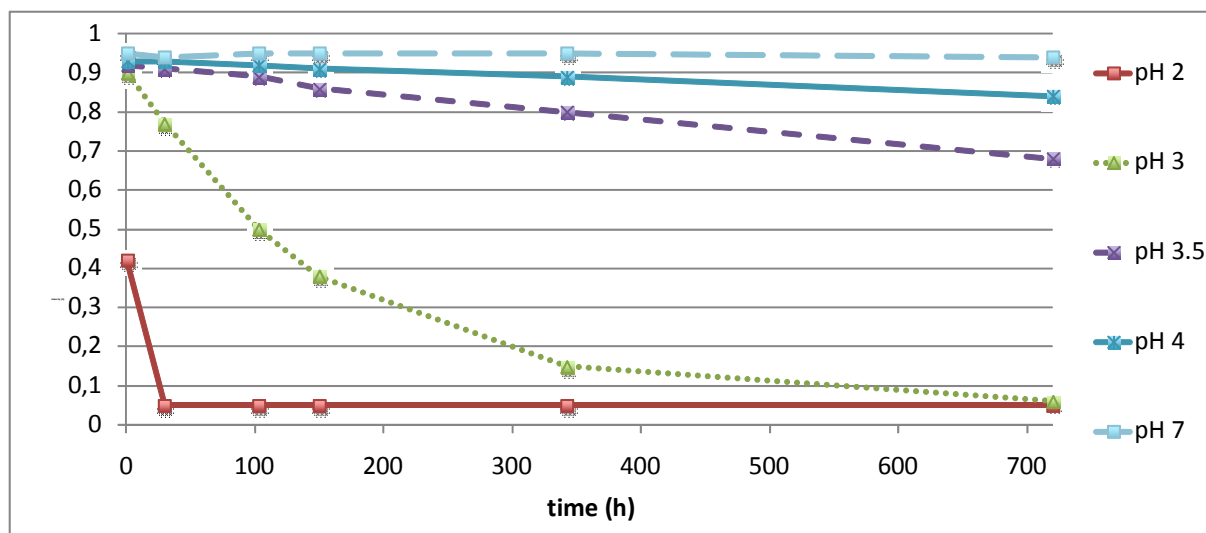


Figure 19: UV-Vis data of magenta dye in different pHs over time with  $\lambda_{\max} = 546 \text{ nm}$ .

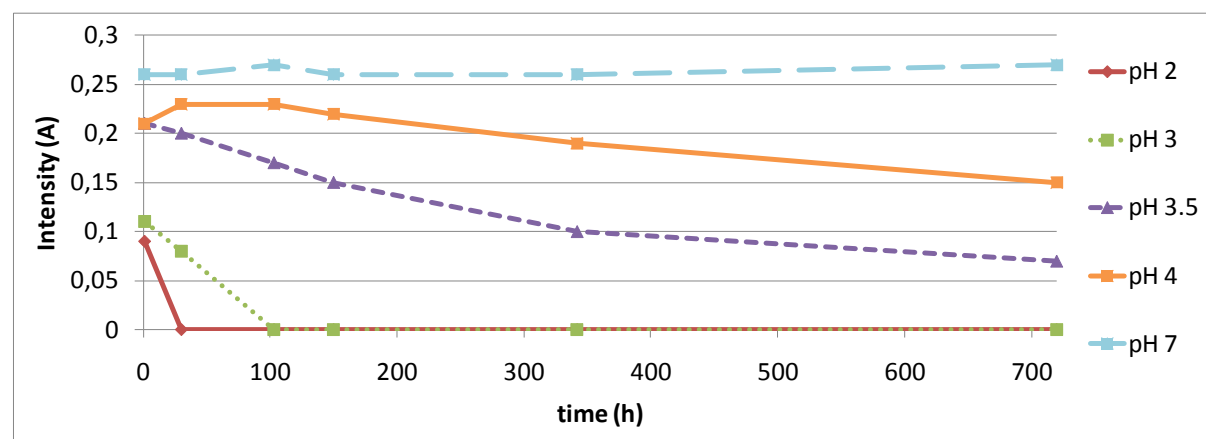


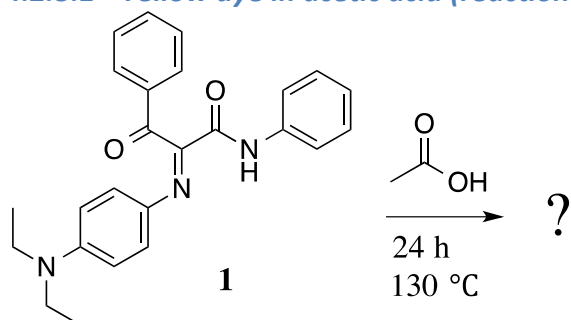
Figure 20: UV-Vis data of cyan dye in different pHs over time with  $\lambda_{\max}$  shifts between 650 and 750 nm.

These results imply that the conjugated system of the yellow dye is damaged the easiest and the magenta dye is the most stable in acidic conditions. In a photograph this means that the yellow dye will fade first in acidic conditions and the magenta dye is the most stable.

#### 4.2.3 Dyes in acid

A reaction of the dyes in acetic acid proceeds too slowly to be of practical use for the analysis of its products. In order to speed up the reactions, the dyes were dissolved and stirred in acetic acid for 24 hours. The products were extracted with water and DCM and the solvents were evaporated. The organic layers were analyzed with  $^1\text{H}$  NMR, UV-Vis and GC/MS. For each dye the analysis of the products are elaborated in the next paragraph.

#### 4.2.3.1 Yellow dye in acetic acid (reaction 1)



Reaction 1: Yellow dye with acetic acid.

Yellow dye **1** was dissolved in acetic acid and this solution was refluxed for 24 hours. The reaction is given in Reaction 1. The GC/MS chromatogram showed no signal. The UV-Vis spectra are given in Figure 21. A decrease of the intensity of the yellow dye is observed. No peak is observed in the region at the  $\lambda_{\text{max}}$  of yellow dye around 450 nm so no clear maximum is observed. The diamine **10** (shown in green as a reference spectrum of diamine in acetone/buffer (pH 4) 1:1 v/v, gives a peak at  $\lambda_{\text{max}} = 480$  nm) is not observed in the UV spectrum.

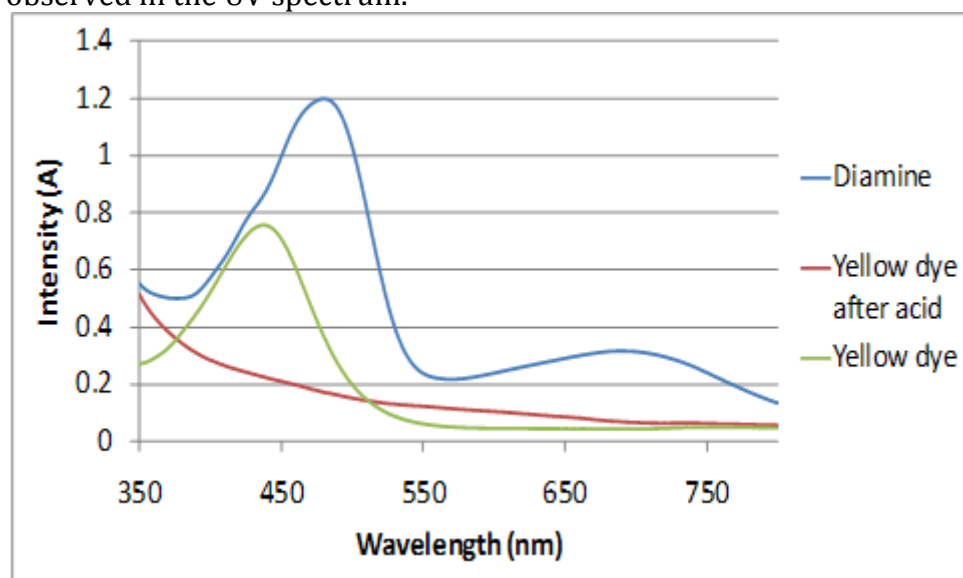


Figure 21: UV- Vis spectra of yellow dye before (blue) and after (red) treatment with acetic acid. The diamine **10** in a buffer of pH 4 (green) is given as a reference spectrum.

$^1\text{H}$  NMR is given in Figure 22 where the yellow dye after treatment with acetic acid (blue) and reference spectrum of yellow dye before the reaction (red) are shown. The ethyl peaks from the dye seem to have disappeared, just like the NH-peak at 9.4 ppm. A myriad of peaks is found in the aromatic region.  $^1\text{H}$  NMR and UV-Vis imply the degradation of the yellow dye into multiple components without notion of the diamine **10**.



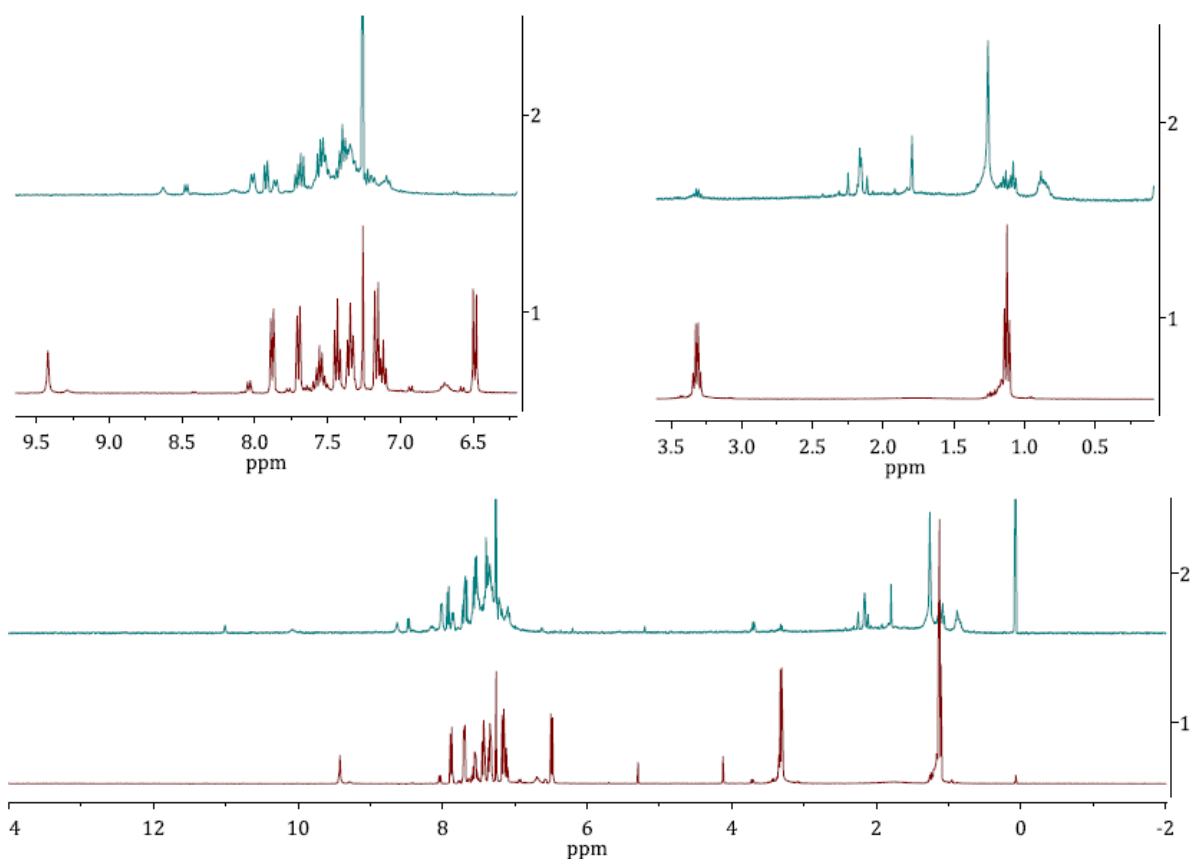


Figure 22:  $^1\text{H}$  NMR spectra of the yellow dye before (red) and after (blue) treatment with acetic acid with a close up of the aromatic (left) and aliphatic (right) region.

#### 4.2.3.2 Yellow dye and acid: other observations

In the UV-Vis spectra of the experiments described in section 4.2.2 (yellow dye in acetic acid buffers) at pH 4 and 3.5 two new peaks were observed over time. In Figure 23 the two extra peaks are indicated with two blue arrows, given are the yellow dye at pH 3.5 after 30 hours and after 720 hours. At  $t = 1\text{h}$ , this peak is not observed. After 30 h this peak is observed at pH 2, 3.5 and 4 at 510 and 550 nm. After 4 weeks at pH 4 and 3.5 two peaks seems to appear at 510 and 555 nm. After a month in pH 3.5 these peaks are still observed, this implies that the formed compounds are stable in acid conditions over time. The yellow-color peak is completely disappeared (with  $\lambda_{\text{max}} = 450\text{ nm}$ ). At lower pHs these peaks are all gone. These peaks seem to be present at pHs between 3 and 4 (different pHs over time). These peaks were not assigned to compounds due to lack of reference compounds.

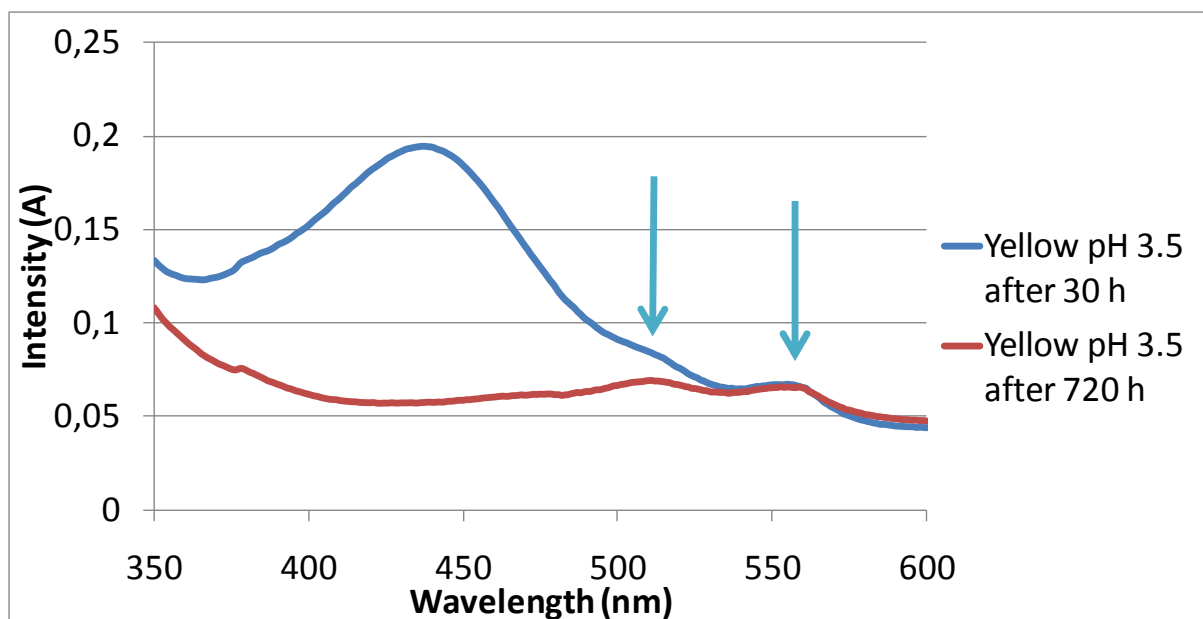
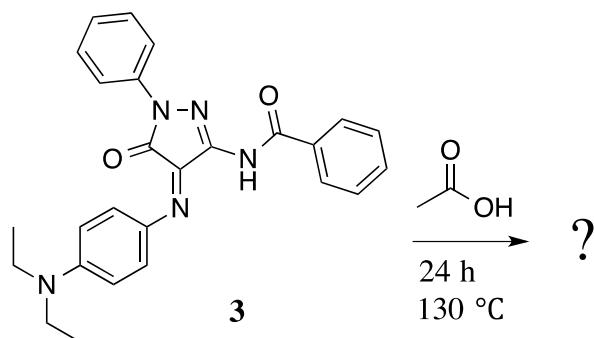


Figure 23: Yellow dye 1 in pH 3.5 after 30 hours (blue) and 720 hours (red).

#### 4.2.3.3 Magenta dye in acetic acid (Reaction 2)



Reaction 2: Magenta dye with acetic acid.

The GC/MS fragmentation pattern gave one signal with a peak with  $m/z$  340. No matching molecular structures were assigned. The UV-Vis spectrum of the organic layer of the product in acetone/water (1:1 v/v) is shown in Figure 24. Reference spectra are given of the magenta dye in acetone/water (1:1 v/v) and the diamine in pH 4 (acetone/buffer 1:1 v/v). The main absorption band at  $\lambda_{\max}$  545 nm is largely quenched and the diamine hydrolysis product is not present either. The spectrum of the dye after treatment with acid shows a new absorption band at 450. This does not resemble the absorption band of diamine **10**, which has a  $\lambda_{\max}$  at 480 nm. This can imply the formation of a new compound. The water layer of the extraction is colorless so no UV-Vis measurements can be done.

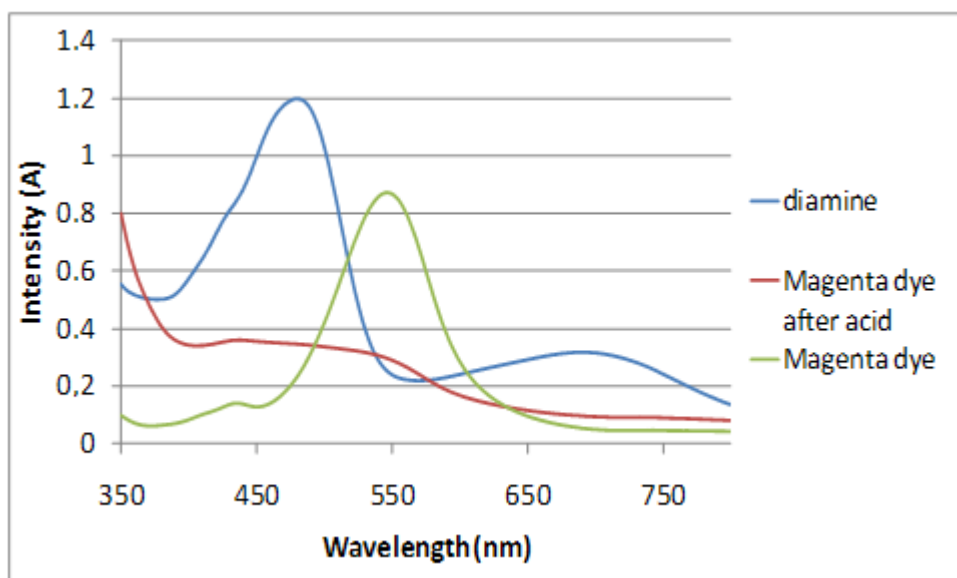


Figure 24: UV-Vis spectra of magenta dye before (green line) and after (red line) treatment with acetic acid. Diamine 10 in pH 4 is shown as a reference (blue line).

The  $^1\text{H}$  NMR of the organic layer is given in Figure 25 where the upper graph (blue) shows the products of the reaction between magenta dye and acetic acid and the lower graph (red) is magenta dye before reaction. The ethyl peaks are gone after the reaction and the aromatic part of the spectrum shows a lot of differences compared with the starting material. The NH-peak of the diamine is not present anymore after the reaction.

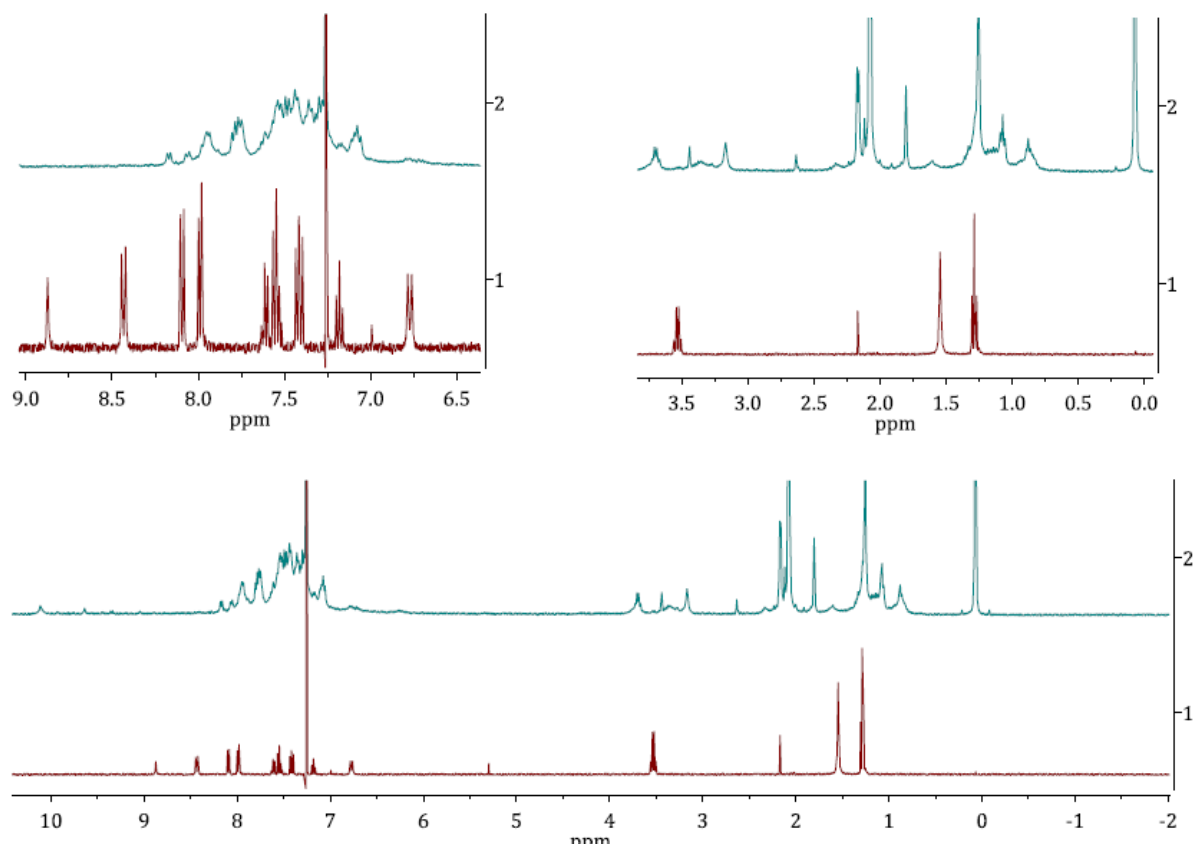
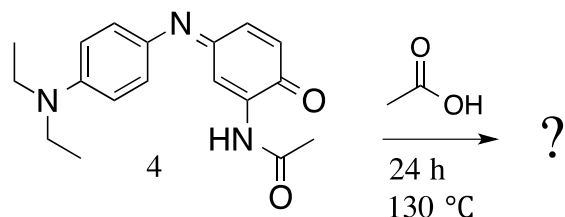


Figure 25:  $^1\text{H}$  NMR spectra of the magenta dye before (red) and after (blue) the reaction with acetic acid with a close up of the aromatic region (left) and aliphatic region (right).

From this experiment the conclusion can be drawn that the dye is decomposed in multiple products, the ethyl peak is missing in the  $^1\text{H}$  NMR and the diamine peak is

missing in both the  $^1\text{H}$  NMR and UV-Vis spectra so this is probably not present in the organic layer. A complex mixture is formed.

#### 4.2.3.4 Cyan dye in acetic acid (Reaction 3)



Reaction 3: Cyan dye in acetic acid.

The GC/MS chromatogram did not show a signal. The UV-Vis spectra are shown in Figure 26 and peak positions are given in Table 4. In Figure 26 the graph "cyan dye" shows the absorption of the cyan dye in acetone/water. The product of Reaction 3 was also analyzed with UV-Vis spectrometry and both the water layer and the organic layer are shown in the graph. The organic layer is measured in acetone and acetone/water (1:1 v/v). The extinction coefficient is not determined due to unknown concentrations of the products. In the organic layer strong solvatochromic effects are observed (Table 4), which can be explained by a larger difference in charge distribution between the HOMO and the LUMO in the products formed than in the cyan dye.<sup>xxx</sup> Both layers do not show the absorption band of the diamine **10**, which has a  $\lambda_{\text{max}}$  at 480 nm (given in Figure 24).

Compound	Peak position $\lambda_{\text{max}}$
Cyan dye in acetone/water	655 nm
Product water layer	648 nm
Product organic layer in acetone/water	587 nm
Product organic layer in acetone	556 nm

Table 4: UV-Vis peaks of the cyan dye before and after reaction with acetic acid.

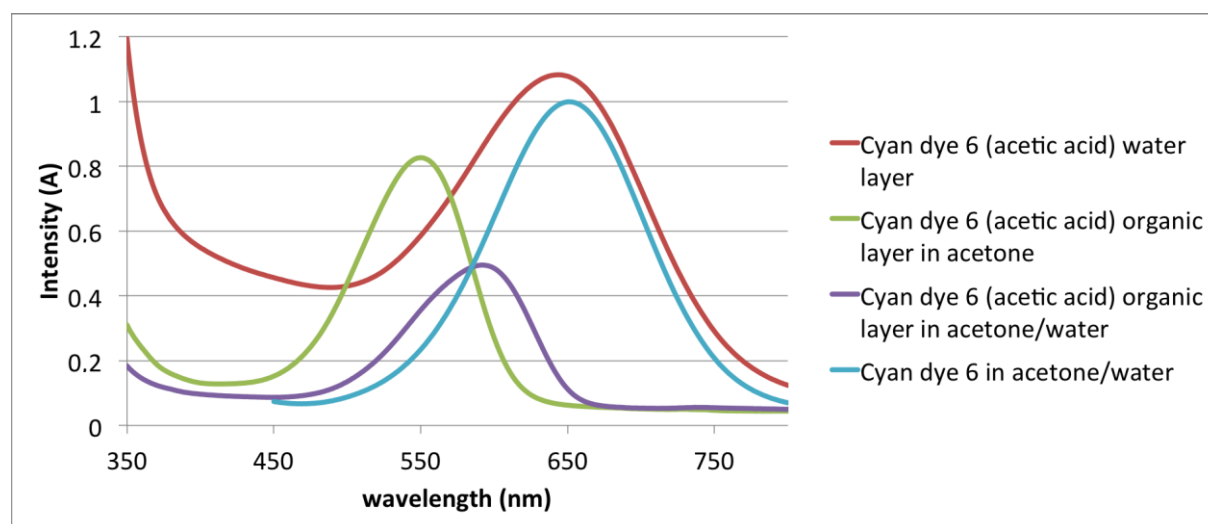


Figure 26: UV-Vis spectra of the cyan dye before treatment with acetic acid (blue), water layer of extraction after treatment with acetic acid (red), organic layer in acetone (green) and organic layer in acetone/water (1:1 v/v) (purple).

$^1\text{H}$  NMR spectra are given in Figure 27 where the upper graph (blue) is cyan dye after treatment with acid and the lower graph (red) is cyan dye before reaction with acetic acid. The NH-peak is gone after the reaction. A lot of peaks are appeared in the aliphatic region (between 0 and 3 ppm).

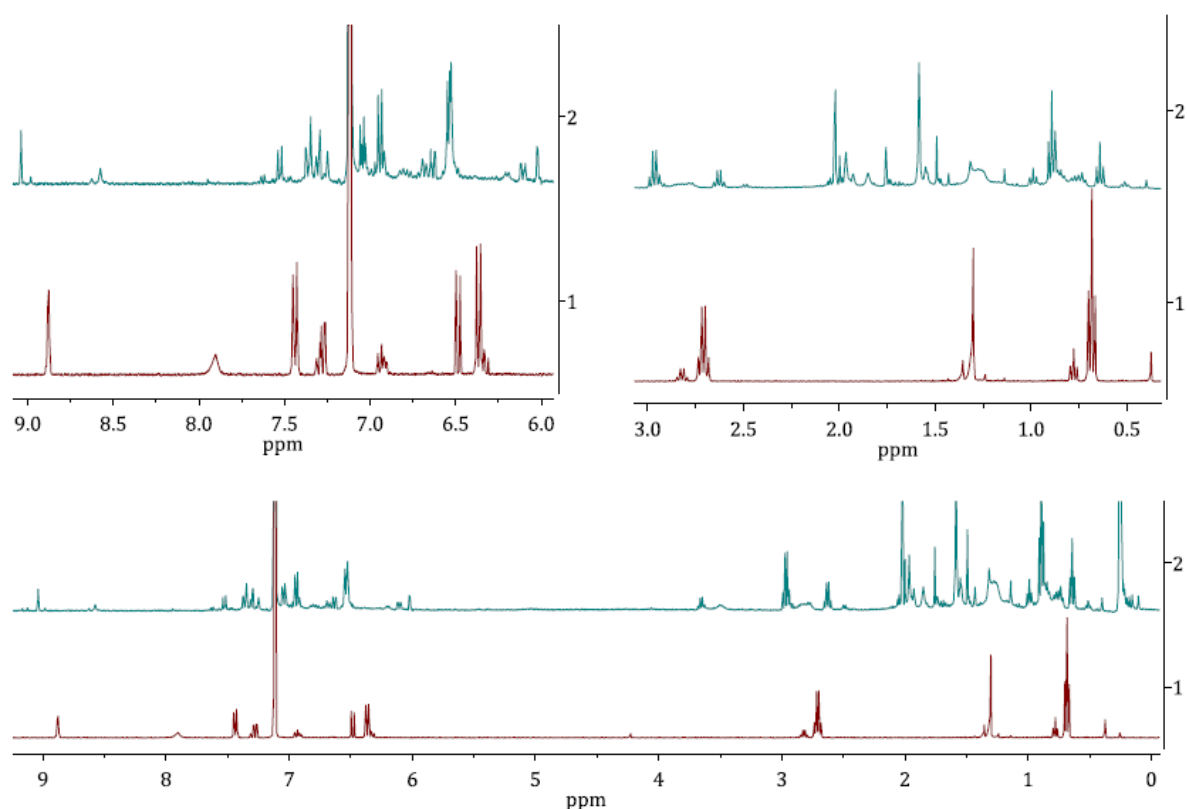


Figure 27:  $^1\text{H}$  NMR of the cyan dye before (red) and after (blue) treatment with acetic acid with a close up of the aromatic (left) and aliphatic (right) region.

A myriad of peaks reveals the presence of more than one compound, with both aliphatic and aromatic parts. UV-Vis shows the presence of cyan dye in the water layer and a new compound formed which shows stronger solvatochromic effects than the cyan dye.

#### 4.2.3.5 Cyan dye with acid: other observations

One of the experiments carried out consisted of the cyan dye with acid in water. The products of this reaction were analyzed with  $^1\text{H}$  NMR, GC/MS and UV-Vis.  $^1\text{H}$  NMR shows multiple products in organic layer. In the GC/MS fragmentation pattern the azocompound **14** in Figure 28 is found and therefore tried to synthesize to use as a reference compound. This synthesis was not successful.

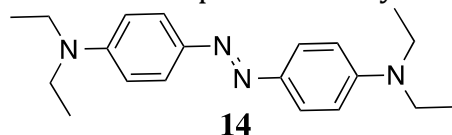


Figure 28: Azocompound **14**.

From the experiments with the three dyes dissolved in acetic acid the general conclusions can be drawn that the dyes did chemically react with acetic acid and the products after extraction of the organic layer do not show signs of the diamine **10**. In the case of the yellow and magenta dye, the color of the reaction mixtures was changed after 24 hours. The  $^1\text{H}$  NMR spectra show multiple products formed. These were not analyzable with GC/MS. UV-Vis spectra do not imply the presence of diamine **10**. The diamine could be protonated and dissolved in the water layers of the extractions, which were not analyzed with  $^1\text{H}$  NMR.

#### 4.2.4 Combined mixture of three dyes and acid

On a black part of a chromogenic photograph, the three dyes are all present with the same intensity. This is the case in *Russian Diplomacy* where a black and white image is printed on a chromogenic photograph. In order to mimic this situation, a mixture of the three dyes in water/acetone (1:1 v/v) was made with concentrations that result in an equal intensity. In Figure 29 the UV-Vis spectrum of this mixture is shown in blue. The mixture was also measured with UV-Vis spectrometry at a pH of 3.5 in an acetone/buffer mixture, which is shown in red (t = 1 h). This measurement was repeated after 16 hours (t = 17 h), which results in the green line.

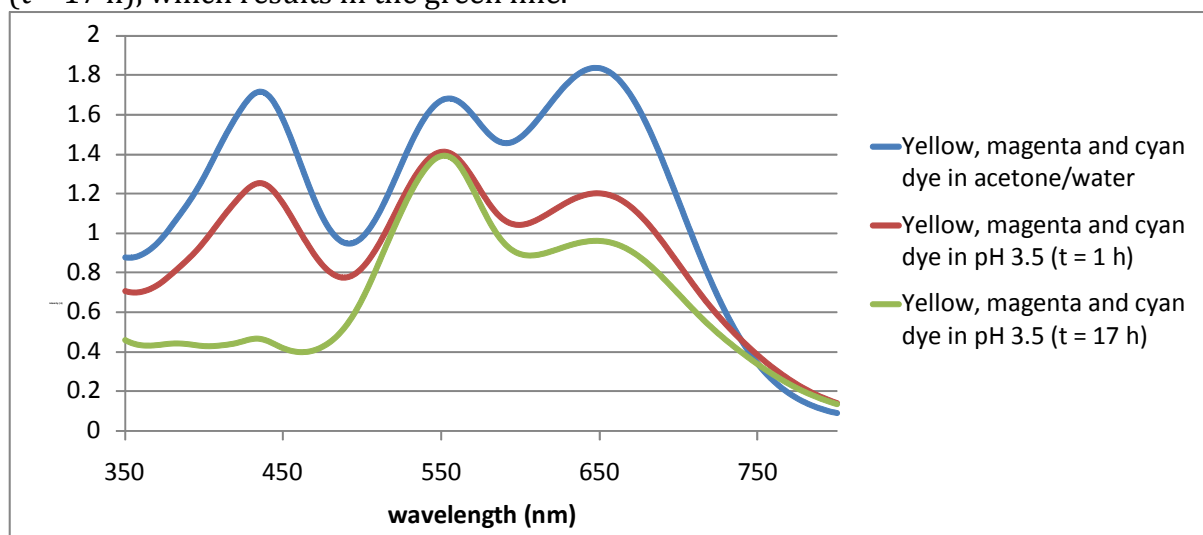


Figure 29: UV- Vis spectra of the yellow, magenta and cyan dye combined under neutral and acidic conditions respectively. The three dyes are compared at pH 7 (blue line), pH 3.5 (red line) and pH 3.5 after 16 hours (green line) in acetone/water or acetone/buffer (1:1 v/v).

As shown in Figure 29, peak positions  $\lambda_{\max}$  are the same as the individual dye measurements. At pH 3.5 the intensity of the three peaks was already decreased at t = 1 hour. As shown in Table 5, after 17 hours the magenta peak was decreased with 1%, the peak of the cyan dye was decreased with 18% and the peak of the yellow dye was decreased with 61% compared with the intensity at t=1 hour.

$\lambda$ peak position (nm)	dye	$\Delta A$ after 17 hours	$\Delta A$ in %
450	yellow	0.6842	61
545	magenta	0.0133	1
650	cyan	0.2102	18

Table 5: Intensities of peak position of the three dyes measured over time.

In Figure 30, the intensities of the dyes at peak positions are plotted over time. The magenta dye is the most stable and the yellow dye the least stable in acidic conditions. This is in line with the long term experiments of the three dyes separately in acidic conditions mentioned previously in 4.2.2 and with the observations mentioned in literature and as seen in *Russian Diplomacy*.<sup>xvii, xxii</sup> Also these results are in line with the experiments done in paragraph 4.2.2 where the yellow dye is the most unstable under acidic conditions and the magenta dye the most stable.

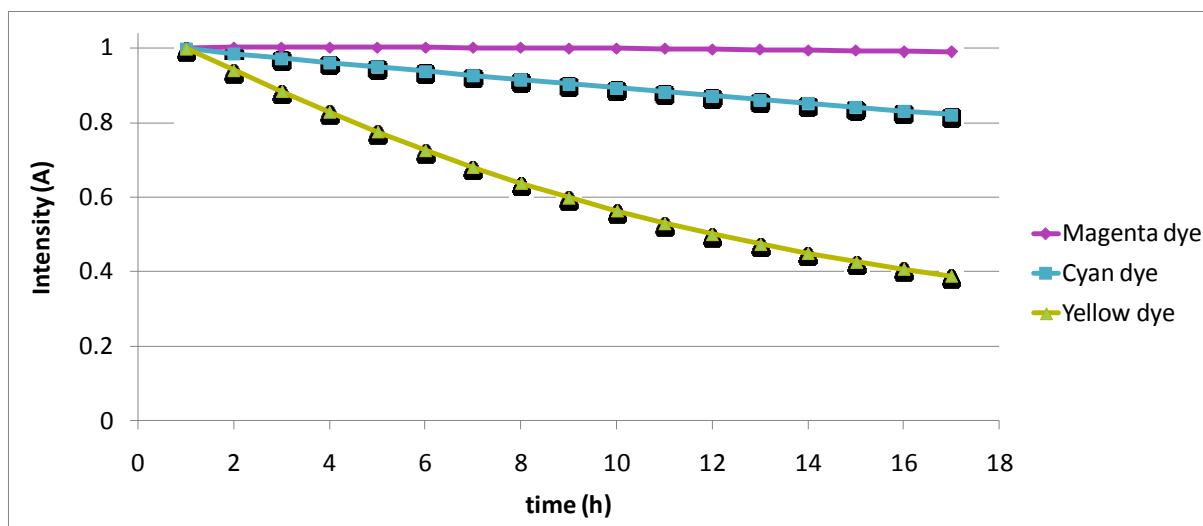


Figure 30: Normalized intensity of peak positions of the three dyes (yellow, magenta and cyan) in acidic conditions (pH 3.5) measured over time.

With the Arrhenius equation used for the data given in Figure 30, (equation 1), the rate constants and activation energies of the reactions are calculated and given in Table 6.

$$\text{--- (1)}$$

In this equation,  $k$  is the reaction rate,  $A$  is a constant which is set on 1 due to unknown values for the specific reactions,  $-E_a$  is the activation energy for the reaction,  $R$  is the gas constant and  $T$  the temperature, which is 293 K in these cases. The yellow dye has the lowest value for  $E_a$  which is in line with the observed UV-Vis measurements. The magenta dye has the highest value for  $E_a$ .

Compound	$k$	$-E_a$
Yellow dye 1	$4 \cdot 10^{-10}$ M/s	-52 kJ/mol
Magenta dye 3	$3 \cdot 10^{-12}$ M/s	-65 kJ/mol
Cyan dye 4	$9 \cdot 10^{-11}$ M/s	-56 kJ/mol

#### 4.2.5 Acid and base treatment

In order to investigate the reversibility of the reactions, yellow dye treated first with acid and neutralized again with base. Previous work in our group has shown that after acid and base treatment, the main absorption peak was partially quenched.<sup>xi</sup>

Yellow dye in 27 mL acetone was treated with 3 mL 1M aqueous HCl until a pH of 1 was reached. After 1 hour of stirring the solution was neutralized with 3 mL 1M aqueous NaOH. A color shift was visible from yellow to orange when the acid was added and back to yellow again when the base was added. A  $^1\text{H}$  NMR was taken of the water layer and organic layer. The  $^1\text{H}$  NMR of the organic layer showed a complex mixture, the  $^1\text{H}$  NMR ( $\text{D}_2\text{O}$ ) of water layer (Figure 31) shows the presence of the diamine used as coupling agent. This implies that the yellow dye degraded to the diamine and other parts of the dye. This is in line with literature.<sup>xvii</sup> From the  $^1\text{H}$  NMR the conclusion can be made that the presence of acid results in a chemical reaction where dye disintegrates in two or more compounds. This is not a complete reversible reaction.

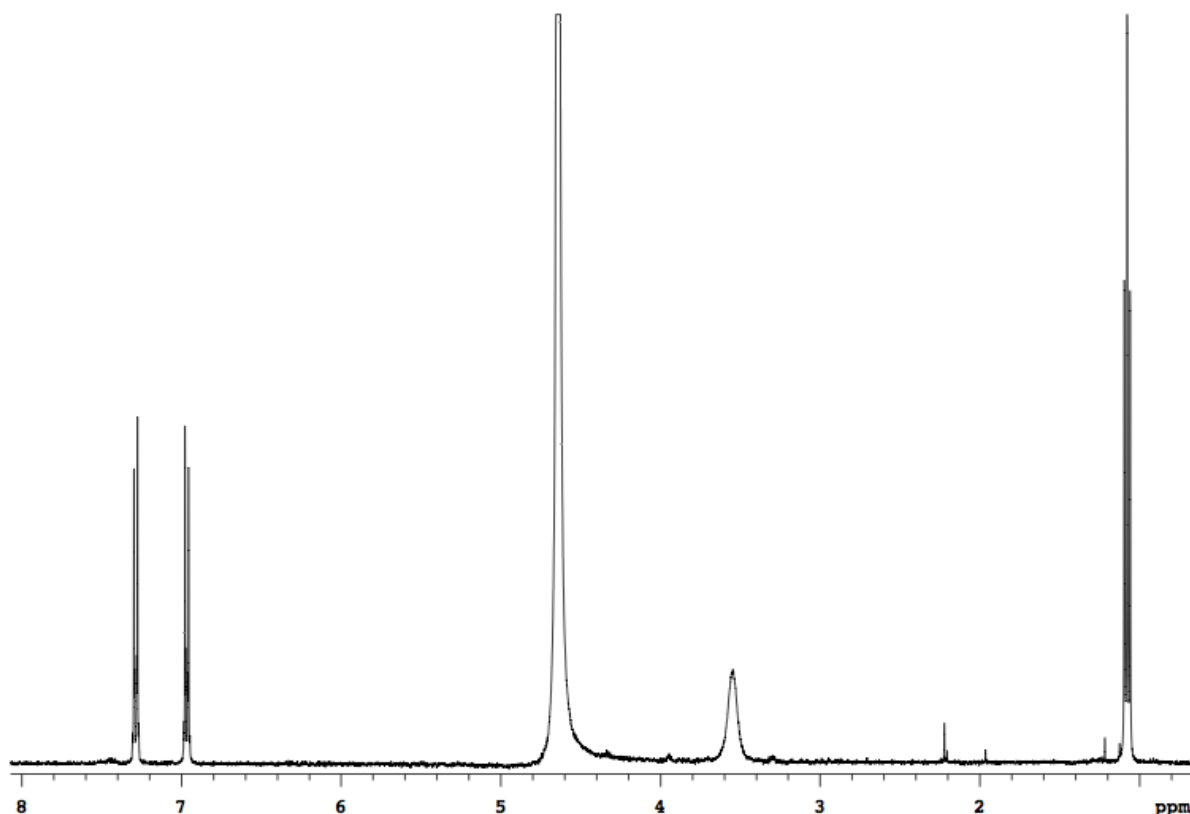


Figure 31:  $^1\text{H}$  NMR of the water layer containing diamine 10.

### 4.3 Dyes and reactivity: study of the molecular orbitals

As shown in chapter 4.2, the three dyes are prone to reactions with acid. From the previous experiments no solid conclusions about the reaction mechanism can be made. The dyes and derivatives were analyzed with several techniques in order to obtain more information of the molecular structures and with the aim to find clues what actually happens when the dyes react with acetic acid. Cyclovoltammetric and solvatochromic measurements and density functional theory calculations were performed to investigate the three-dimensional structure and localization of the HOMO and LUMO of the dyes.

#### 4.3.1 Cyclovoltammetric measurements

Cyclovoltammetric measurements were done with the cyan dye **4** and its two derivatives **5** and **6** in order to determine the differences in availability for electron transfer in the HOMO and LUMO. When measuring from 0.0 V, a compound is first reduced (towards a positive potential) so an electron is added to the molecule. The reduced compound is then re-oxidized until the starting voltage is reached. First oxidation (from 0.0 towards a negative potential) and then reduction (back to a positive potential) can be measured in order to see if there is a difference between the oxidation and the reduction pathway. Reference graphs are shown in appendix C.

In Figure 32 the voltammograms of cyan dye **4**, aminoquinone **5** and aminoquinone **6** are shown. For cyan dye **4** the starting potential was 0 V, vertex 1 was 2 V and vertex 2 was -2 V (first reduction, than oxidation). For aminoquinone **5** the starting potential was 0 V, vertex 1 was 3 V and vertex 2 was -3V (first reduction than oxidation). For aminoquinone **6** the starting potential was 0 V, vertex 1 was -3 V and vertex 2 was 3 V (first oxidation than reduction).



From Figure 32 it is clear that the oxidation- and reduction process do not follow the same path and not the same amount of peaks are visible in both processes. This implies that with the application of electric current the cyan dye and its derivatives are irreversible damaged and not capable of following the same pathway of oxidation/reduction.

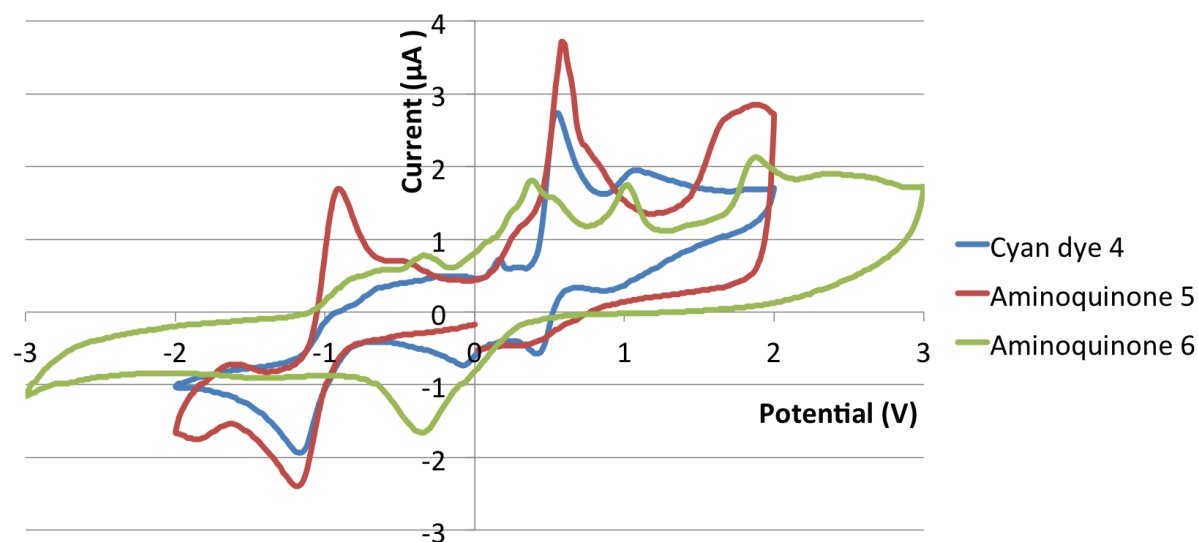


Figure 32: CV measurements of cyan dye 4 (blue), aminoquinone 5 (red) and aminoquinone 6 (green).

#### 4.3.2 DFT calculations

DFT calculations were performed in order to investigate the molecular structure of the dyes and the energy levels. This computational chemistry method is capable to make estimations of the 3D-structure and of the molecular orbitals of the organic compounds. A visualization of the HOMO and LUMO can show where the molecules are more prone to chemical reactions, in this case where the dyes have a localization of electron density that is available to react with protons. In literature, for the cyan and yellow dye data are given concerning the three dimensional structure and the HOMO and LUMO.

For the three dyes the HOMO and LUMO were calculated and visualized. Localization of the HOMO and LUMO was observed in the case of the yellow and magenta dye, as shown in Figure 33 and Figure 34 respectively. The cyan dye calculation shows a more delocalized HOMO and LUMO as shown in Figure 35. Calculations were run where the cyan dye, compound 4, was protonated at the heteroatoms but the calculation finished in a separation of the proton and the dye. This could imply that the protonated dye is a transition state and in the DFT calculation this results in the lapse towards the starting material and an unbound proton.

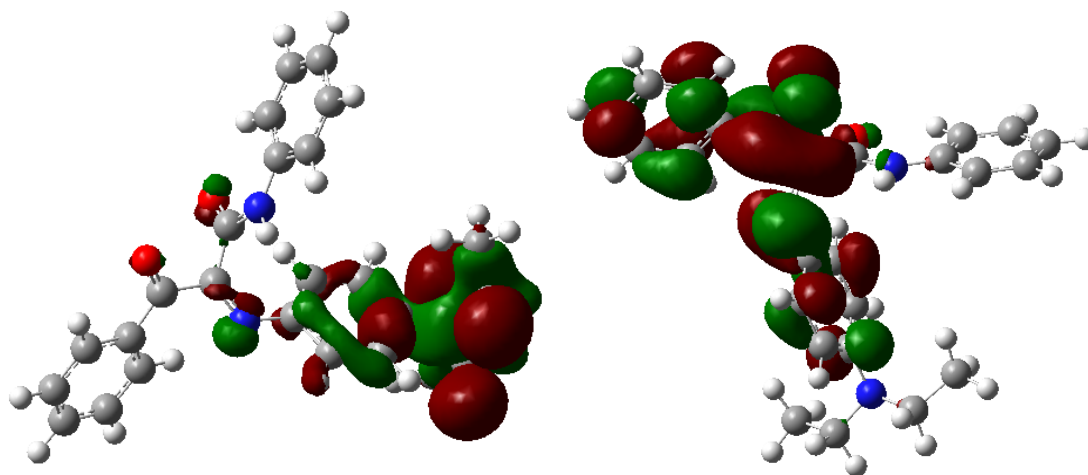


Figure 33: DFT visualization of the HOMO and LUMO of the yellow dye.

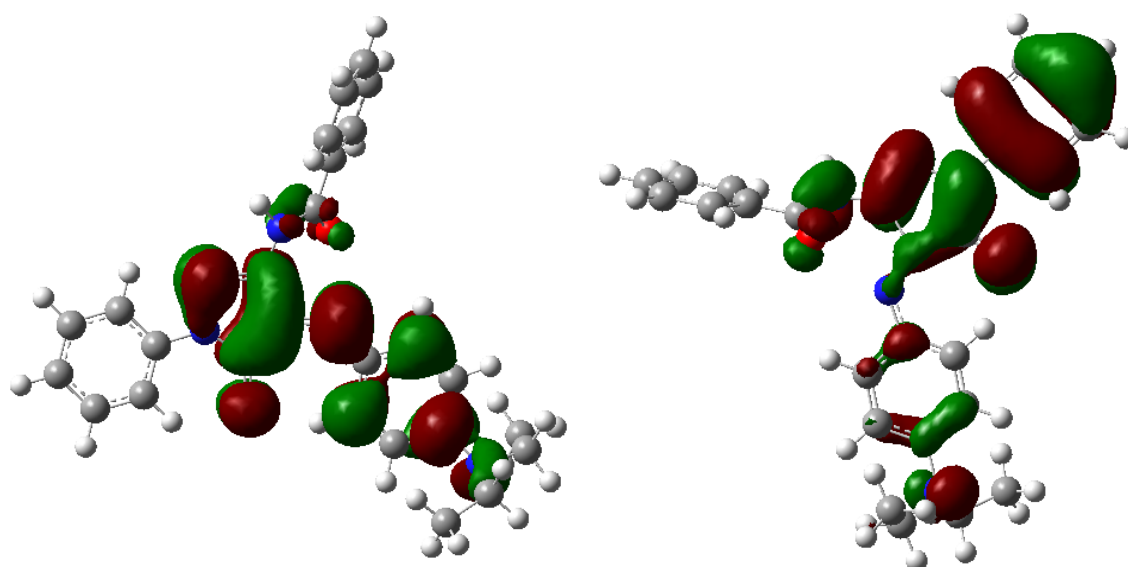


Figure 34: DFT visualization of the HOMO and LUMO of the magenta dye.

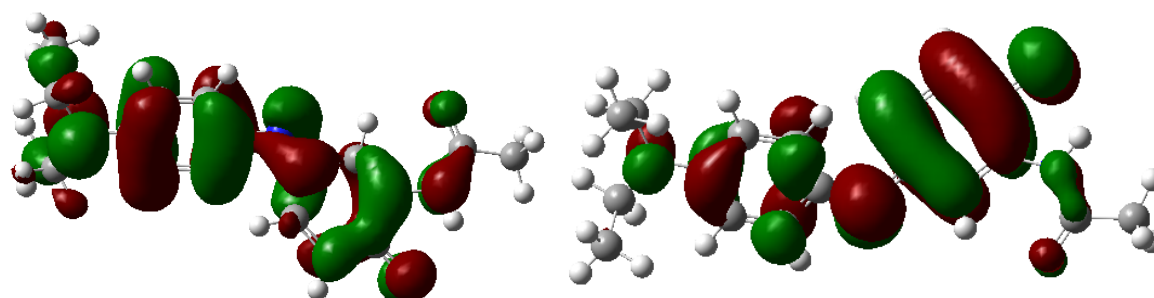


Figure 35: DFT visualization of the HOMO and LUMO of the cyan dye.

For the cyan dye time-dependent calculations were run of the dye in ethanol via the SCRF approximation. This resulted in a UV-Vis spectrum shown in Figure 36. Since the difference ( $\Delta \lambda_{\max}$  150 nm) with experimental values is relatively large, these calculations can be regarded as insufficiently accurate. This deviation is known in literature as a normal number.<sup>xli</sup> More accurate calculations with PCM (polarizable continuum model) approximations may give accurate calculations, DFT can then be used as a supportive technique to mimic UV-Vis spectra of protonated dyes and provide more information about the three dimensional structure of the dyes in solvents.

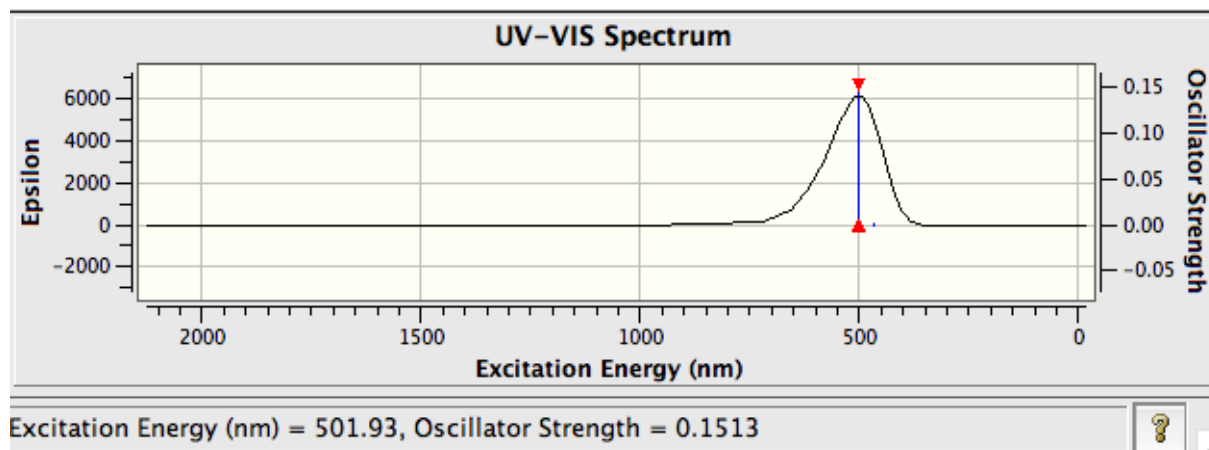


Figure 36: UV-Vis spectrum of the cyan dye calculated with TDDFT.

### 4.3.3 Solvatochromic effects

For the three dyes the solvatochromic effects were measured because these effects can provide information about sensitivity of the HOMO and LUMO for polarity and therefore are directly linked with the charge localization separation of the LUMO. The yellow, magenta and cyan dye were dissolved in different solvents and measured with UV-Vis spectroscopy to investigate the solvatochromic effects that may occur. Concentrations were 20  $\mu\text{M}$  per sample.

The most notable solvents in the series of the yellow dye are shown in Figure 37. A shift of peak position of 33 nm and an increase of intensity of 0.35 was observed between the highest and lowest absorption. In Figure 38 the most notable solvents are shown for the magenta dye. The peak position differ 54 nm and the intensity of the absorption differ 0.56. In Figure 39 the cyan dye in the most notable solvents is shown. A shift of 155 nm for the cyan dye and an increase in 0.55 in intensity were observed. In the appendix D a table is given of all peak positions and intensities.

For all three dyes, the most non-polar non-protic solvent results in the lowest wavelength and therefore the highest energy (hypsochromic shift). This implies the destabilization of the LUMO, which enlarges the band gap between HOMO and LUMO. The LUMO must therefore consist of molecules that can adapt more charge transfer character; the charges in the molecule are more localized than in the HOMO. This is much more present with the cyan dye. For the cyan dye this is also known in literature.<sup>xxxix</sup> The yellow dye does not show a big shift in energy, which implies that the charge formed in the LUMO is much better stabilized over the conjugated system by delocalization. The magenta dye also show some shift but not as large as the cyan dye. The HOMO/LUMO transition that results in the color of the dyes has more charge transfer character in the case of the cyan dye compared to the yellow and magenta dye.

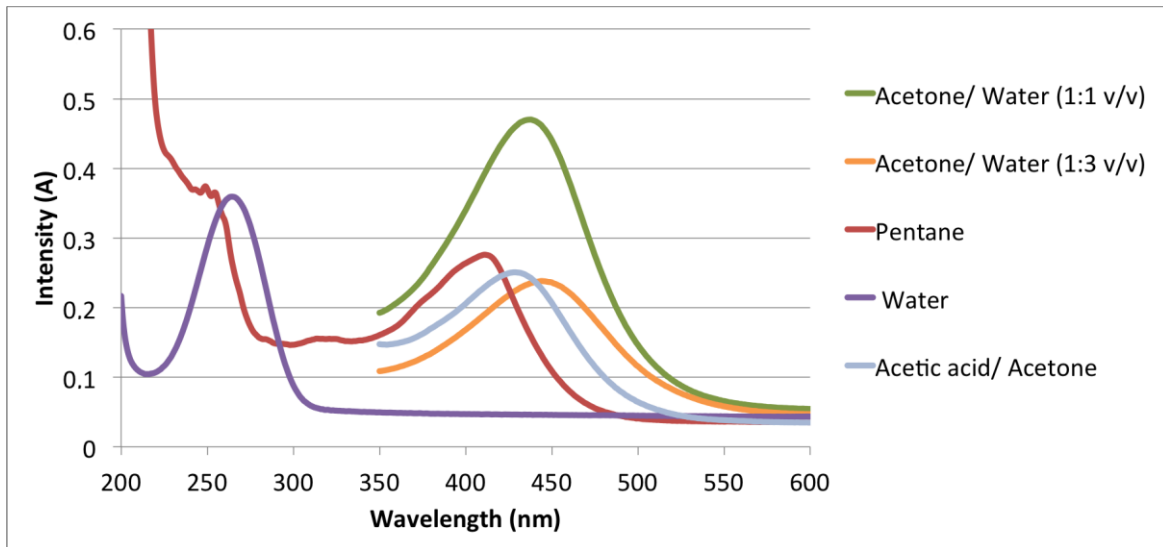


Figure 37: UV-Vis spectra of yellow dye in various solvents.

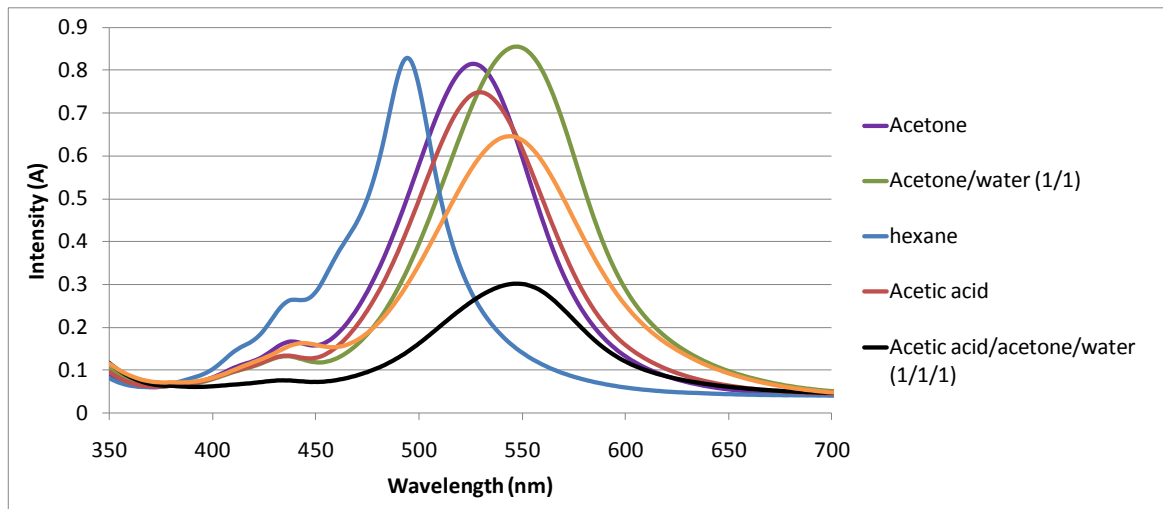


Figure 38: UV-Vis spectra of magenta dye in various solvents.

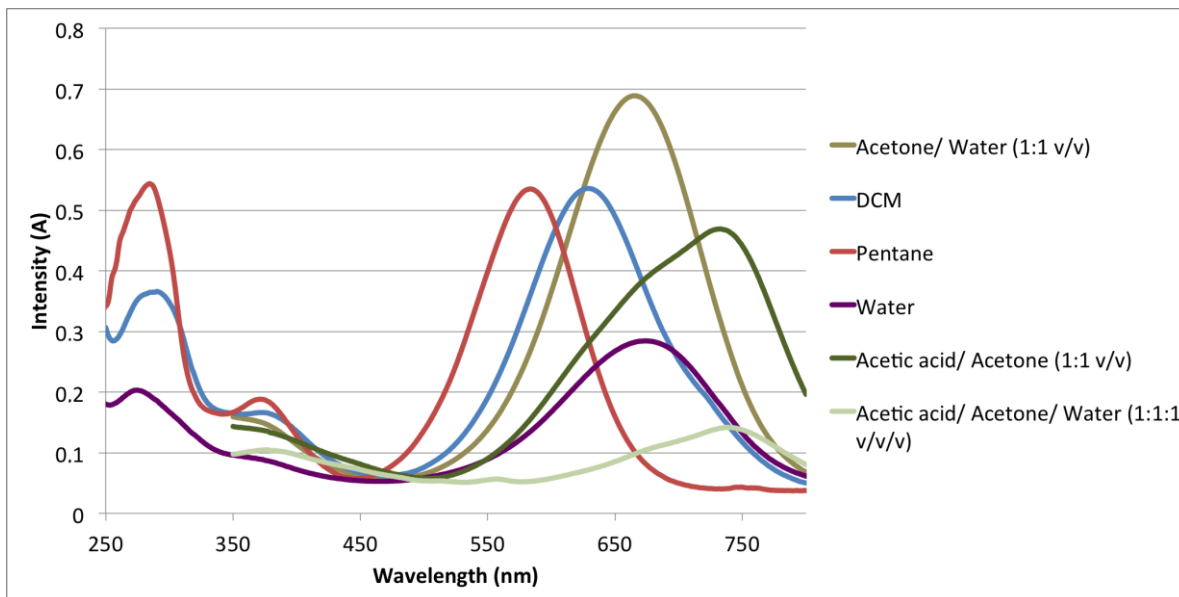


Figure 39: UV-Vis spectra of cyan dye in various solvents.

## 4.4 Dyes in photographic context

### 4.4.1 Extractions

Extractions of dyes from photographic paper were performed with yellow, magenta and cyan parts of calibration photographic paper. These extractions were performed in order to see if the UV-Vis data from the synthesized dyes are comparable with dyes from real photos. It was also not found in literature what the concentration of the dyes is in photos. By extraction and UV-Vis analysis an approximation is made of this concentration, using reference UV spectra to compare the intensities with.

A mixture of ethanol and TFA was made. The ester formed in this mixture was used to extract the dyes.<sup>xxxix</sup> This was done 2:1 v/v ratio for the yellow, magenta and cyan dye, and also in 1:1 v/v ratio for magenta dye in order to see what the influence of more acid is. After extraction the solvents were removed and the dyes were dissolved in acetone/water (1:1 v/v) in order to compare with model dyes compound **1**, **3** and **4**. In Figure 40, the extraction of the magenta dye is shown in both ratios. When more acid is present (in the 1:1 ratio), the sample was more turbid than the sample in the 2:1 v/v ratio. An explanation can be that more gelatin was dissolved during the extraction due to the acid, which can protonate the amino acids in gelatin and make it more soluble. The sample also had a magenta color, but a less defined peak was observed in the UV-Vis spectrum at 550 nm. The extraction with the 2:1 v/v ratio shows a peak around 550 nm. The intensity of the extracted dye resembles the intensity of the reference peak of magenta dye (20  $\mu\text{M}$ ) in acetone/water 1:1 v/v but because gelatin can influence the intensity of the UV-Vis data and the concentration gelatin in the samples is unknown, the concentration does not need to be comparable with the reference spectra in acetone/water. Assuming that the size is comparable with the model dyes used, the concentration will be in the range of  $10^{-5}$  M.

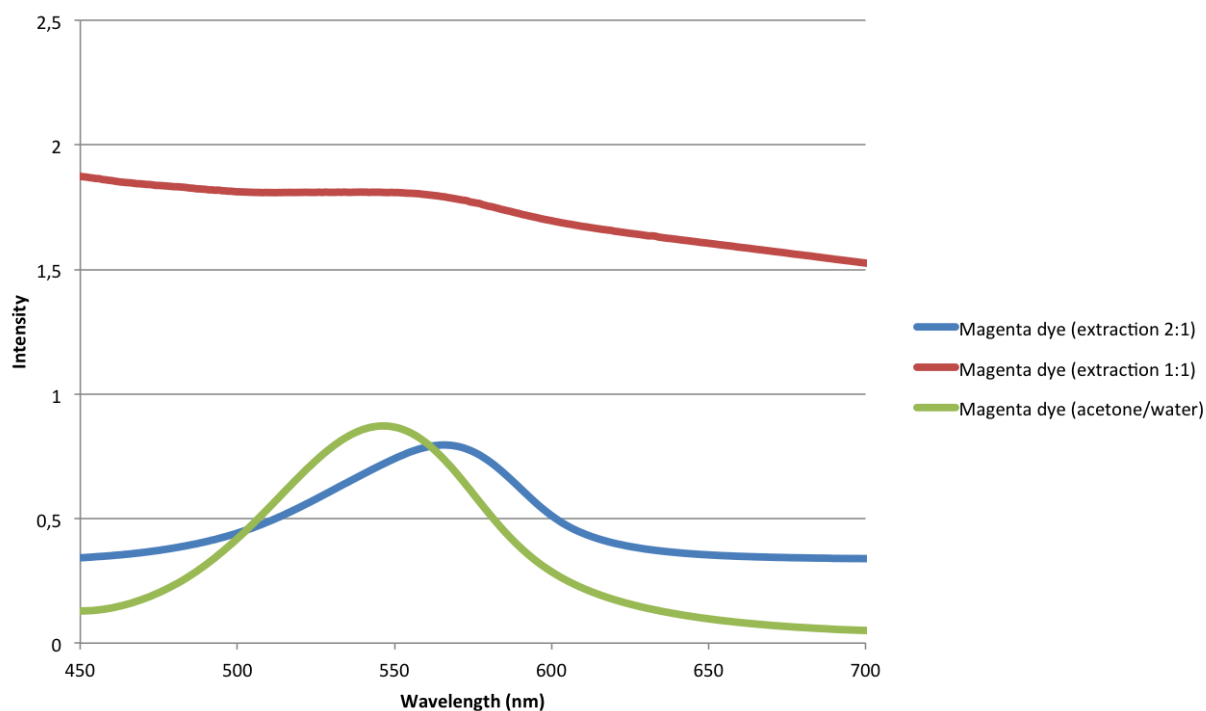


Figure 40: UV-Vis spectrum of extracted magenta dye from photographic paper, measured in acetone/water 1:1 v/v.

#### 4.4.2 Dyes in gelatin

In order to approach an actual photograph UV-Vis spectroscopy of the magenta dye in gelatin/water was performed (Figure 41).

Gelatin dissolved in water can only be measured with transmission UV-Vis apparatus when liquid, so above 30 °C. When cooled, the gelatin structure changes, which results in scattering of the electromagnetic waves, so no data were obtained with regular UV. The cooled gelatin samples measured are an opaque gel. Measurements were performed with melted gelatin/water mixtures (samples were put in hot water) and with cooled gelatin/water mixtures (samples were put in ice). For the magenta dye in warm gelatin, a peak was visible around 560 nm (Figure 41 and Figure 42). This is in line with the measurements done with dye in other solvents and with the extracted dye from the photographic paper. When cooled, the peak is disappeared due to the scattering of the gelatin. A next step will be to measure gelatin with reflectance UV-Vis spectroscopy and compare these spectra to spectra obtained from photographic paper.

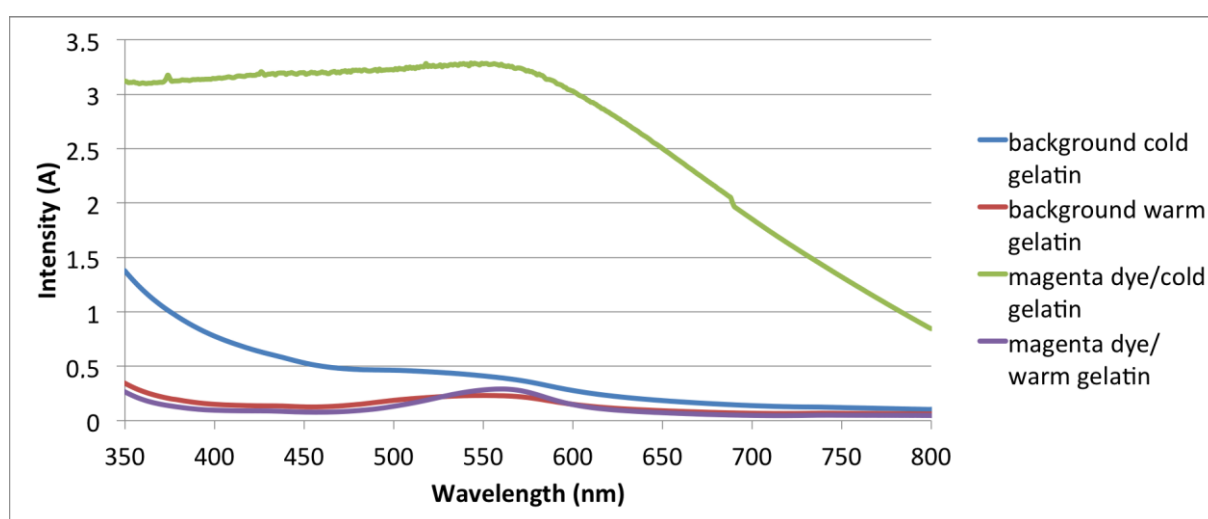


Figure 41: UV- Vis spectra of magenta dye in warm (purple) and cold (green) gelatin. Reference spectra are warm (red) and cold (blue) gelatin without dye.

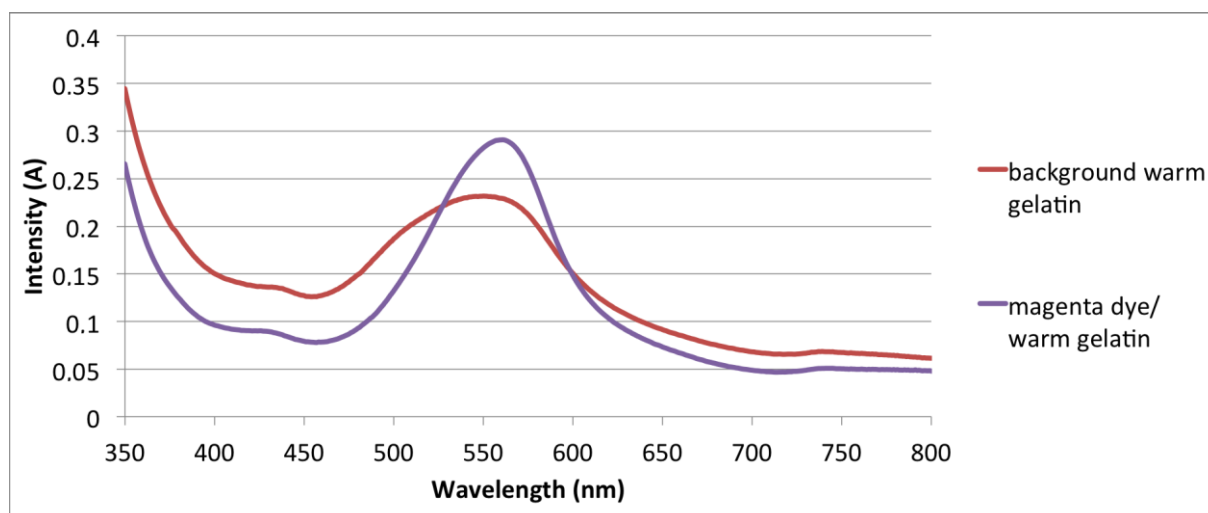


Figure 42: UV- Vis spectra of the magenta dye in warm gelatin (purple) with a reference spectrum of warm gelatin without dye (red).

## 4.5 Schiff base hydrolysis theory

In order to find a molecular explanation for the discoloration of the artworks, the dyes were studied structurally to point out reactive parts and possible reactions were investigated. Due to the lone pair on the imine nitrogen and the degradation in acidic conditions, the hydrolysis of the Schiff base seems to be a logic possibility. In literature also this hydrolysis is mentioned regarding the yellow dye (section 2.1.3). In order to find more evidence for this reaction to take place when acid reacts with the dye, the products of reactions between dyes and acid were analyzed with GC/MS chromatography,  $^1\text{H}$  NMR and UV-Vis spectroscopy.

### 4.5.1.1 Yellow dye

In Figure 43 the Schiff base hydrolysis reaction of the yellow dye is given.

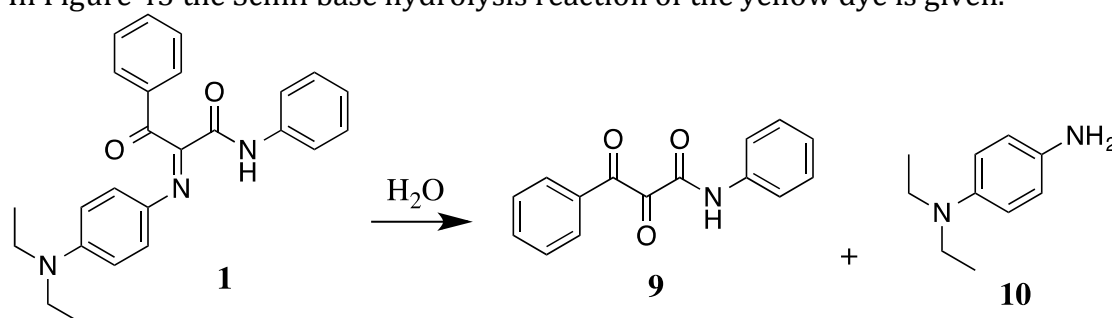


Figure 43: Schiff base hydrolysis of the yellow dye.

As described in the experiment done in section 4.2.5, diamine **10** was found in the water layer of the reaction between **1** and acid. The proposed Schiff base hydrolysis was mentioned in literature and this experimental procedure was tried to repeat. The product of this reaction, triketone **9**, was not soluble in both water and several organic compounds and therefore analysis with NMR was not performed successfully. An IR was made but the triketone was not found. The GC/MS chromatogram shows a possible degradation product: compound **11** (Figure 44). Compound **11** was tried to synthesize, but this was not successful.

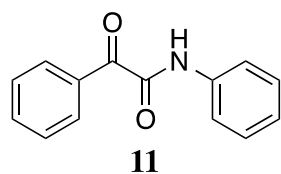


Figure 44: Diketone **11**

#### 4.5.1.2 Magenta dye

In Figure 45 the Schiff base hydrolysis reaction of the magenta dye is given.

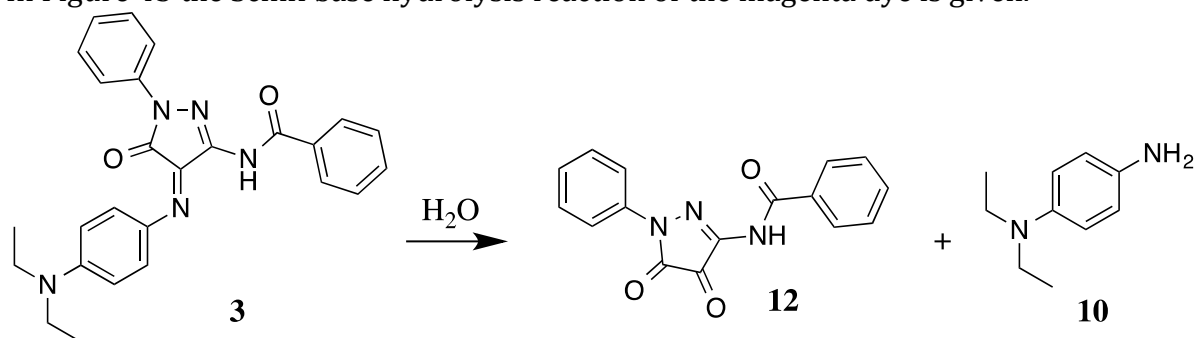


Figure 45: Schiff base hydrolysis of the magenta dye.

This reaction would imply the formation of the diamine **10** and the diketopyrrole **12**. The product mixtures between acid and dye were analyzed with NMR, GC/MS and UV-Vis and did not show the presence of the pyrrole or diamine. No syntheses were carried out to form the pyrrole **12**. This could be a next step in order to compare the analysis results in a proper way with reference compounds.

#### 4.5.1.3 Cyan dye

In Figure 46 the Schiff base hydrolysis reaction of the cyan dye is given.

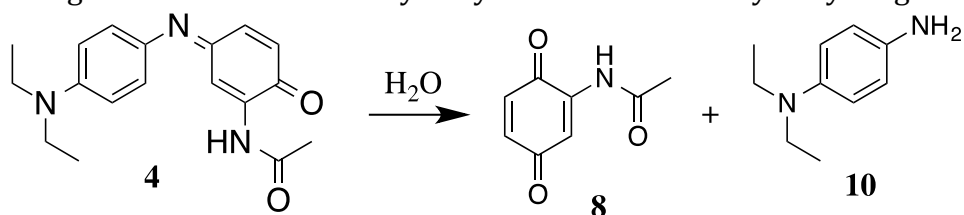


Figure 46: Schiff base hydrolysis of the cyan dye.

The Schiff base hydrolysis of the cyan dye would imply the formation of quinone **8** and diamine **10**. Both products were not found in the UV-Vis spectra or NMR data. The quinone **8** was successfully synthesized but analysis shows no overlap between the quinone and the degradation products of the dye in UV-Vis spectra. The reaction was also tried to be carried out in a retrosynthetical way: quinone **8** and diamine **10** were stirred in an acidic buffer (pH 4). A blue mixture was formed which gave two peaks in the UV-Vis spectrum between 350 and 800: at 610 nm and 450 nm (450 nm is the peak of diamine **10**).  $^1H$  NMR shows the presence of diamine **10** and multiple products.

An experiment between the cyan dye and HCl in anhydrous conditions was carried out. This was done in order to see the difference in reaction products to compare these with the reactions where water was present. The product of this reaction gave a different UV-Vis spectrum (Figure 47) a new peak was observed at 443 nm. This does not resemble the peak of diamine **10** or the quinone. This difference in products between the acidic conditions with or without water implies the role of water in the cyan dye degradation. This is in line with the Schiff base hydrolysis theory.



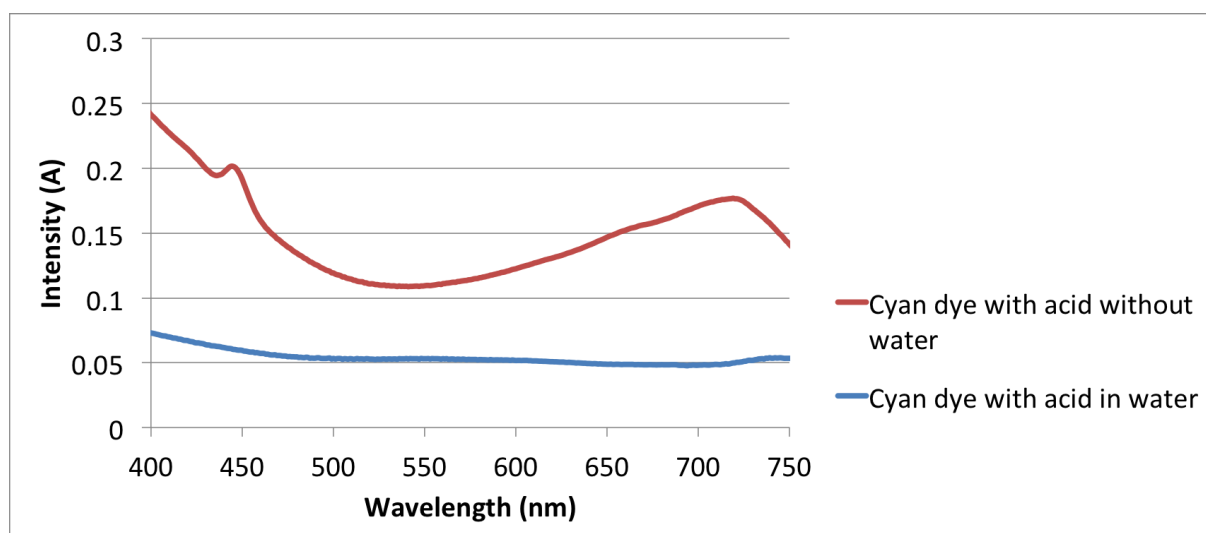


Figure 47: UV-Vis spectra of cyan dye with acid with and without water.

#### 4.5.1.4 Compound 6

In Figure 48 the hydrolysis of the Schiff base of compound **6** is shown.

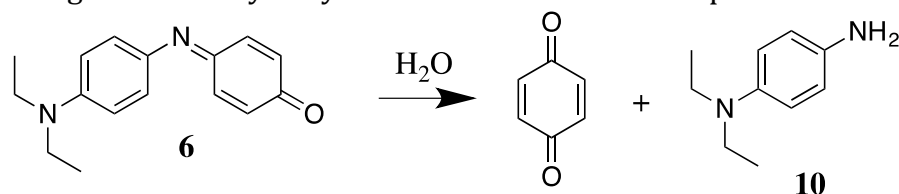


Figure 48: Schiff base hydrolysis of aminoquinone **6**.

This reaction would imply the formation of a quinone and the diamine. Both were not found in the UV-Vis spectra and NMR data taken from the product mixture of compound **6** with acid.

Thus, indications are found for Schiff base hydrolysis but the investigations are still ongoing.

## 5 Conclusion

In order to investigate the role of pollutants in the shift in colors observed in photographic artworks, the dyes that are responsible for colors in photographs, compounds **1**, **3**, and **4** have been synthesized. These dyes were studied structurally with DFT, CV and solvatochromic effects were measured with UV-Vis spectrometry. The reactivity of the dyes towards acid was studied with several types of acid. The dyes were dissolved and stored in several acidic conditions; a pH calibration set was made for the three dyes from pH 1 to 7 and measured over a period up to a month. The yellow dye seems to be more vulnerable for acid degradation; the magenta dye seems to be the most stable in acidic conditions. Variants of the cyan dye were synthesized to compare the reaction products of compounds **5** and **6** with acid with those of compound **4** with acid. The hydrolysis of the Schiff base present in the three dyes was a theory that was applied, some indications are given that Schiff base hydrolysis may take place but no conclusive evidence was found. The magenta dye being the most stable and the yellow dye being the least stable in acidic conditions are measurements that are in line with the observations found in *Russian Diplomacy*, a photographic artwork that was used as a case study for this thesis.

## 6 Outlook

### 6.1 Dyes in solid gelatin

For this thesis most of the UV-Vis measurements were done by using solutions of dyes in acetone/water mixtures due to the low solubility of the dyes in water and the ease of transmission UV-Vis spectroscopy. Dyes dissolved in gelatin are a closer approximation of a real photograph. Solid state UV-Vis spectroscopy of these gelatin samples can be compared with UV-Vis spectroscopy data of calibration photographic paper. Then, these gelatin samples can be treated with acid in order to measure the optical changes of the dyes in gelatin.

### 6.2 Analysis of reaction products

In this thesis indications for the Schiff base hydrolysis theory were found. In order to find more evidence for this theory several approaches can be performed. The reaction products of the dyes with acid now show in NMR spectra multiple components. The product mixtures only consist of a few milligrams of product mixtures, too less to separate properly. The dyes can be synthesized in a larger amount in order to carry out these reactions on a larger scale, the products will be in a higher quantity and therefore more doable to separate and analyze these products properly in order to get a better view on the formation of the chemicals formed after the reaction takes place.

Another way to find more evidence for the hydrolysis of the Schiff base can be by using heavy-oxygen water  $\text{H}_2\text{O}^{18}$ . The labeled oxygen can then be traced in the products by the use of ESI-MS spectrometry. In the case of the hydrolysis of the Schiff base the carboxyl group formed will contain  $\text{O}^{18}$ . This implies that the products formed must be stable enough to not react further after the reaction with acid and be analyzable.

The yellow dye shows in the UV-Vis spectrum of dye with acid at pH 3.5 and 4 two new peaks between 500 and 550 nm. These indicate the formation of degradation products. The reaction products of the Schiff base hydrolysis of the yellow dye would imply the formation of triketone **10**. This product is unstable and therefore not analyzed with NMR spectroscopy. A possible degradation product is diketone **11**. This compound could be synthesized and compared to the UV-Vis spectra of the yellow dye in pH 3.5.

All of these reactions could gather more information about the reaction mechanism that is applicable to the reaction between photographic dyes and acetic acid.

## Acknowledgements

I would like to thank Bas Reijers for supervising me. I think I was not the easiest student but even when the project did not proceed as we wanted, you helped me to challenge myself to find new ways to approach my problems and be creative in this process. You are not only a good supervisor but you made me feel I was a part of a team, we worked together many hours in the lab and it was much more fun with you around.

I would like to thank professor Leo Jennekens for supervising me and helping me find new ideas for my research. You taught me (fundamental) organic chemistry, which was very useful. You were always willing to help me with my project, which I appreciate a lot.

I would like to thank Alexander for synthesizing compound Aminoquinone **8**. The complete technical staff, Johann, Henk, Jord and Adri, I would like to thank you for the technical support I needed. Besides that, you were always there to discuss my chemistry with me, teaching me some tips and tricks in the lab and help me whenever I needed it. I also want to thank the whole OCC group for the nice coffee breaks, UMC lunches, good conversations and making me feel welcome in the group. At last I would like to thank NWO for funding this thesis.

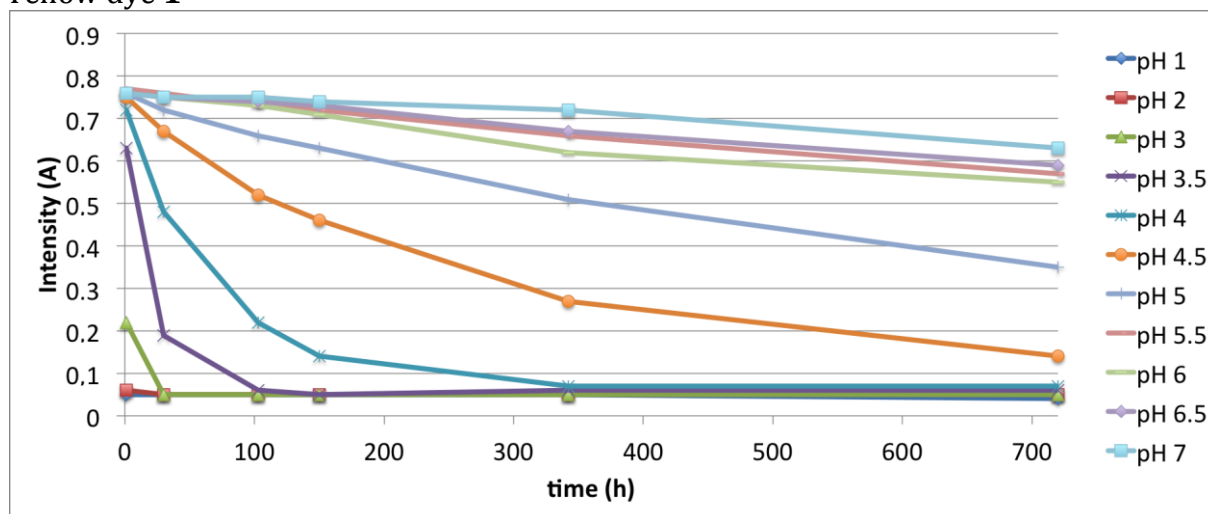
## References

---

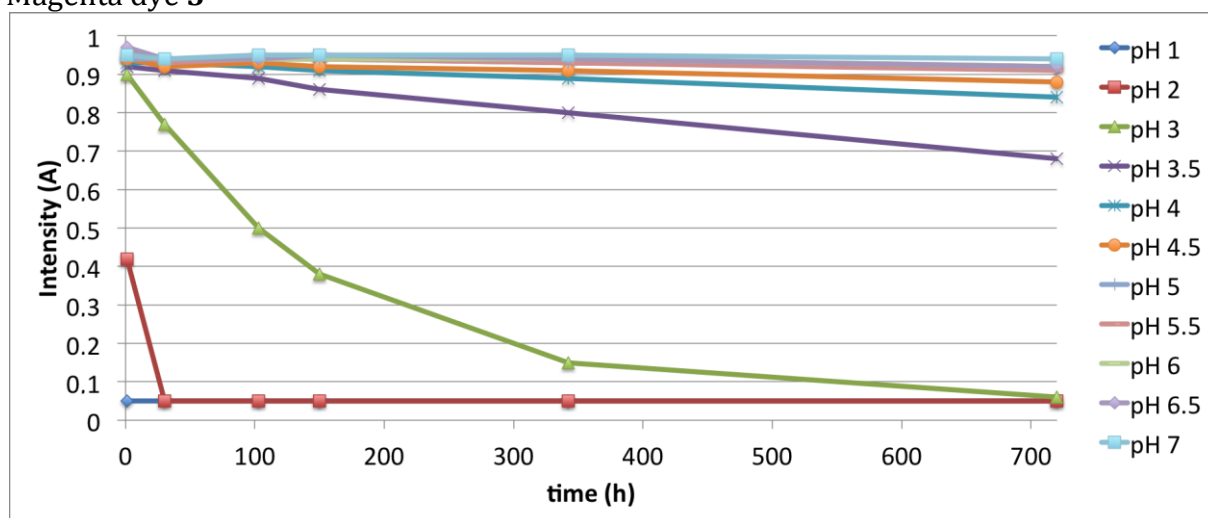
- <sup>i</sup> Oxford dictionaries. <http://www.oxforddictionaries.com/definition/english/art> (accessed April 4 2015).
- <sup>ii</sup> Dissanayake, E. *What is art for?* 4th ed.; University of Washington press: Washington, 1998.
- <sup>iii</sup> Bahn, P. *The Cambridge Illustrated History of Prehistoric Art*. Cambridge university press, 1998.
- <sup>iv</sup> Marien, M. W. *Photography, a cultural history*. 2<sup>nd</sup> ed.; Laurence King Publishing, 2006.
- <sup>v</sup> National geographic, wallpapers, first color photograph. <http://photography.nationalgeographic.com/wallpaper/photography/photos/milestones-photography/color-tartan-ribbon/> (accessed April 4, 2015).
- <sup>vi</sup> Photographic resource center, timeline of color photography related to the Leopold Godowsky Jr. Color Photography Awards. <http://www.bu.edu/prc/GODOWSKY/timeline.htm> (accessed April 4, 2015).
- <sup>vii</sup> Furthering the fold: three-dimensionality and the photographic sculpture. <http://www.modern-edition.com/art-articles/photographic-form/folded-photographs.html> (accessed April 18, 2015).
- <sup>viii</sup> Condition Mapping Rapport: "*Russian Diplomacy*" by Ger van Elk, Clara von Waldthausen, October 2013.
- <sup>ix</sup> Wilhelm, H. *The permanence and care of color photographs: traditional and digital color prints, color negatives, slides, and motion pictures*. 1th ed.; Preservation Publishing Company: Iowa, 1993.
- <sup>x</sup> Photographs and Preservation. How to save photographic works of art for the future? <http://www.nwo.nl/onderzoek-en-resultaten/onderzoeksprojecten/34/2300169034.html> (accessed April 4, 2015).
- <sup>xi</sup> Theys, R. D.; Sosnovsky, G. Chemistry and Processes of Color Photography, *Chem. Rev.*, **1997**, *1*, 83-132.
- <sup>xii</sup> Bergthaller, P. Couplers in colour photography, chemistry and function, *The image science journal*, **2002**, *5*, 153-230.
- <sup>xiii</sup> Kumar, A. PhD. Dissertation, Punjab technological University, 2013.
- <sup>xiv</sup> Cordes, E. H.; Jencks, W. P. On the Mechanism of Schiff Base Formation and Hydrolysis. *J. A. C. S.*, **1962**, *84*, 832-837.
- <sup>xv</sup> Cordes, E. H.; Jencks, W. P. The mechanism of hydrolysis of schiff bases derived from aliphatic amines, *J. A. C. S.*, **1963**, *85(18)*, 2843-2848.
- <sup>xvi</sup> Balenovic, L. Arhiv za Kemiju 1955 vol 27 p 219.
- <sup>xvii</sup> Tuite, R. J. Image stability in color photography, *Journal of applied photographic engineering*, **1979**, *5*, 200-207.
- <sup>xviii</sup> De Hoffmann, E.; Bruylants, A. Synthèses et Propriétés des Bases de Schiff. II. — Propriétés acidobasiques et vitesses d'hydrolyse acide des  $\alpha$ (p, N-diméthyl-aminophényl) iminobenzoylacétanilides (PIBA), *Bulletin des Sociétés Chimiques Belges*, **1966**, *75*, 91-106.
- <sup>xix</sup> Martin, R. B. Relative Humidity, *Chemistry everyday for everyone*, **1999**, *74*, 1081-1082.
- <sup>xx</sup> Fenech, A. et al. Volatile aldehydes in libraries and archives, *Atmospheric environment*, **2010**, *44*, 2067-2073.
- <sup>xxi</sup> Adelstein, P. Z.; Bigourdan, J. L.; Reilly, J. M. Moisture relationships of photographic film, *J. A. C. S.*, **1997**, *36*, 193-206.

- 
- xxii Reilly, J. M. Storage guide for color photographic materials, Image permanence institute, **1998**.
- xxiii Fenech, A. PhD. Dissertation, Bartlett School of Graduate Studies, 2011.
- xxiv Ralmaho, O. et al. Emission rates of volatile organic compounds from paper, *e-preservation science*, **2009**, *6*, 53-59.
- xxv Pénichon, S.; Jürgens, M.; Murray, A. *Light and dark stability of laminated and face-mounted photographs: A preliminary investigation*. Congres at Baltimore 2-6 September.
- xxvi M Ryhl-Svendsen. Pollution in the photographic archive. *9th IADA Congress Preprints*, **1999**, 211–215
- xxvii Conjugated Systems, Orbital Symmetry, and UV Spectroscopy, [http://wps.prenhall.com/wps/media/objects/340/348272/wade\\_ch15.html](http://wps.prenhall.com/wps/media/objects/340/348272/wade_ch15.html) (accessed April 4 2015).
- xxviii Benzene reactions, chemical properties of benzene, <http://chemistry.tutorvista.com/organic-chemistry/benzene-reactions.html> (accessed April 4, 2015).
- xxix Abu-Hasanayn et al. Energy Transfer to the Low-Energy Triplet States of 1,3-Dicarbonylazomethine Dyes: The Role of Unique Geometries and Nonadiabatic Behavior, *J. Phys. Chem.*, **2001**, *105*, 1214-1222.
- xxx Reichardt, C. Solvatochromic Dyes as Solvent Polarity Indicator, *Chem. Rev.*, **1994**, *94*, 2319-2358.
- xxxi Figueras, Hydrogen Bonding, Solvent Polarity, and the Visible Spectrum of Phenol Blue and Its Derivatives, *J. A. C. S.*, **1971**, *93*, 3255-3263.
- xxxii Kazuya, S. The alkaline hydrolysis of yellow azomethine dyes. *J. O. C.*, **1986**, *37*, 2076- 2080.
- xxxiii Cusan. C. et al, Synthesis and biological evaluation of a new class of acyl derivatives of 3-amino-1-phenyl-4,5-dihydro-1H-pyrazol-5-one as potential dual cyclooxygenase (COX-1 and COX-2) and human lipoxygenase (5-LOX) inhibitors, *Il Farmaco*, **2004**, *60*, 327-332.
- xxxiv Vittum, P.; Duennebier, F. The Reaction between Pyrazolones and their Azomethine Dyes, *J. A. C. S.*, **1950**, *72*, 1536–1538.
- xxxv Adachi M.; Murata Y.; Nakamura S. The relationship between the structures and absorption spectra of cyan color indoaniline dyes, *J. O. C.*, **1993**, *58*, 5238–5244.
- xxxvi Wilstaetter, Moore. *Chemische berichte*. **1907**, *40*, 200-202.
- xxxvii Gould, S.; Shen, B.; Whittle, Y. Biosynthesis of Antibiotic LL-C 10037a: The Steps beyond 3 -Hydroxy anthranilic Acid, *J. A. C. S.*, **1989**, *111*, 7932-7938.
- xxxviii Nawrat, C.; Lewis, W.; Moody, C. Synthesis of Amino-1,4-benzoquinones and Their Use in Diels\_Alder Approaches to the Aminonaphthoquinone Antibiotics, *J. O. C.*, **2011**, *76*, 7872-7881.
- xxxix Fenech, A. et al. Stability of chromogenic colour prints in polluted indoor environments, *Polymer Degradation and Stability*, **2010**, *12*, 2481–2485.
- xl Wiggen, van M. *Degradation of photo dyes by treatment with acid*, Bachelor thesis, O. C. C., July 2014.
- xli Mahmood, A et al. Assessing the quantum mechanical level of theory for prediction of UV/Visible absorption spectra of some aminoazobenzene dyes, *Journal of Saudi chemical society*, **2015**, *19*, 436-441.
- xlii Documentation and characterization of photographic surfaces by edge reflection analysis, [http://notesonphotographs.org/index.php?title=Pollmeier,\\_Klaus.\\_%22Documentation\\_and\\_Characterization\\_of\\_Photographic\\_Surfaces\\_by\\_Edge\\_Reflection\\_Analysis.%22](http://notesonphotographs.org/index.php?title=Pollmeier,_Klaus._%22Documentation_and_Characterization_of_Photographic_Surfaces_by_Edge_Reflection_Analysis.%22). (accessed November 6, 2015).

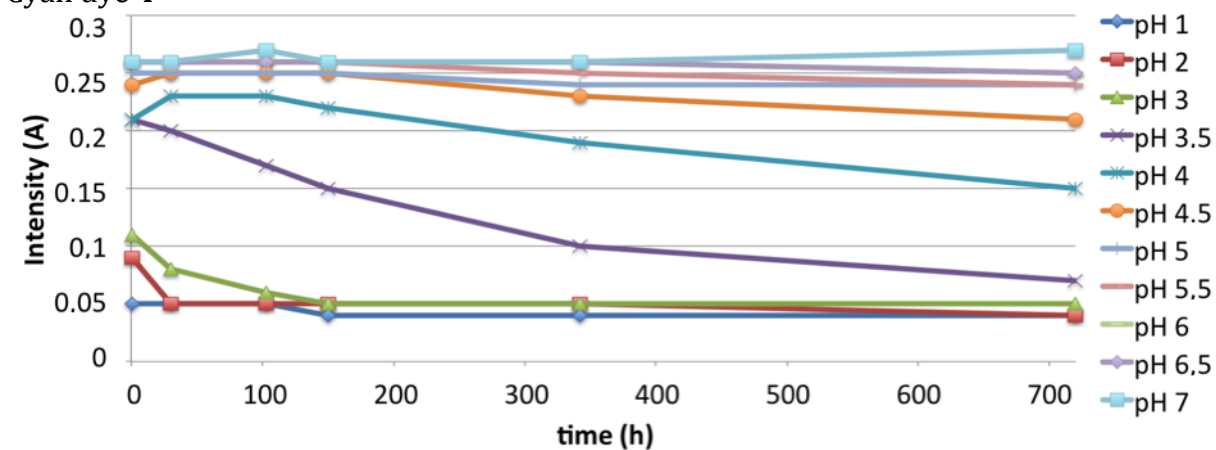
Appendix A: Dyes in acid over time  
Yellow dye 1



Magenta dye 3



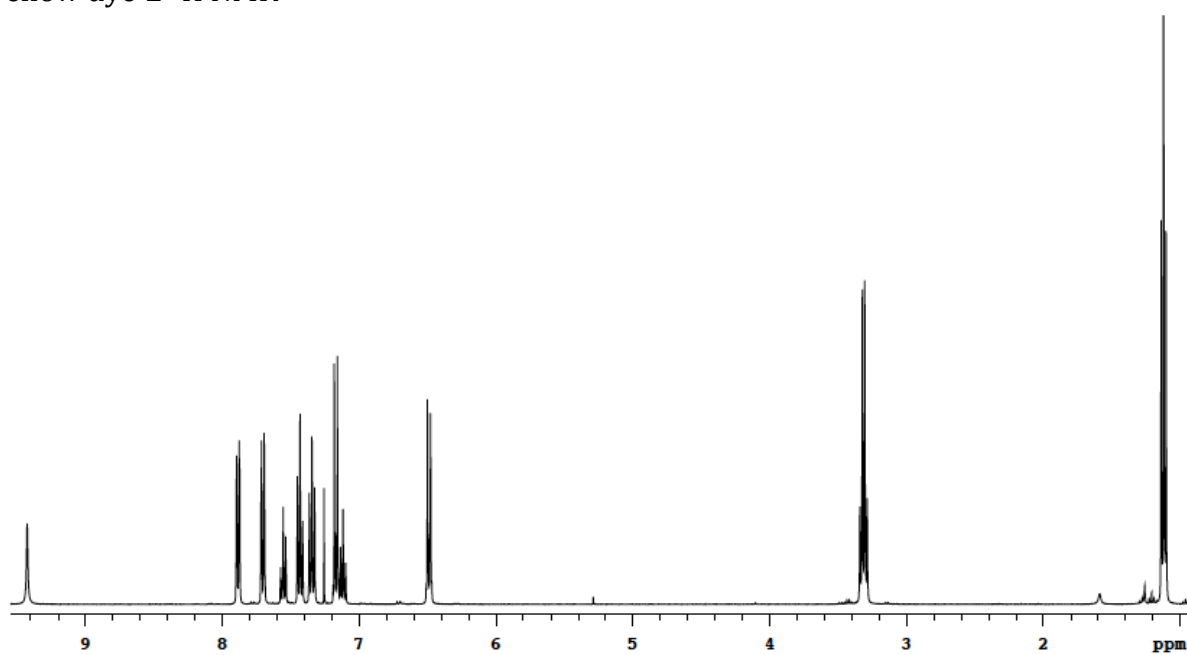
Cyan dye 4



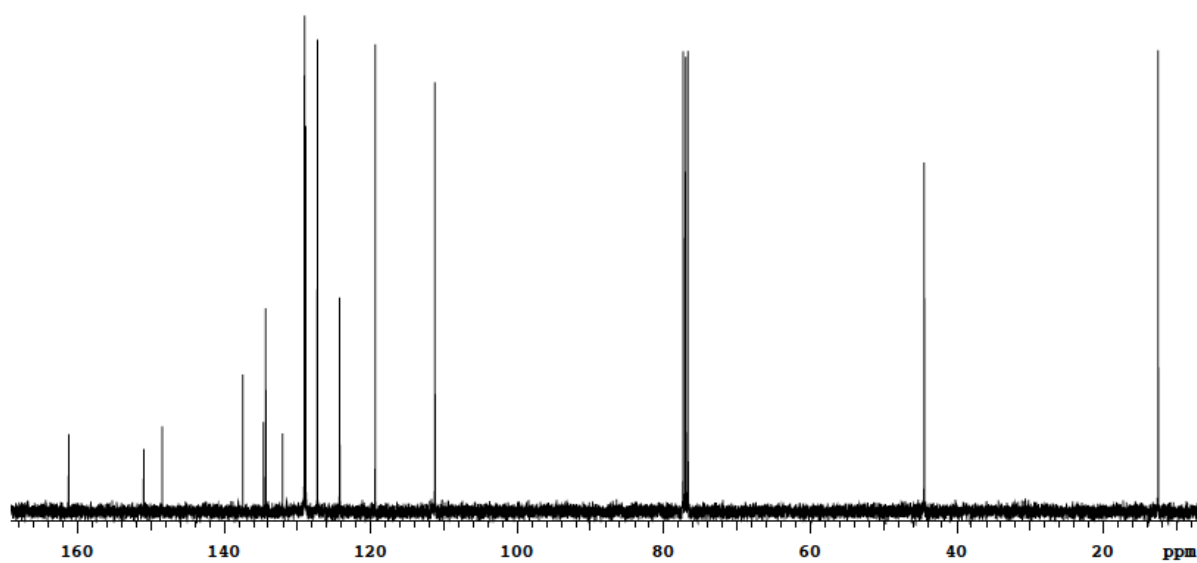
---

Appendix B: NMR spectra

Yellow dye **1**  $^1\text{H}$  NMR

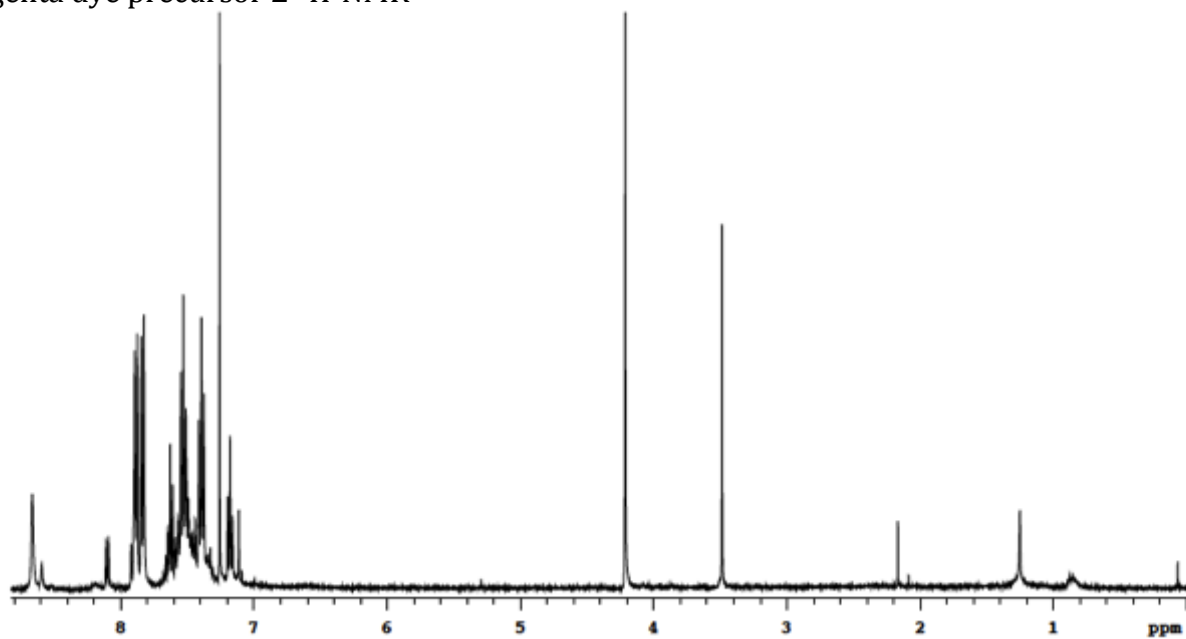


Yellow dye **1**  $^{13}\text{C}$ -NMR

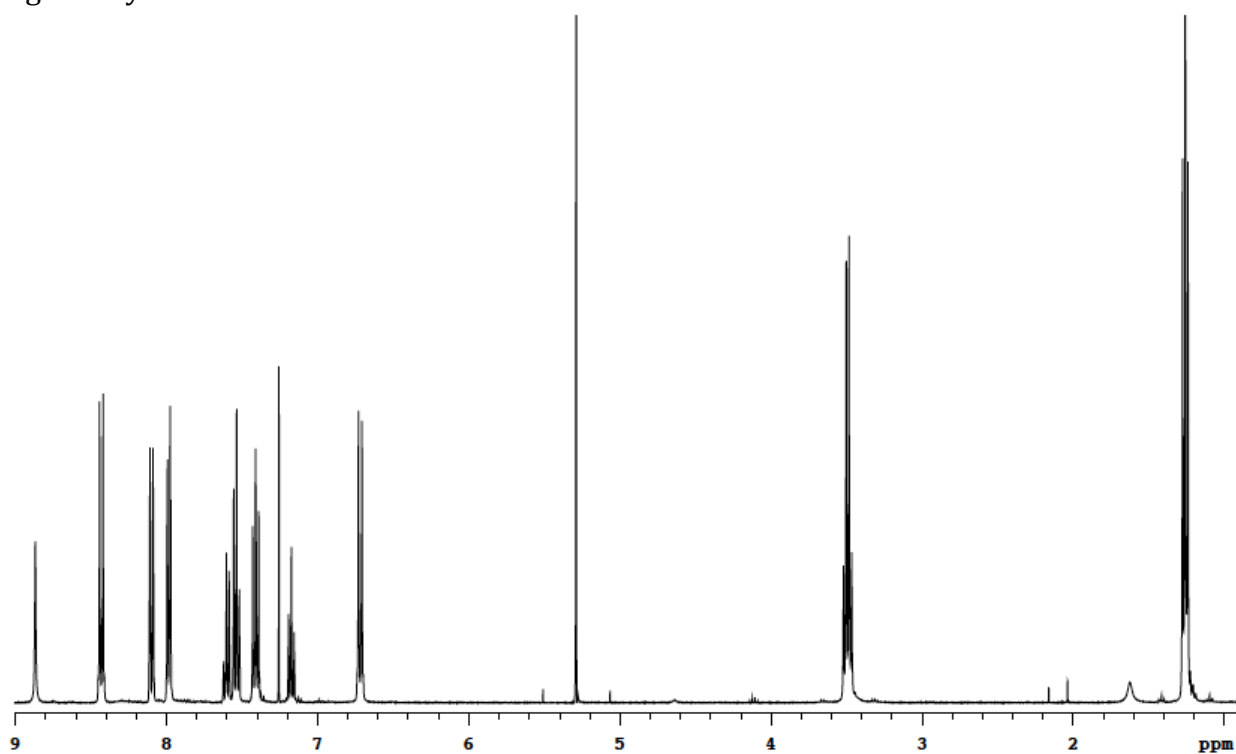




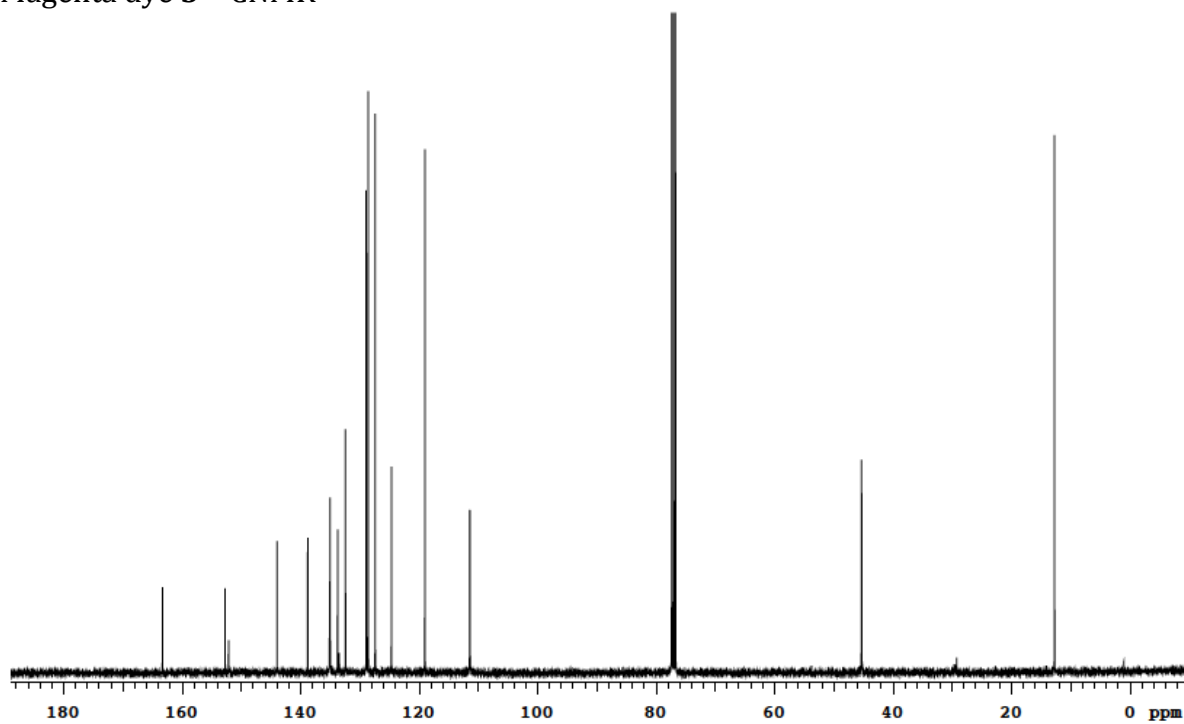
Magenta dye precursor 2  $^1\text{H-NMR}$



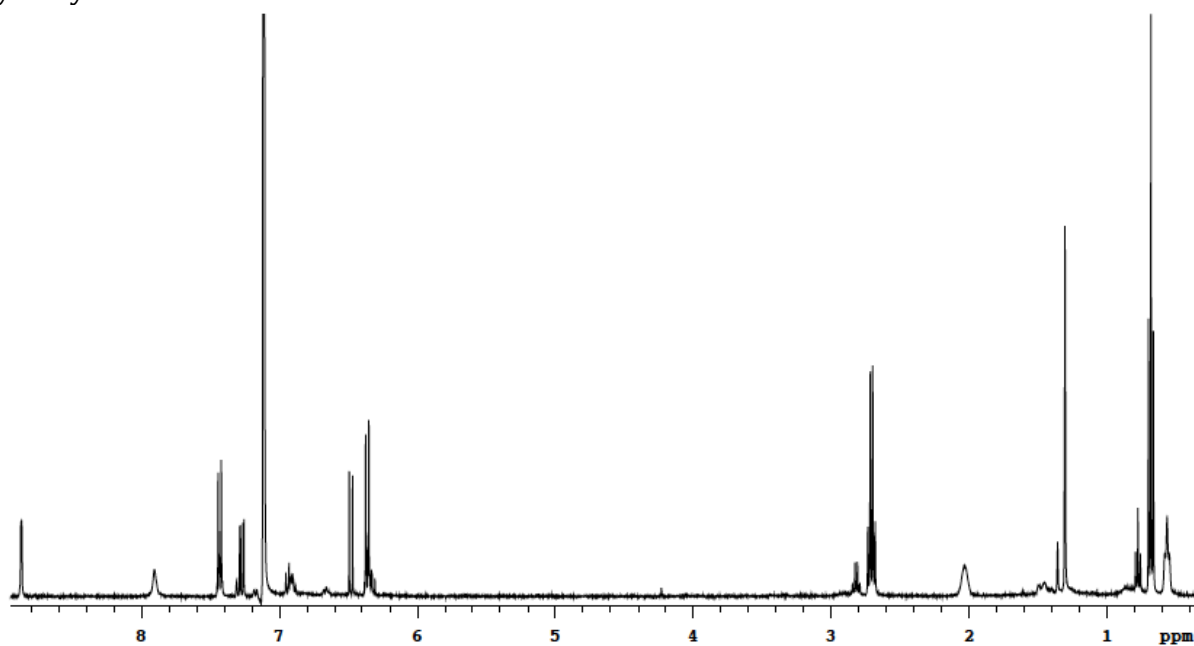
Magenta dye 3  $^1\text{H-NMR}$



Magenta dye 3  $^{13}\text{C}$ NMR

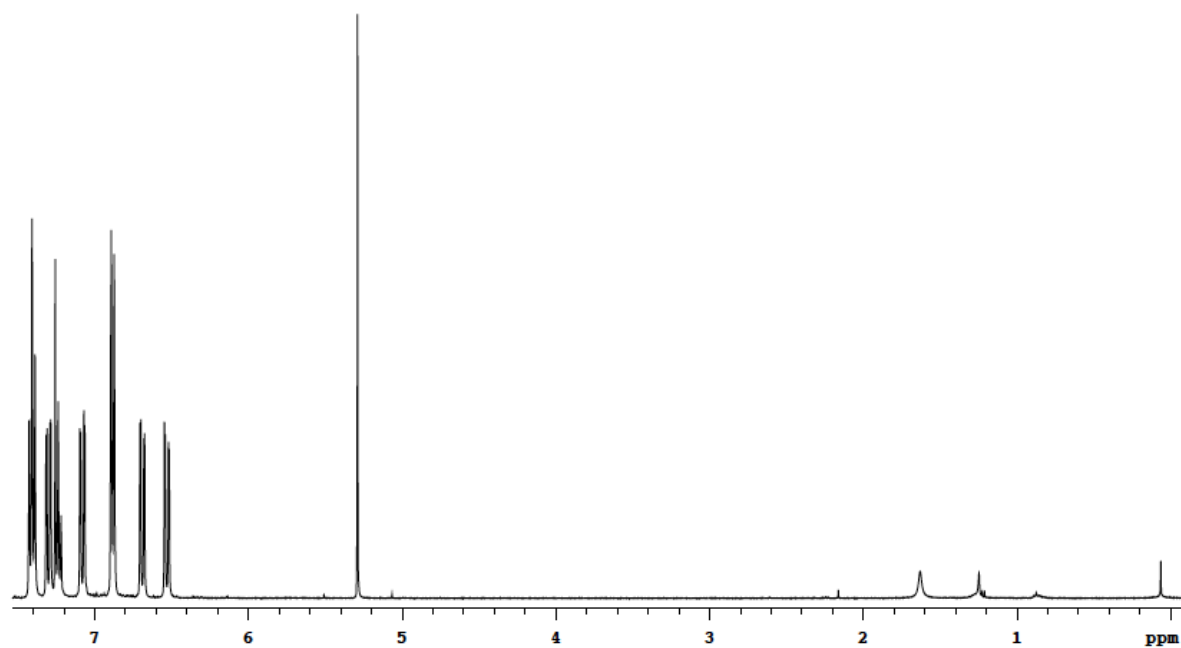


Cyan dye 4  $^1\text{H}$ NMR



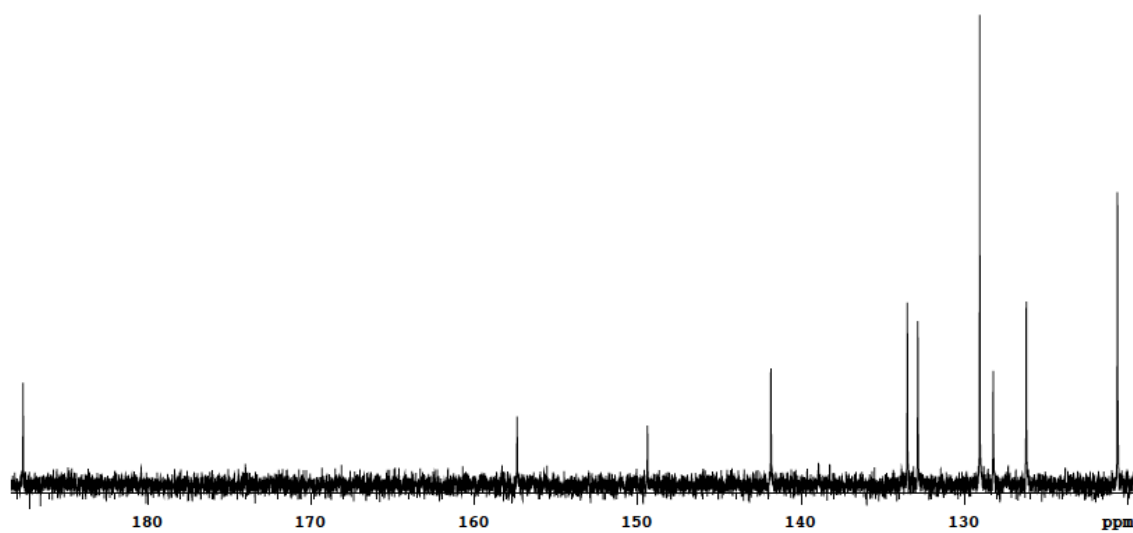
---

Aminoquinone 5  $^1\text{H}$ NMR

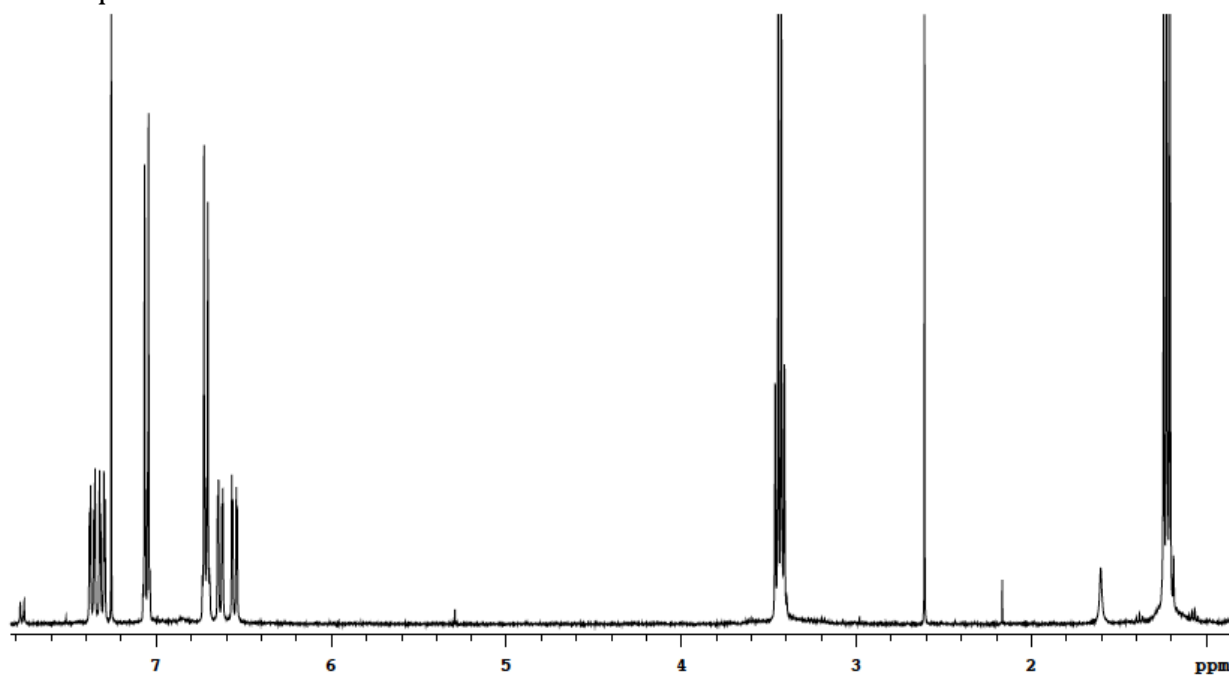


---

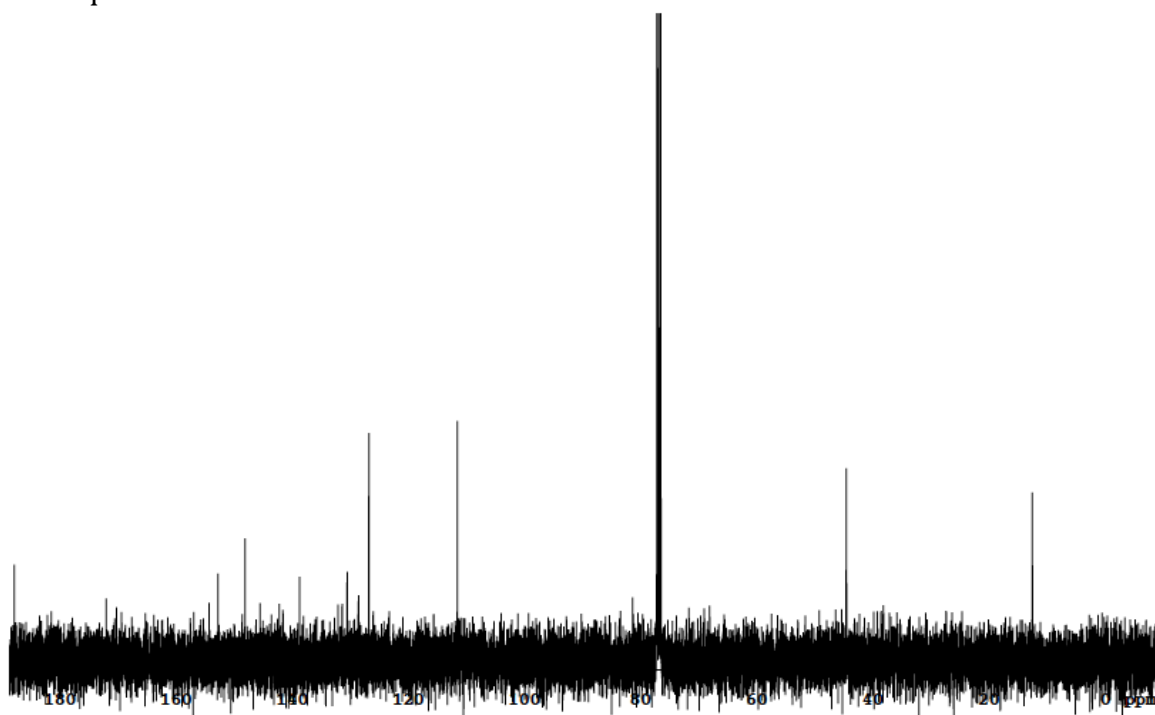
Aminoquinone 5  $^{13}\text{C}$ NMR



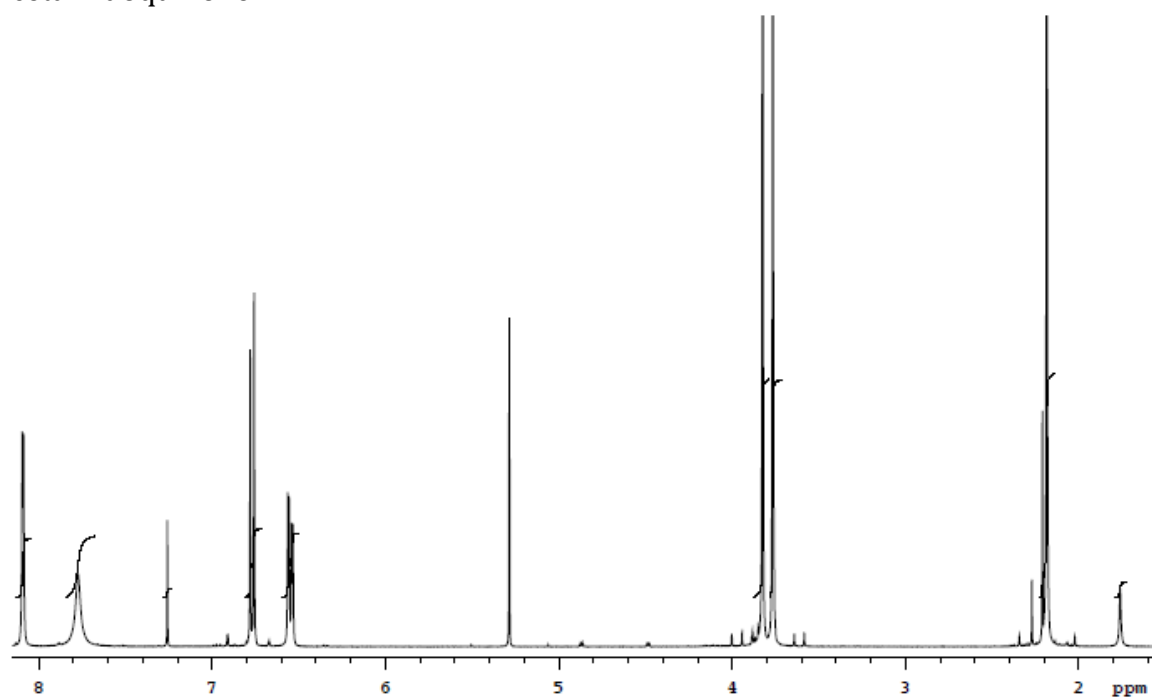
Aminoquinone 6  $^1\text{H}$ NMR



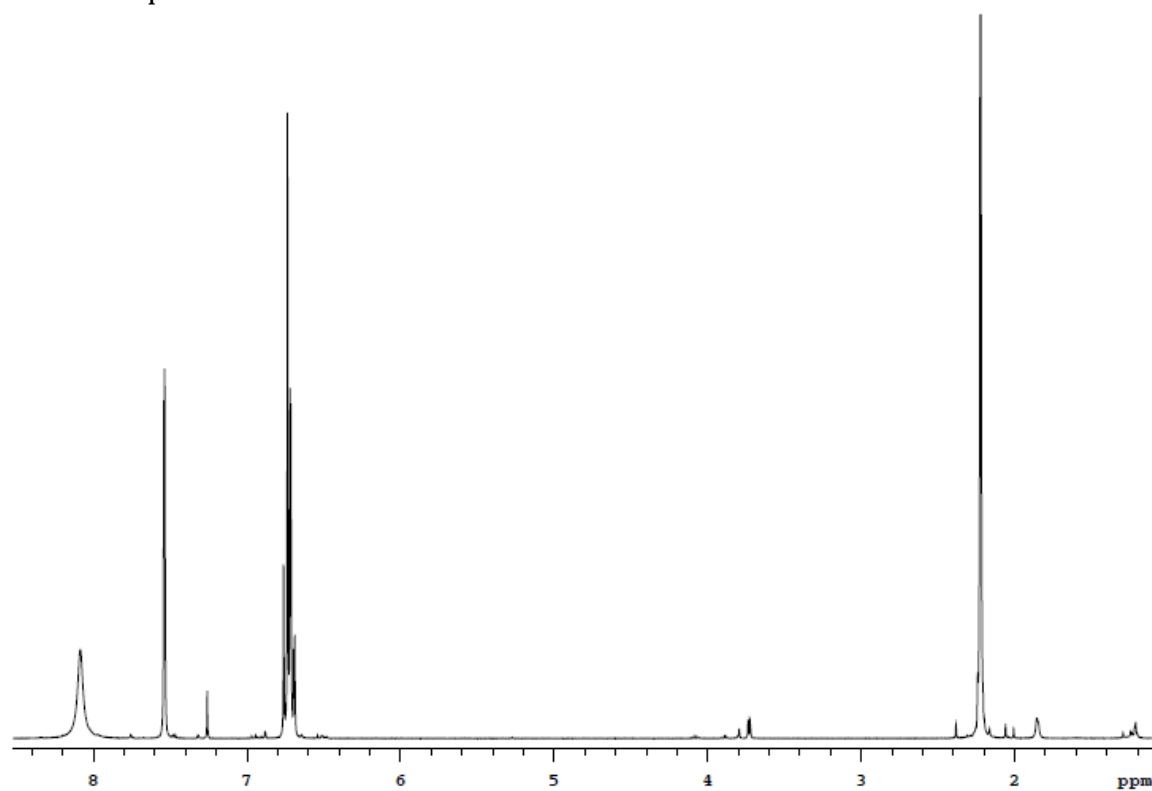
Aminoquinone 6  $^{13}\text{C}$ NMR



Acetamidoquinone **7**  $^1\text{H}$  NMR

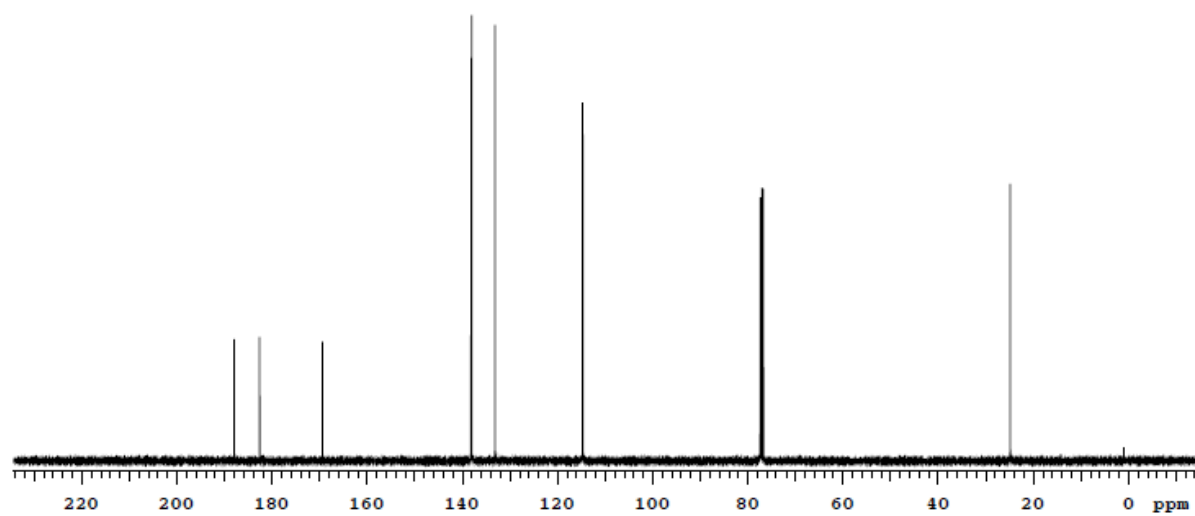


Acetamidoquinone **8**  $^1\text{H}$  NMR



---

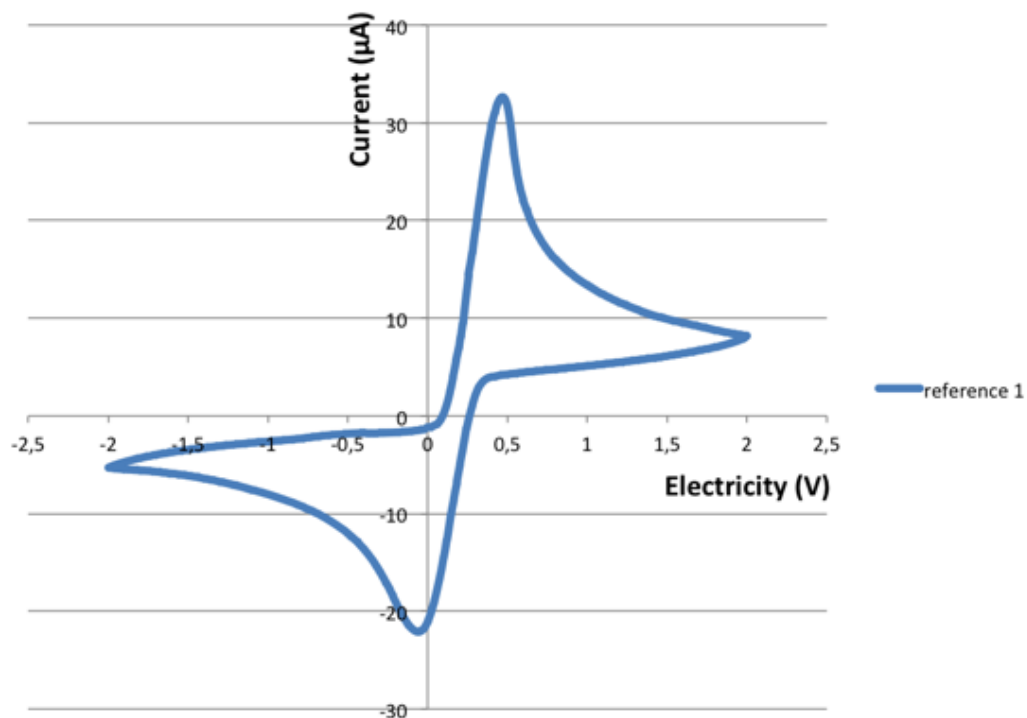
Acetamidoquinone **8**  $^{13}\text{C}$  NMR



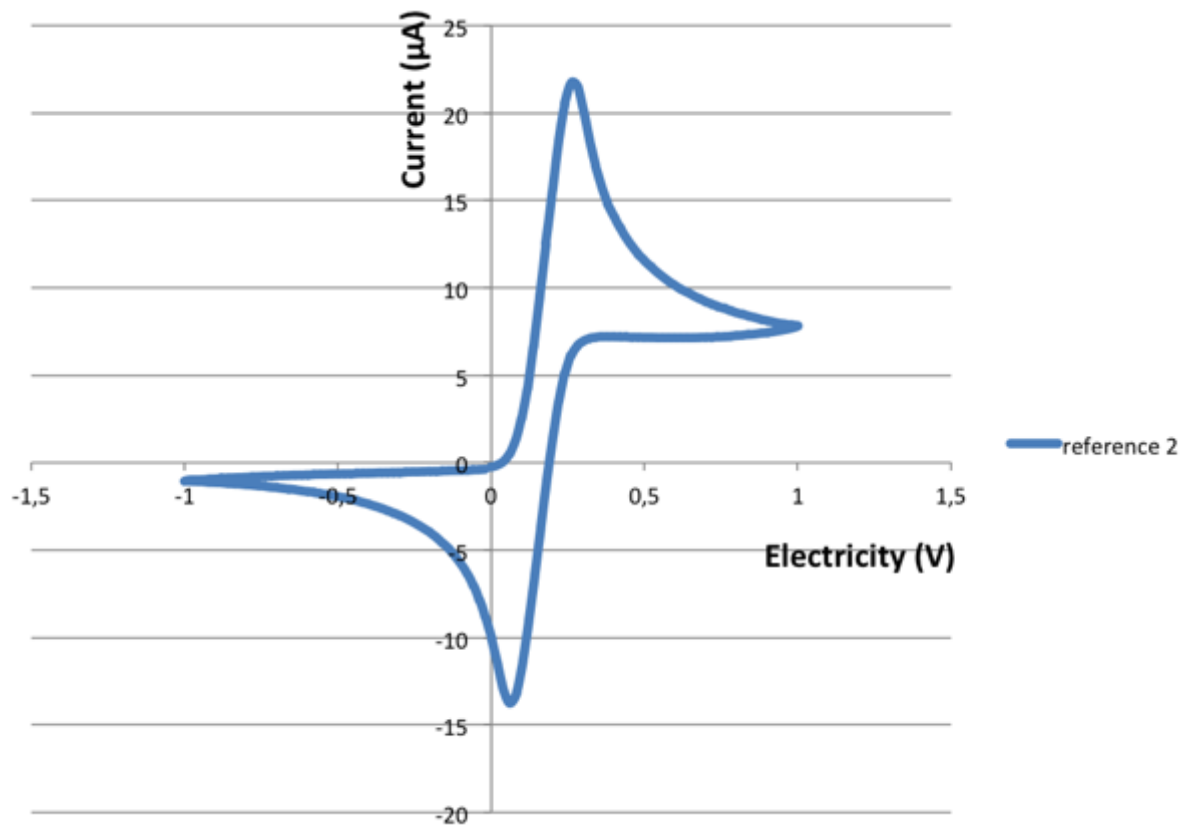
---

Appendix C: CV reference spectra

Ferrocene in electrolyte, reference for compounds cyan dye **4** and aminoquinone **5**.



Ferrocene in electrolyte, reference for aminoquinone **6**.



Appendix D: UV-Vis data of solvatochromic series.  
Yellow dye 1

Number	Solvent	$\lambda_{\max}$ (nm)		Intensity	
1	acetone	426		0,46	
2	acetone/water (3:1)	432		0,44	
3	acetone/water (1:1)	437		0,47	
4	acetone/water (1:3)	444		0,24	
5	CHCl <sub>3</sub>	434		0,46	
6	DCM	434	262	0,45	0,69
7	hexane	413	254	0,28	0,40
8	pentane	411	249	0,28	0,37
9	EtOH	431	253	0,41	0,54
10	water	264		0,36	
11	toluene	426		0,41	
12	acetic acid	429		0,12	
13	acetic acid/acetone (1:1)	428		0,25	
14	acetonitrile	429	259	0,44	0,62
15	acetic acid/acetone/water (1:1)	no peak		no peak	
16	THf	424		0,41	
17	DMSO	438		0,38	
19	dioxane	422	277	0,40	2,32
20	benzene	428		0,43	
21	ethylacetate	422	261	0,40	2,00

Magenta dye 3

Number	Solvent	$\lambda_{\max}$ (nm)	Intensity
1	acetone	526	0.82
2	acetone/water (3:1) vol: 8mL	560	0.63
3	acetone/water (1:1)	548	0.86
4	acetone/water (1:3) vol: 8mL	537	0.62
5	CHCl <sub>3</sub>	530	0.79
6	DCM	530	0.83
7	hexane	494	0.83
8	EtOH	531	0.75
9	water	No peak	No peak
10	toluene	514	0.77
11	acetic acid	530	0.75
12	acetic acid/acetone (1:1)	530	0.77
13	acetonitrile	528	0.80
14	acetic acid/acetone/water (1:1:1)	548	0.30
15	THF	520	0.77
16	DMSO	544	0.65



Cyan dye 4

Number	Solvent	$\lambda_{\max}$ (nm)		Intensity	
1	acetone	612		0.54	
2	acetone/water (3:1)	635		0.63	
3	acetone/water (1:1)	652		0.69	
4	acetone/water (1:3)	665		0.69	
5	CHCl <sub>3</sub>	634	279	0.60	0.50
6	DCM	629	290	0.54	0.37
7	hexane	586	282	0.51	0.68
8	pentane	584	284	0.54	0.54
9	EtOH	626	273	0.58	0.55
10	water	673	274	0.28	0.20
11	toluene	610		0.57	
12	acetic acid	715		0.40	
13	acetic acid/acetone (1:1)	733		0.47	
14	acetonitrile	616	280	0.52	0.44
15	acetic acid/acetone/water (1:1)	739		0.14	
16	THf	608		0.54	
17	DMSO	632		0.55	
19	dioxane	608	277	0.53	3.03
20	benzene	615		0.58	
21	ethylacetate	605	278	0.52	0.63